Prepared for publication in PASP

Faint BVRI Photometric Sequences in Selected Fields

A. Saha[1,2], A. E. Dolphin[1,3] and F. Thim[1,4]

NOAO, P.O. Box 26732, Tucson, AZ 85726

`saha@noao.edu, adolphin@as.arizona.edu, thim@noao.edu`

and

B. Whitmore

Space Telescope Science Institute, 3700 San Martin Drive, Baltimore, MD 21218

`whitmore@stsci.edu`

ABSTRACT

The results from work done to extend the Johnson-Cousins *BVRI* photometric standard sequence to faint levels of $V \sim 21$ mag in compact fields is presented. Such calibration and extension of sequences is necessary to fill a calibration gap, if reliable photometry from modest aperture telescopes in space (e.g. *HST*), or terrestrial telescopes with apertures exceeding 4-m is to done. Sequences like the ones presented here, which cover a large range in brightness as well as color, will allow photometric calibration to be done efficiently, as well as for such work to be less prone to systematic sources of error.

Photometry of stars in approximately 10×10 arc-minute fields around 3 globular clusters, NGC 2419, Pal 4 and Pal 14 are presented from data acquired over several photometric nights. In each field, several stars are measured in B, V, R and I passbands, with standard errors in the mean less than 0.015 mag from random errors, to levels fainter than $V = 21$ mag. It is shown that standard errors in the mean from systematic errors when tying to the Landolt standards on the Johnson-Cousins system are typically well below 0.01 mag in all 4 bands (except for B in NGC 2419, and R in Pal 4), thus justifying the claim that these fields have been correctly calibrated.

The primary context for the work presented here is that parts of these fields were observed repeatedly by the Wide Field Planetary Camera-2 (WFPC2) of the *HST*, and thus these newly calibrated sequences can be used to retro-actively calibrate WFPC2 at over various times of its operating life. In the past, WFPC2 data have had typical photometric zero-point uncertainties of a few hundredths of a magnitude, largely due to a lack of suitable standard stars. The sequences presented here have standard errors at the 0.01 mag level. They agree at the 0.02 mag level with

[1]NOAO is operated by the Association of Universities for Research in Astronomy, Inc. (AURA) under cooperative agreement with the National Science Foundation

[2]Sabbatical Visitor, Indian Institute of Astrophysics, Koramangala, Bangalore 560034, India

[3]present address: Steward Observatory, University of Arizona, 933 North Cherry Avenue, Tucson, AZ 85721

[4]present address: Brandenburg GmbH, Technologiepark 19, 33100 Paderborn, Germany; thim@brandenburg-gmbh.de

other extant calibrations of the targets presented here, except in the I band, where there are color dependent deviations of up to 0.05 mag versus one other photometric sequence. There is no clear resolution of this difference: we present as much verification of the sequences presented here as possible. We argue that a very likely reason for such discrepancies is differences in the filter bandpass.

Subject headings: globular clusters: individual (NGC 2419, Pal 14, Pal 4) — standards

1. Introduction

Accurate absolute photometric measurements of stars and galaxies lie at the very heart of modern astronomy. Modern day measurements, both from space with the *Hubble Space Telescope*, as well as with large aperture telescopes from the ground are routinely being used for projects that require accurate photometry. Examples range from the distance scale based on Cepheid or RR Lyrae variables or supernovae, to metallicity estimates from the position of the red giant branch, to the ages of globular clusters and dwarf galaxies throughout the Galactic halo. With each improvement in accuracy it becomes possible to attack whole new classes of problems.

It is fundamental to precision measurement, that calibrators and science targets be observed in exactly the same way to minimize systematic errors. This has not been possible for most photometric observations using the *Hubble Space Telescope* (*HST*) or large ground-based telescopes, due to the lack of faint standards. For instance, the photometric zeropoints for the Wide Field Planetary Camera 2 (WFPC2) on board *HST* have been monitored using exposures of a few seconds of a $V = 13$ star, while most science observations utilize exposures of typically 500–2000 s, and are interested in much fainter targets (e.g., Cepheids from $V = 24$ to 26).

In 1994, Peter Stetson (see Kelson et al. (1996) and Saha et al. (1996)) first noticed that his WFPC2 photometry from short and long exposures of Palomar 4 and NGC 2419 did not agree at the few percent level. This led to a more complete analysis by Casertano & Mutchler (1998)[1], and by Stetson (1998) which confirmed that the WFPC2 has a non-linearity problem, which is responsible for absolute photometric uncertainty that could be as large as 0.05 mag. Thus far, zero-points reported by various investigators scatter with rms values like 0.02 mag for V and I, and 0.03 to 0.04 mag for B and U (Heyer et al. 2004)[2]. A brief history of attempts to understand and mitigate the anomalous behavior of WFPC2 can be found in Dolphin (2000b).

The obvious solution is to obtain fainter standards for use with *HST* and large ground-based telescopes which have similar problems. In a recent compilation, Stetson (2000) presented $> 15,000$ new photometric standards in $BVRI$. While Stetson's current database[3] does contain samples of standard stars in a number of globular clusters and dwarf galaxies that have been observed over the past decade with WFPC2, it is still highly desirable to increase the number density on the sky, the magnitude limit, and the accuracy of faint standard stars in a number of historically popular science fields for two reasons:

---

[1]see http://www.stsci.edu/instruments/wfpc2/Wfpc2_isr/wfpc2_isr9802

[2]see http://www.stsci.edu/instruments/wfpc2/Wfpc2_isr/wfpc2_isr0401.html

[3]http://cadcwww.dao.nrc.ca/cadcbin/wdb/astrocat/stetson/query

1. Fields suitable for direct observation with *HST* instruments must have sufficient number of stars per square arc-minute to efficiently map the Quantum Efficiency (QE) and Charge Transfer Efficiency (CTE) of all the component CCD chips.
2. Observing established standards *now* with WFPC2 would not tell us anything about the historical calibration of the instrument, since it has been shown (Whitmore et al. 1999) that the calibration of WFPC2 for faint objects has evolved with time. Rather, fields that have been observed with WFPC2 at multiple epochs during its active life should be calibrated as best as possible, so that the time varying behavior of the instrument can be characerized after the fact.

We have therefore used WIYN, with its relatively large aperture and excellent seeing, to extend the Landolt *BVRI* photometric system (Landolt 1992, 1983) to fields that have already been repeatedly observed with *HST* and which are known to have a suitable density and magnitude range of stars to provide an effective retroactive calibration of WFPC2. We are able to obtain consistent photometry to levels of 0.01 mag down to $V \approx 22$ mag in our targets. In this paper we describe our experiment and present the results of this calibration for three such suitable targets: the globular clusters NGC 2419, Pal 4, and Pal 14. We demonstrate that systematic and random errors have been contained sufficiently well so that stars in these fields have been tied to the Landolt system with accuracy ~ 0.01 mag or better.

The results from this project should improve the magnitude gap between photometric standards and science targets. For instance, typical corrections for WFPC2 linearity will be over a dynamic range of ≈ 10 (between photometric standards and extragalactic Cepheids, for instance) rather than the prior range of $\approx$ 100,000. These calibrated fields will also help calibrate new generations of *HST* imagers. Our photometry of NGC 2419 has already been used to verify the calibration for the *Advanced Camera for Surveys (ACS)* (Sirianni et al. 2004) and will provide an efficient way to perform nightly photometric calibrations for imagers on 8-m class telescopes.

In the following sections we describe the observations used, followed by a discussion of the peculiarities of the instrument configurations used, and the methods required to properly process the photometry extraction that successfully removes the instrumental signatures. The photometry for four target fields (NGC 2419, Pal 14, Pal 4 and Pal 3) are presented. The exposure to exposure and night to night consistency is examined in a way that gives separate estimates for systematic and random errors in calibration. Lists of stars in each of the four fields are presented, with the measured magnitudes and error estimates. Comments on how they may be best utilized as standard stars is discussed.

2. Instrumental Setup

Observations were made primarily with the WIYN 3.5-meter telescope at the Kitt Peak National Observatory. The Mini-mosaic (*MIMO*) camera mounted on one of the Nasmyth focii was used. This instrument has two 4096×2048 *SITE* CCD chips, mounted side by side, providing a roughly square field of view (FOV). The 15 micron pixels project to ~ 0.14 arc-seconds on the sky at the $f/6.4$ Nasmyth focus of the telescope. This is an excellent match to the superb image quality delivered by the telescope (median $FWHM = 0.7$ arc-sec), and also provides an FOV of about 9.6 arc-minutes on a side. The imaging performance of this telescope and instrument combination is described in Saha et al. (2000). Each chip is read out by two amplifiers as two 4096×1024 sub-sections.

The instrument was commissioned with rigorous tests which cover linearity, shutter timing performance, charge transfer efficiency, dependence of accumulated counts from a star with background level, and geometrical distortion of the focal plane. The complete retinue of tests is described in the commissioning report, which can be found at the website: *http://www.noao.edu/wiyn*. The charge transfer inefficiency is too small to be noticed, even at the lowest background levels. Shutter timing and/or shading corrections are unnecessary at the 0.2% level, even for exposures as short as 0.3s. No measurable dependence of aperture photometry on position in the field of view (due to geometric distortion, for instance) could be detected. With the exception of a few issues that we mention below, the photometric performance of *MIMO* is better than 0.2%. Throughout the course of the observations reported in this paper, one of us (AS) continually monitored the performance of the instrument, to ensure that it remained satisfactory.

The only real issue of note has been the existence of a cross-talk between amplifiers: if a pixel is saturated in the A/D counter of one amplifier, the corresponding pixel in the sub-section read by each of the other amplifiers can be contaminated. This problem is described in the commissioning report, and methods to mitigate it in the data reduction process are provided in an anonymous ftp area that can be reached from the *Documentation/* tag on the website: *http://www.noao.edu/wiyn* under the sub-heading *Saha's notes on reducing MINIMO data*. Pixels that are affected by cross-talk were masked, and not used in subsequent analysis.

The spectral response of the chips from 380 nm to 850 nm varies smoothly from about 80% in the middle of this range to no worse than 50% at the ends. The response drops sharply from 850 to 950 nm, a spectral region that is within the I-band. The two chips are very similar in their spectral response, although that does not alleviate the need to evaluate color terms separately for each. The filters used ($BVRI$) are the so called 'Harris set', which closely resemble the canonical passbands. The transmission data for the actual filters used are available on the website: *http://www.wiyn.org/filters*, where they are designated *W2, W3, W4*, and *W5* (B, V, R and I respectively). The point to note is that the filters are well bounded, and have no red-leaks even beyond 1000 nm. Photometry of standard stars shows that the overall spectral response (telescope plus filters plus detector) requires only linear color terms with coefficients smaller than 0.05.

There are a few items of note regarding the telescope and instrument combination. Since this is an alt-az telescope, the pupil rotates with respect to the image plane, and any azimuthal asymmetry in pupil illumination will require flat-field correction to be a function of the image rotator position. Dome flats were obtained covering many orientations of the instrument base. The worst peak to valley differences in flat-field images taken in different image rotater positions was 0.5%. The next issue is that the image port was designed to include a field-flattener, which is also an atmospheric dispersion compensator. Unfortunately this optical component produces considerable light loss, especially in the blue, and so is not used. Over the FOV of *MIMO*, the lack of the field flattener can produce small but noticeable changes in the shape of the PSF, especially when the seeing is good. This must be accounted for when doing PSF photometry. It appears that there is also a 'vertical' displacement in the relative mounting of the two chips of perhaps a few microns, which is sufficient to produce a subtle discontinuous change in the PSF shape as one steps from one chip to the other. In total, the PSF changes have been confirmed to be a function only of the radial position in the field (as one would expect if the source of the problem is the absence of the field-flattener) plus a step from one chip to the next. The resulting complications for PSF fitting photometry are adequately handled if aperture corrections are determined as a function of radial position on *MIMO* in addition to a step function going from one chip to the other. The third item of note is the imperfect baffling at the Nasmyth port, which allows some stray scattered light to enter the camera. We have ascertained that this produces only an elevation of the background ('sky') level, and changes over spatial scales that are much much larger than a stellar PSF. As a result there is no contribution due to this on aperture or PSF photometry of stars.

It is thus clear that there are no issues with this setup that would preclude obtaining photometry with systematic errors much smaller than one percent. The telescope-instrument-site combination has delivered R band images with *FWHM* as small as 0.28 arc-sec (without any adaptive optics corrections) which is as well as one can expect to do from the ground. Median delivered image quality is between 0.6 and 0.7 arc-sec. In order to calibrate faint sequences within small fields of view, which is necessary for the retro-active calibration of the *HST* image archives as well as being best suited for work with current 8-m class telescopes, optimal image quality is essential to minimize confusion noise. The *WIYN/MIMO* combination is thus as good as one might expect to have. The only net disadvantage is the slow read-out time of the chips, which limits the efficiency when observing the bright Landolt standards. It would have been better to observe more standard stars than we were able to do, but on pristine photometric nights the self consistency in the photometry of standard stars was seen to be more than satisfactory, leaving us confident about the results.

In addition, our target fields and standard stars were also observed at the WIYN 0.9-m telescope at Kitt Peak, using S2KB, a 2048×2048 SITE chip. Photometry of our target fields with this independent setup (telescope, detector, filters, are all different) is restricted to brighter magnitudes, but is adequate for revealing any systematic errors that arise from either telescope, i.e. concordant photometric results is a strong argument for absence of systematic errors in both setups.

2.1. Observations

Observations of NGC 2419, Pal 4, and Pal 14, all of which are distant globular clusters in our galaxy and have the additional virtue of having being observed repeatedly with the *WFPC2* camera of the *HST*, were made on nights that appeared to be cloudless. Contemporaneous observations of Landolt equatorial standards were also made. Pointings that include several Landolt stars within the FOV of *MIMO* were chosen, taking care also to choose fields that contain standard stars with a wide range of colors. Exposure times on the Landolt fields were set to optimize the signal-to-noise (S/N) ratios for the standard stars. Varied exposure times were used on the target fields, which allows the calibration of stars over a wider range of magnitudes, while also providing a running check on the linearity of the system (i.e. by comparing the measured magnitudes of stars that appear bright on long exposures, but faint on short ones). On some nights images were taken so that different exposures were taken with two camera base orientations set 180^o from one another. This not only puts each star once on each chip, but also reverses the direction of charge transfer with respect to the field, thus providing closure tests not only on chip-to-chip response variations, but also on losses from charge transfer problems. Standard star fields were observed over a wide range of airmasses, so that target field observations were well bracketed. Exposure times for standard stars were always at least one second.

The true test of whether a given night was photometric was decided after reducing the standard star data. On good nights, typical rms residuals in the photometry for standard stars per measurement are ~ 0.01 mag or smaller: errors in the mean are typically ~ 0.003 mag. Only nights which proved to be photometrically pristine were used in the final analysis. A list of these nights, with a summary of the observations made, is given in table 1. The processed images from all the nights are being made available in the STScI archive.

3. Data Processing and Photometry

The raw images were pre-processed to identify and mask out known cosmetic flaws on the detectors, and saturated pixels and pixels affected by the cross-talk described in §2. A program written in IDL by one of us (AS) was used. Bias subtraction for the *MIMO* CCDs is best done on a line by line basis, which was also done as part of the pre-processing. Flat-field corrections were done in *IRAF*, using the external *mscred* package.

3.1. Instrumental magnitudes of the Standard Stars

Aperture photometry of the Landolt stars were done interactively, using an IDL program written by AS. A measuring aperture of 35 pixel radius was used, which corresponds to an aperture of ~ 5 arc-sec radius. This is a large aperture in pixels, as a result of the fine spatial sampling of 0.14 arc-sec per pixel, and so the standard stars need to be well exposed in order to avoid read-noise of the CCD (or shot noise from the sky) from contributing uncertainty. An initial background value was estimated from an annular aperture from 40 to 60 pixels in radius, and the value of the sky was interactively adjusted so that an aperture growth curve is flat near 35 pixel radius. This procedure works well for images with seeing $FWHM \leq 1.8$ arc-sec, which sets the limit for the worst delivered image quality (DIQ) that can be tolerated. There is some low level light in the PSF even beyond the 35 pixel aperture boundary, but as long as the $FWHM \leq 1.8$ arc-sec, it is entirely due to scattered light in the optics (mostly from the tertiary mirror), which does not change from one exposure to the next in the same passband. In other words, the 35 pixel aperture measures the same fraction of light from a star in different exposures with different *FWHM*, as long as the $FWHM \leq 1.8$ arc-sec.

3.2. PSF Photometry and Instrumental Magnitudes of the Target Stars

PSF photometry was run on the target fields with a modified version of the *DoPHOT* program (Schechter, Mateo & Saha 1993). For a given image, the PSF is not allowed to vary with position in the field of view. The private version of *DoPHOT* that was used, produces two sets of aperture magnitudes (for a range of measuring aperture radii) of the brighter relatively uncrowded stars *in isolation* (i.e. with all other objects subtracted after fitting). One set is for background value chosen so that the growth curve is flat near 15 pixel radius, and the second set is for background value chosen so that it is flat near 35 pixels. Let us designate the instrumental aperture mag at 15 pixel radius from the first set by $m(15)$, and that at 35 pixel radius from the second set by $m(35)$. The latter is equivalent to the interactively measured instrumental aperture magnitude described above for the standard stars. The advantage here is that we measure the star in isolation (with all neighbors subtracted), and do so automatically for all the stars (from several to several hundreds, depending on the target field), that have adequate S/N. The disadvantage is that an automatic algorithm for flat growth curve background determination can go awry from specious or unsubtracted features in the image. However, this problem is mitigated by the number statistics from a large number of stars.

If $m(fit)$ is the PSF fitted magnitude, one needs simply to find the dependence of $apcorr_{35} = m(35) - m(fit)$ with detector position (x, y) to account for the subtle spatial variation of the PSF. This is not easy in practice, since there are not always a sufficient number of stars in the FOV for which $m(35)$ can be measured with sufficient S/N. However, since the PSF variation is primarily due to subtle focus changes and lack of perfect field flattening over the field area, only the core of the PSF varies with position on the FOV, while the wings of the PSF remain unchanged. Experimentation shows that the PSF variation due to position in the FOV is essentially all contained within a 15 pixel radius of the center of the stellar profile. Thus the spatial variation of the PSF can be compensated by calculating $apcorr(15) = m(15) - m(fit)$, and mapping it as a function of position in the FOV. There are more stars for which one can obtain $m(15)$ with high enough S/N than there are for $m(35)$.

Using even a few stars for which both $m(15)$ and $m(35)$ are measured with high S/N, we can derive the additive offset required to go from a 15 pixel radius aperture magnitude to a 35 pixel radius aperture mag, since we only need one quantity, which is invariant over the FOV. Thus,

$$offset_{15}^{35} = \langle m(35) - m(15) \rangle \tag{1}$$

Meanwhile, $apcorr_{15} = m(15) - m(fit)$ is fitted as a function of position x and y on the FOV:

$$apcorr_{15} = apcorr_{15}(x, y) \tag{2}$$

With experimentation, we have found that a quadratic polynomial with circular symmetry about the optical axis (center of the FOV) is adequate (a general two dimensional quadratic function has the risk of being unconstrained in the corners if there are not enough stars to define it), plus an additional term to correct the discontinuity going from one chip to the next, as described in §2. The sign and magnitude of the variation depends on the seeing, as well as on the focus setting (i.e. how far, and in which direction, the telescope is from true focus). Once the polynomial description of $apcorr_{15}$ (in terms of x and y), and the value of $offset_{15}^{35}$ are known, the PSF fitted magnitude $m(fit)$ for any star anywhere in the FOV can be put on the system of 35 pixel apertures, which we designate as the instrumental magnitude m^{instr}.

$$m^{instr} = m(fit) + apcorr_{15} + offset_{15}^{35} \tag{3}$$

This brings the target star instrumental magnitudes to a common footing with the instrumental magnitudes of the standard stars.

Software necessary to determine and apply the aperture corrections as above were custom written in the *IDL* language.

3.3. Nightly Photometric Solutions

To account for extinction due to airmass, and to allow for color-terms and zero-point adjustment in order to transform to m^{true}, the true magnitude on the Landolt system, we can write a system of equations of the kind:

$$m_i^{true} = m_i^{instr} \ + \ C_i \ + \ \alpha_i X \ + \ \beta_{i,j}(m_i^{instr} - m_j^{instr}) \tag{4}$$

where i and j are indices for the various passbands ($i \neq j$), and X is the airmass at which the object is observed. The standard star observations are used to solve for the coefficients C, α, and β.[4] C_i and $\beta_{i,j}$ are in general different for each chip, and were solved for separately for each chip. Higher order color terms might be required, but with our setup, as described in §2, were found to be unnecessary. Also, no cross-terms of airmass with color were used. Such terms are sometimes necessary, since selective absorption by

[4] Note that in this formulation, one can additionally use the instrumental mags of any stars in the object fields that were observed more than once, and at significantly different air-masses to assist in the determination of α.

the atmosphere can alter the effective central wavelength for a passband, i.e. a star (particularly if it is of extreme color) observed at high airmass is seen with a different effective wavelength than if observed at low airmass. All of our target observations were made at airmass less than 1.7, and observations of Landolt stars were done up to airmasses of 2.0. The use of such cross-terms did not improve the nightly solutions: typical star by star rms scatter in the standard star solutions was ~ 0.015 mag or smaller, with no discernible trends in the residuals with the product of airmass and color.

In the following set of equations, the solution for the night of 2003 Feb 9 (UT) for one of the CCD chips (using 22 measurements in each passband) is shown, illustrating typical values for the coefficients. The lower case symbols b, v, r, i denote instrumental magnitudes in units of $-2.5\log(ADU s^{-1}) + 30.00$, whereas B, V, R, I denote magnitudes on the Landolt system. To derive the coefficients in the equations below, Landolt's published photometry (Landolt 1992) was used to derive the constants and coefficients in the equations below (and for each night of observations in this program). The errors in the mean are shown in parentheses. Not all color combinations are displayed.[5]

$$B = b - 4.120 - 0.262X + 0.013(b - r) \quad (\pm 0.003) \tag{5}$$

$$V = v - 4.095 - 0.146X - 0.010(v - i) \quad (\pm 0.002) \tag{6}$$

$$R = r - 3.978 - 0.103X - 0.012(b - r) \quad (\pm 0.002) \tag{7}$$

$$I = i - 4.714 - 0.065X - 0.024(v - i) \quad (\pm 0.003) \tag{8}$$

Over the course of the several nights of observations, we noted quite significant changes in the extinction coefficients. The pattern in the night to night differences is that a roughly equal value is added to the extinction coefficients of *all* passbands. For instance, on the night of 2003 June 4 (UT), the extinction coefficients as above for B, V, R, I were $0.350, 0.221, 0.169$, and 0.124 respectively. The extinction in all bands is uniformly increased by $0.07 \pm .02$ relative to 2003 Feb 9. It is possible that dust, water-vapor and aerosol play a role in this, and it is wise, therefore, to restrict observations to relatively low airmass, since the scale height of these contaminants may be different from other atmospheric sources of scattering.

Once the photometry solution for a night is obtained, as above, the instrumental magnitudes m^{instr} of each star on a set of target observations (obtained from aperture correction of the DoPHOT PSF fitting magnitudes according to the procedure described in §4.2) in at least 2 passbands can be converted to the Landolt system. DoPHOT reports good estimates of the (random) measurement errors from the photon statistics, read-noise characteristics and fit residuals for each star. These were propagated along with the calibrated magnitudes for the next steps in analysis.

[5]While it is common practice to express the night constants and color coefficients with the true magnitudes and colors as the independent variables, and instrumental magnitudes as the dependent terms, we have chosen to do the opposite, as in the above, for ease of computing the true magnitudes for the target stars, and because this formulation can be used to estimate atmospheric extinction by comparing the instrumental magnitudes of stars in the target fields when they are observed at different airmasses. This enables the inclusion of the lower end of airmass values not available from Landolt's equatorial standard stars when observing from mid-latitudes. In the absence of non-linear color terms, the two forms are algebraically identical. Further, the errors in measurement, i.e. of the instrumental magnitudes, are insignificant, and the direction of the regression makes no difference. Nevertheless, we have verified this assertion by computing the regression the other way, and find there is no difference at the 0.001 mag level in how these equations are specified and calculated.

4. Analysis of Errors

The procedures described above yield magnitudes that are nominally calibrated on the Landolt system for each set of exposures (in the various passbands). We see that the nightly photometric solutions themselves carry errors that are smaller than one percent, which gives us the expectation that the systematic errors are also adequately small. However, it is necessary to see how well the systematic errors are indeed contained, by comparing the results obtained across several nights of observations, particularly since extinction coefficients have been seen to vary significantly from night to night. We have data from several nights for each of our targets, including some observations made with an independent setup (0.9m telescope and a different physical set of filters). We also sometimes have several determinations for magnitudes from different exposure sets on the same night. However, there is no external estimate of how well the aperture correction procedures worked, and systematic errors from that are not separately accounted for. In the final analysis, the repeatability of the magnitudes from all of these different measurements is the true test of how well systematic errors have been contained. Also the final reported magnitudes for each star should be a mean that is adjusted and weighted appropriately from all the photometric epochs at which observations were made.

We describe here the adopted procedure, using as an example, the case of V magnitudes for the NGC 2419 field. There are 14 epochs over 7 nights. After cross-matching the stars from all the epochs, an initial weighted mean value $\overline{V_k}$ for the k^{th} star was calculated using the inverse of the variance of individual magnitude errors reported by DoPHOT as weights. The stars that are common to all 14 epochs were then identified: in the case at hand, 74 such stars were found. If V_j^i denotes the i^{th} measurement for the j^{th} such common star, and e_j^i is the corresponding measurement error estimate reported by DoPHOT, the quantity

$$\Delta V^i = \frac{\sum_j w_j^i (V_j^i - \overline{V_j})}{\sum_j w_j^i} \tag{9}$$

where

$$w_j^i = \frac{1}{(e_j^i)^2} \tag{10}$$

is the best estimate of the systematic zero-point offset for magnitudes measured in the i^{th} epoch, relative to the mean of all epochs. More specifically, the error in the mean from the rms scatter of the ΔV^i's is a measure of the systematic error in the values of $\overline{V_k}$, and we denote it by ϵ_{sys}.[6]

$$(\epsilon_{sys})^2 = \frac{\sum_i (\Delta V^i)^2}{N(N-1)} \tag{11}$$

ΔV^i was then subtracted from the magnitude of every star as measured in the i^{th} epoch (for each of the epochs), i.e.:

$$\mathcal{V}_j^i = V_j^i - \Delta V^i \tag{12}$$

from which we recompute the final weighted mean magnitude of the k^{th} star as:

$$\overline{\mathcal{V}}_k = \frac{\sum_i w_k^i \mathcal{V}_k^i}{\sum_i w_k^i} \tag{13}$$

where the w's are the same as in equation 10. We also obtain the reduced chi-square for each star as:

$$\chi^2_{\nu,k} = \frac{\sum_i w_k^i ((\mathcal{V}_k^i - \overline{\mathcal{V}}_k)^2}{\nu - 1} \tag{14}$$

[6] We adopt the convention of reporting rms scatter with σ, 'errors in the mean' with ϵ, and measurement uncertainties with e.

where ν is the number of available observations for star k.

The weighted random error in the mean for the k^{th} star, ϵ_k, is then given by:

$$(\epsilon_k)^2 = C.\frac{1.}{\sum_i w_k^i} \tag{15}$$

where C is set to unity if $\chi^2_{\nu,k} \leq 1$, and $C = \chi^2_{\nu,k}$ otherwise. This formalism deals optimally with the fact that the various exposures are of different depth, and thus a given star in general has very different signal-to-noise from one exposure to the next. Further, ϵ_k's are reliable estimates of the uncertainty in the individual $\overline{\mathcal{V}}_k$'s, irrespective of whether the DoPHOT reported error estimates e_k^i's are correct. In the case of a variable object, the value of ϵ is the uncertainty in the mean brightness.

In reporting our results, we will keep the systematic errors ϵ_{sys} separate from the random/variability uncertainties ϵ. The latter are reported star by star, whereas the former are the same for all stars for any target field and filter. Table 2 gives the values of ϵ_{sys} for each target and passband. Random errors will be reported in later sections regarding the individual targets.

5. Results

For each of 3 targets for which we have sufficient data (namely NGC 2419, Pal 14 and Pal 4) we present here the following data products:

1. A deep reference image of the target field is shown both in print, as well as a *FITS* file in the electronic version of this paper. The *FITS* files are appointed with a 'world coordinate system') (WCS) calibrated to J2000 coordinates on the sky. All positions of individual stars for these target fields are referred to positions (X and Y in pixels) on the corresponding image and/or their J2000 positions.
2. For each target, a table of the stars for which there are at least 3 measurements in each of the four passbands B, V, R, and I, and where ϵ_k (as in equation 15) is less than 0.015 mag in each passband. These are the best stars to be used as standards. This table is given both in printed form, and also in the electronic version of this paper. This table is numbered for easy reference to individual stars. In using these values, one should be mindful also of the additional systematic errors tabulated for each passband and target field in Table 2.
3. A table of all available objects with measured magnitudes in at least V and I is presented as an electronic table.
4. A table identifying objects flagged as variable stars, where the selection criterion is that the star have $\chi^2_{\nu,k}$ (as in equation 14) higher than 20 in all of B, V, R, and I, with at least 6 measurements in each passband. Also, the rms scatter ϵ_k) is required to be greater than 0.05 mag in V, R, and I, and greater than 0.1 mag in B. This table is also numbered for easy reference to individual stars.

   In the following sub-sections, we identify and comment on these data products target by target.

5.1. NGC 2419

The reference field for NGC 2419 is shown in Fig. 1. The *FITS* image supplied in the electronic version reveals much more detail, depth, and dynamic range, and shows individual stars much further into the cluster core than the printed version.

Table 3 gives the magnitudes and uncertainties (from random errors) in four passbands for all the stars in the field (designated 'best' stars) for which the random uncertainty in the mean is less than 0.015 mag in all the passbands. The corresponding data for all stars for which V and I magnitudes are available are given in Table 4. Finally, the stars which are most likely variables (at least 6 available measurements in each of the four passbands, and with $\chi^2_\nu > 20$ in each passband) are listed in Table 5.

A color-magnitude diagram (CMD) in V and I for stars in the NGC 2419 field (utilizing all the objects listed in Table 4) is shown in Fig. 2. The 'best' stars are marked in bold, and the variables are also identified. In addition to cluster stars, there are clearly several foreground stars, including a few 'best' stars with colors redder than $V - I \sim 1.5$ mag. There are also 'best' stars among the blue horizontal branch stars in the cluster to colors as blue as $V - I \sim 0.0$. While the 'best' stars go no fainter than $I \sim 20.5$ mag, taking ensemble averages for the large number of fainter stars still permits one to directly calibrate photometry with uncertainties from random errors contained below 0.01 mag.

The systematic error estimates (given in Table 2) in V, R and I for NGC 2419 are below 0.006 mag rms. This includes 3 nights of observations with the independent setup at the WIYN 0.9-m telescope, and these small values thus strengthen our confidence that the magnitudes given in the tables in this paper are truly on the Landolt system. The systematic error estimates must be added in quadrature to the individual rms estimates for random errors. The larger systematic error of ~ 0.02 mag in B is disappointing. The seeing was often poorer in B, and bright uncontaminated stars with sufficient S/N that are common to exposures that range in depth by a factor of 100, and observed in common on two telescopes of very different aperture, were few. This has resulted in poor S/N for anchoring the B photometry to the Landolt scale.

A total of 92 objects were deemed to be variables. Fig. 2 shows that the majority of these are in the location of the RR Lyrae region in the CMD, with a few that are brighter than the horizontal branch by ~ 0.5 mag. A few lie along a suggestive track that leads up along where the AGB should be, with a few more yet up among the brighter red giants. There is a solitary variable among where one find SX Phe or W UMa stars. No attempt was made to cross identify with known variables.

5.2. Pal 4

The reference field for Pal 4 is shown in Fig. 3. As before, the *FITS* image supplied in the electronic version reveals much more detail, depth, and dynamic range.

Table 6 gives the magnitudes and uncertainties from random sources for the 'best' stars in Pal 4, i.e. those for which the uncertainties are less than 0.015 mag in each of the four passbands. Table 7 presents the magnitudes for all stars in the field for which at least V and I magnitudes are available. The likely variables are identified in Table 8. The systematic uncertainties for each passband listed in Table 2 for Pal 4 must be added (in quadrature) in all cases to get the true uncertainties with respect to the Landolt system.

The CMD for the target field is given in Fig 4. It is much sparser than for NGC 2419: even the numbers of foreground stars is fewer for this field, which is less than 20 degrees from the North Galactic Pole. Also, the data from the 0.9m telescope did not have enough stars with high enough S/N at levels faint enough for a good overlap with the 3.5m data. As a result, there are no calibrated stars in this field that are brighter than ~ 16 mag. There is only one 'best' quality star bluer than $V - I = 0.5$ and only two that are redder than $V - I = 1.5$. However, there are several stars in the giant branch and red clump which can be used as photometric standards to $I \sim 20$ mag, and fainter calibration can be had from the ensemble average of stars to $I \sim 22$ mag.

Three variable stars are identified: from their location on the CMD, one is likely an RR Lyrae star, another an SX Phoenicis star, and the brightest object is either an AGB variable (if it is a cluster member—it does lie in the line of sight of the cluster) or a field variable of as yet unknown type.

5.3. Pal 14

The reference field for Pal 14 is shown in Fig. 5. Once again, the *FITS* image supplied in the electronic version reveals much more detail, depth, and dynamic range.

Table 9 presents the photometry for the 'best' stars, which have uncertainties less than 0.015 mag in each passband. Table 10 gives the available magnitudes for all stars for which V and I magnitudes could be measured, and Table 11 lists the likely variables. As before, systematic errors with respect to the Landolt system as listed in Table 2 must be added in quadrature to all listed uncertainties.

The CMD is given in Fig. 6. The field surrounding the cluster is more populous than for Pal 4, and the 'best' stars span the range of colors better. Unfortunately again, as in the case of Pal 4, the 0.9m observations do not produce enough stars with sufficient overlap to allow the calibration of standard stars brighter than $I \sim 15.5$ mag. At the faint end, the sub-giant branch is well defined by numerous stars, and (as in the case for NGC 2419 and Pal 4) even though they do not individually qualify in the 'best' category, ensemble averages of several of these stars can carry the calibration well beyond $I \sim 21$ mag.

Seven variable stars are identified, some of which are likely to be foreground field stars.

6. Comparison with other sequences

6.1. Comparison with Stetson's sequence in NGC 2419

Stetson (2000) has presented a photometric sequence in NGC 2419 that spans a similar field size and brightness range. A comparison with this independent calibration is instructive. For NGC 2419, there is also an older unpublished sequence in *UBVRI* by L. Davis in the KPNO consortium fields Christian et al. (1985). Comparison with that is also of interest.

The comparison in all four passbands with the Stetson (2000) sequence for NGC 2419 is shown in Fig. 7: the small dots show the difference in magnitudes star by star versus the mean magnitude of the objects as reported in this paper. The annotations in the figure give the net differences (unweighted means for all objects, and the errors in the mean) in the sense of Stetson minus this work. The mean differences are larger than can be accounted by the sum (in quadrature) of the error in the mean and the systematic error estimates in Table 2 (except in the B band where the systematic error estimate is atypically high). Thus, they cannot be ignored, and must be discussed. In V and R bands, the Stetson sequence is on average brighter by ~ 0.015 mag, but in the I band it brighter by almost 0.04 mag. In comparison, the 0.9m and 3.5m observations reported in this paper when taken separately, differ (in the sense of 0.9m minus 3.5m) by $-0.005 \pm .006$, $+0.020 \pm 0.004$, and $+.024 \pm 0.010$ mag in V, R, and I respectively, which are smaller than the difference between the Stetson sequence and this work. Note also, that there is no obvious brightness dependence in the difference between the Stetson scale and the work in this paper: non-linearity is not the culprit.

The large dots in Fig. 7 show the difference between the L. Davis unpublished sequence (Christian et al. 1985) and the present work. On average the Davis sequence appears to lie midway between the Stetson and current work values. We should note that formally the Davis sequence is tied to Landolt (1983), not Landolt (1992), though differences due to this are not expected to be significant beyond a few milli-mags.

An important characteristic of the difference between the Stetson (2000) sequence (especially in I) and the work in this paper is revealed in Fig. 8, where the differences between the two sequences is shown star by star as a function of color $(V-I)$. Note how both in V and especially in I, the differences are a function of color. Specifically at $V-I\sim 0.2$ there is no difference on average in either V or I, whereas at $V-I\sim 1.2$, The Stetson sequence is brighter in I by ~ 0.05 mag, and in V by ~ 0.02 mag. There are not enough data in R to see if a color dependence exists, and in B the differences are within the systematic error estimate (which is regrettably large).

6.2. Comparison with other photometry in NGC 2419

The equivalent comparison of magnitude difference as a function of color against the Davis standards in NGC 2419 is shown in Fig. 9. The annotations show the net differences and level of significance similar to those given for the Stetson sequence in Fig 7. The color dependent trends seen against the Stetson sequence are not present here.

One of us (AED) has obtained photometry in V and I of stars with WFPC2 in a field south of NGC 2419, which overlaps in area with our ground based field here. The photometry were obtained using the *HSTPHOT* program described in Dolphin (2000a), using a procedure that corrects for the CTE anomalies described in Dolphin (2000b). Independent photometry zero-points and color-terms derived from photometry in ω Cen by Walker (1994) were used. The comparison of these magnitudes with those in this paper is shown in Fig 10. The data span a smaller range in color than in Fig 8, and the blue stars show significant scatter (because the blue horizontal branch stars are faint on these relatively shallow WFPC2 exposures). Despite these shortcomings, the two sets of photometry show better agreement than the comparison with the Stetson NGC 2419 sequence. Specifically, if the color trend seen against the Stetson sequence were present, it would be revealed by these data, but no such comparably strong trend is seen.

We have private communication from Sirianni that the synthetic photometry calibration of the ACS on *HST* is in close agreement with the results presented in this paper.

The various comparisons detailed above are summarized in Table 12.

We see that there is still a lack of concordance between different independent investigations regarding the calibration of the I band at the few percent level. Systematic differences of a few hundredths of a magnitude, especially in the I band, are apparently not uncommon. Many I filters in use at various observatories allow out of band transmission in the infrared. While detectors like the S20 extended response photomultipliers were blind at near infra-red wavelengths, CCDs can have substantial response at 1.0 to 1.2 μ. At these wavelengths, the spectra of cool stars have pronounced bands, and simple color transformations (even with higher order terms) may not adequately account for out of band transmission, since color 'excesses' become discontinuous. In addition, as we show in the Appendix, the form of the standard color equations used in practice is a poor match to physical reality unless the color response mis-match between the employed and the original measuring systems are small, i.e. correctable by a term that depends only on the first moment in frequency/wavelength of the spectral energy distribution.

Whether the above is in fact the reason for the difference between the Stetson sequence and the one derived here, is not established beyond doubt. In practice we see much smaller deviations because of bandpass mis-match, which arises out of the fact that the spectral energy distribution of stars vary only in highly constrained ways. Synthetic simulations with a possible extreme variant of the I band (see §7.3) shows that at most half of the discrepancy seen can be explained this way. The idea of using the 0.9m data as an arbiter, while sound in principle, is only marginally useful because of the lack of S/N at faint magnitudes. While the comparison through the HSTPHOT photometry of WFPC2 observations in the NGC 2419 field against the system of Walker (1994) is consistent with the sequence derived in this paper, it is at least a little bit circular, given that we are trying to set up a sequence to retro-actively calibrate WFPC2. The agreement of the NGC 2419 photometry presented here against the ACS photometry by Sirianni et al. (2004) (priv. comm.) as discussed above, is an endorsement of the sequence derived here. However the agreement may be viewed with some reserve since the ACS Photometry results are from a synthetic calibration.

7. Verification of our own photometry

As a sanity check to test that there is not some hidden error in our reduction, one of us (AED) has independently reduced observations on the night of 2003 Feb 09. All measurements were made independently, including PSF fitting, which was done using a modified version of HSTPHOT (Dolphin 2000a) and solving for extinction and color terms. The results from identical data frames were compared. The comparison in V and I bands are shown in Fig 11. The ensemble mean differences in photometry, derived from stars that are reported individually (by the respective reduction procedures) to have measurement errors less than 0.05 mag, is only a few milli-mags for both passbands. No color dependent trends are visible.

7.1. Testing the Assumptions in the Calibration Procedure

Our discrepancy with Stetson's sequence begs further introspection. It can be asked whether inclusion of a quadratic term in the color equation for the I band color-equation would bring the results from our data into better agreement with Stetson sequence. In other words, have we neglected a color term that needed to be included? It can be alleged, that our sparse observations of Landolt standards (due to instrument read-out time limitations) does not permit a quadratic term to be well constrained from a single night's worth of data. To refute this argument, we demonstrate below that while our observations are much less extensive than Stetson's, it is adequate for asserting that the discrepancy seen is a real disagreement, and not an artifact of inadequate data.

The first argument is that ϵ_{sys} in Table 2 value for I in NGC 2419 is .0058 mag. This value comes from 14 measurements on 7 different nights on 2 different set-ups. The extinction coefficients and color equations were derived independently for each night using only observations from the same night. Despite noting quite large changes in extinction from one night to another, and observing on two different set-ups, the value of ϵ_{sys} is satisfactorily small. Since this is an 'external' estimate of the systematic error, it is very unlikely that systematic errors in calibration have been made at the 0.04 mag level.

The second argument involves a combined analysis of standard star observations made on 4 different nights when V and I observations of NGC 2419 were made with the WIYN 3.5-m telescope set-up. In this check, we assume for simplicity that the color equations are the same for both CCD chips (their spectral responses are very close), and that they do not change from one night to another. Allowing for a different zero-point for each night, we wish to derive the color coefficients. We use the extinction coefficients for I as originally derived: recall that our original procedure corrects the instrumental magnitudes, and the atmospheric coefficients are derived not just from the standards, but from all high S/N stars (including those in our target fields) that were observed at different airmasses. This correction reduces the instrumental magnitudes to zero air-mass. An error as large as 0.04 in the extinction coefficient for I will produce relative errors between standard stars observed at the extremes of airmass range (1.15 to 1.95) of 0.03 mag. The rms scatter (per star) in determining the extinctions is seen to be at least a factor of 3 smaller, and errors in the mean from all the measured standards are thus a few milli-mags at most. Thus extinction determination cannot itself be a significant source of systematic error. Let i denote the instrumental magnitudes corrected to zero air-mass. We then write the usual expression:

$$i - I = L_0 + L_1(V - I) \tag{16}$$

which is the linear form of the color equation, and where V and I are Landolt's values for the standard stars. According to the discussion above, L_0 can change from night to night, but L_1 is assumed the same for all observations of standards. Similarly, one can write the quadratic form as:

$$i - I = Q_0 + Q_1(V - I) + Q_2(V - I)^2 \tag{17}$$

We can solve these equations for the standard stars, allowing only one value each for L_1 and for Q_1 and Q_2, but allowing L_0 and Q_0 to differ from night to night. The residuals for the fit to equation 16are shown in the top panel of Fig. 12, with data points from the four different nights coded in four different colors. The middle panel shows the residuals for the same observations for the fit to equation 17. In each of the above panels, the dashed lines shows the locus about which the points would lie had we fitted the instrumental mags of stars in NGC 2419 to the Stetson sequence. These figures demonstrate that the difference seen with respect to the Stetson sequence is real, and not the figment of inadequate data. Nor is the difference attributable to using a linear color term when a higher order term is demanded. The continuous black lines in the third panel of Fig. 12 show the fits to equations 16 and 17 (with respective L_0's and Q_0's subtracted). The dashed shows the equivalent quadratic fit, if instead of fitting Landolt standards, the instrumental mags of stars in NGC 2419 are fitted to the Stetson sequence. The red line shows the difference purchased by fitting a quadratic versus a linear color equation to the Landolt stars alone: note that in the range $-0.1 < V - I < 2.0$, the difference is always smaller than 0.01 mag. Contrast this with the green curve, which shows the difference between fitting a quadratic color equation to the Stetson sequence in NGC 2419 versus a linear fit to Landolt standards. Since the fit to Stetson's sequence produces a discrepancy with the Landolt standards at a level of significance that is clear from the 3 panels of Fig. 12, the discrepancy cannot be an artifact of inadequate observations of standards. It is a real discrepancy, clearly evident in the data, even though it lacks a clear physical explanation (except possibly the discussion in the Appendix).

7.2. Is the subset of Landolt standards actually used skewed from the Overall Landolt System?

Another possibility is that the subset of Landolt standard stars used in our calibration is somehow skewed from the parent set of all Landolt standards. In particular, Landolt's photo-electric measurements were made with a 14 arc-sec aperture, whereas here we used 10 arc-sec (diameter). In the present work we preferred those fields where a number of standard stars are present within the instrument's field of view, so that we could maximize the number of standards observed while keeping the number of exposures (and accompanying large overhead in read-out time) manageably small. Thus we preferred those fields where the chance of having another star within a 14 arc-sec aperture is increased relative to fields with relatively fewer available stars. We made all our standard star measurements interactively, and any gross cases of such object confusion were immediately apparent, and the offending object was not used further. However, no explicit procedure to guard against such an occurrence was used in a systematic manner, and it is possible, though unlikely, that systematic differences between Landolt's measurements and ours have been introduced in this manner. It is further unlikely that such an error has occurred only in one of the four bands, and even more so that the difference is correlated with color.

Fig. 13 shows the results of the photometry of Landolt stars. Each point on the ordinate for each pass band is the residual (observed minus calculated, after fitting the photometric solution for the relevant night) for each standard star measurement (one point per star per observation). The filled circles are for observations on nights that have contributed to the calibration of NGC 2419. This is like the first panel of Fig. 12, but for each of the four bands, and using the color terms evaluated independently for each night. No perceptible systematic difference is seen for the observations relevant to NGC 2419 when compared to the rest.

In Fig. 14, the same data are shown, but only for the average residuals of objects that have been observed three or more times. The error bars show the standard errors. Note that some objects have standard errors that are much smaller than their average residual—possibly indicating that there are small but significant differences between the Landolt measurements of these stars and ours. A possible source of such differences might be the difference in aperture sizes used. The mean deviations are less than ~ 0.02 mag.

There is no systematic trend with color (or brightness—not shown), and the differences, if real, are random from star to star. This is a possible indication of the inherent uncertainties in using these standard stars. The worst scatter is in the I band, but even there, any systematic color dependent trend exceeding $\sim .01$ mag is ruled out. The same data, and also the mean residuals for stars measured less than thrice, are presented in Table 13. This table also identifies exactly which Landolt stars were used.

7.3. Can differences in the I bandpass explain the differences in I band photometry versus Stetson's magnitudes?

One can ask if red giants in NGC 2419, which are all very metal poor ($[Fe/H] \sim -2$), produce systematically different response through different I filters, as compared to the Landolt standards at the same $V-I$ color. This can be studied by synthetic photometry. The standard I passband is described numerically by Bessell (1990), in his Table 2. The actual filter and CCD response combination used for data in this paper from $MIMO$ is a close match to this standard passband: we will refer to it as the WIYN I passband. There is a wide range of I filters being vended by commercial suppliers, from filters that are really on the *Johnson* rather than Landolt (based on Cousins) system, to ones touted as "Bessel" I filters that have quite large red extensions. We have taken one such example as a 'Bad I' filter. From simulations we find that the WIYN I filter deviates from the standard filter by ~ 0.009 mag (fainter) for giants with $V-I \sim 1.5$ mag and $[Fe/H] = -2.0$ (as compared with giants of the same color with solar metallicity). The 'Bad' filter shows a deviation of ~ 0.025 mag in the same sense with respect to the standard passband. The sense of the differences is correct for explaining the discrepancy between our photometry and that of Stetson, but the magnitude of the predicted difference is only 0.015, whereas the observed difference is nearly 3 times larger. While we have no detailed information on the filter(s) used by Stetson, it is very unlikely that it was as bad a mis-match as the example used here for our case study. Thus, this too is a very unlikely source of the discrepancy.

8. Concluding Remarks

Despite the caveats raised in §6, this work is a significant contribution towards reconciling the large archive of *HST* imaging in broadband filters with the *BVRI* photometric system as realized via the Landolt standards (Landolt 1992). The targets presented here have been observed repeatedly with *WFPC2*, and comparing the instrumental photometry from images taken at different times will not only add to what we know of the temporal variation in CTE of that instrument, but will allow the unambiguous calibration of the photometric characteristics over the lifetime of the instrument. In other papers, we will present the confrontation of *WFPC2* photometry with data obtained at various times and with different reduction procedures.

This paper, and our understanding, has benefitted greatly from work done on these data by Peter Stetson, and from our subsequent discussions with him. We are indebted to Marco Sirianni and collaborators for sharing their results of the ACS calibration with us before publication. Support for this work was provided by NASA through grant HST-AR-09216.01-A from Space Telescope Science Institute, which is operated by the Association of Universities for Research in Astronomy, Inc., under NASA contract NAS 5-26555. The WIYN Observatory is a joint facility of the University of Wisconsin-Madison, Indiana University, Yale University, and the National Optical Astronomy Observatory.

A. The Consequence of Spectral Response Mis-match between Measuring Setups

Here we examine from first principles, the impact and consequences arising from the usually encountered situation where the measuring system does not have exactly the same wavelength dependence as the system that defined the standards (in this case the latter refers to Landolt's original setup). We show that the form of the color equation that is usually used does not follow the physical demands, except in the case when the difference in frequency/wavelength response is small.

Consider a source with an energy distribution f_ν. Let the overall (telescope, filter and instrument response) response of the original (or standard) system be denoted by α_ν^S, and that of the measuring system being used by α_ν. The response of the original system is then

$$S^S = \int \alpha_\nu^S f_\nu \mathrm{d}\nu \tag{A1}$$

and that of the 'current' measuring system is

$$S = \int \alpha_\nu f_\nu \mathrm{d}\nu \tag{A2}$$

We can write

$$\alpha_\nu = C_\nu \alpha_\nu^S \tag{A3}$$

where C_ν tracks the changes in response of the measuring system with respect to the original standard system. If ν_0 is the central frequency of the passband under consideration, we can expand C_ν as a Taylor series about ν_0:

$$C_\nu = C_0 + C_1(\nu - \nu_0) + C_2(\nu - \nu_0)^2 + \ldots \tag{A4}$$

And so we can write:

$$S = C_0 \int \alpha_\nu^S f_\nu \mathrm{d}\nu + C_1 \int \alpha_\nu^S (\nu - \nu_0) f_\nu \mathrm{d}\nu + C_2 \int \alpha_\nu^S (\nu - \nu_0)^2 f_\nu \mathrm{d}\nu + \ldots \tag{A5}$$

In magnitudes, the left hand side is the instrumental magnitude on the 'current' measuring setup, and the first term on right hand side (RHS) is a constant (zero-point adjustment) plus the true standard magnitude. In the absence of any color dependent terms (i.e. further terms on the RHS) we would just get (by taking the logarithm):

$$m_{observed} = \text{Offset} + m_{standard} \tag{A6}$$

The $n - th$ moment of the spectral energy distribution about the central wavelength of the passband is denoted by μ^n, and given by:

$$\mu^n = \frac{\int \alpha_\nu^S (\nu - \nu_0)^n f_\nu \mathrm{d}\nu}{\int \alpha_\nu^S f_\nu \mathrm{d}\nu} \tag{A7}$$

Equation (A5) can thus be re-written as:

$$S = C_0 \left(\int \alpha_\nu^S f_\nu \mathrm{d}\nu \right) \quad (1 + c_1\mu_1 + c_2\mu_2 + \ldots) \tag{A8}$$

where $c_r = C_r/C_0$.

Contrast the above equation, which is derived from physical principles, to the *ad hoc* equation that is used in practice to describe the response variation, which is:

$$m_{observed} = \text{Offset} + m_{standard} + B(color) + C(color)^2 + \ldots \tag{A9}$$

The form of equation (A9) can be strictly derived from (A8) only in the case where when $c_1\mu_1 < 1$ and $c_r\mu_r = 0$ for $r \geq 2$.[7] One must also assert that *color* in eqn (A9) is proportional to μ_1 (which behaves like a change in the effective wavelength for the passband). The failure of either of these conditions will make eqn (A9) inadequate (to varying degrees, depending on the specifics of the situation).

It should be evident that the *ad hoc* form in common use (eqn A9) is thus applicable only if the two measuring systems are a very near match. If the conditions mentioned above are not satisfied, fitting eqn (A9) is tantamount to fitting the wrong function. Depending on the severity of the mis-match, this could result in systematic color-dependent errors in the photometry. If the entire range of colors is evenly sampled, one should notice an increase in the systematic scatter when solving for the night constants using the standard stars, as the severity of the mis-match increases. This scatter is systemic in nature, and will not be mitigated by observing a large number of standards. If the range of colors sampled by the standards is patchy, the fitted solution could 'run away' in the unsampled regions of color.

In the presence of out of band leaks, the mis-match could be acute, since one expects the color moments (of progressively higher order) to be large as a consequence of the large moment 'arms'. In addition, in such situations color will not remain proportional to the first moment of the energy distribution. In practice, however, for stellar work in particular, the progression of the spectral energy distribution (SED) with changing physical parameters in the photosphere is very constrained. This is manifest in the way that

---

[7]The McLaurin series expansion of $\ln(1 + x)$ can then be applied to get the log of $(1 + c_1\mu_1)$.

two color diagrams of stars define very constrained loci. For this reason, the standard form of the color equations in fact work "better than they should." However trouble should be anticipated for non-stellar sources, and in regions of the spectrum where stellar SEDs have large dispersion, e.g. at the Balmer Jump.

The above is the mathematical persuasion that filters being used in combination with CCDs to reproduce a photometric system established with photo-cathodes be very carefully selected, and that they be free of red leaks. We believe that the set used in the study presented in this study is as close an approximation as practical. Further, the V and I filters used here are a very good match to the $F555W$ and $F814W$ filters used with the WFPC2 on *HST*.

This analysis strongly urges use of bandpasses that be reliably realized by filters that are well bounded so that they work with pan-chromatic detectors. This is in contrast to $BVRI$, where some of the bands relied on the detector or atmosphere for blocking, since such bandpasses are often hard, if not impossible, to reproduce when using detectors with very different response, or when they are used in space above the atmosphere. Model spectral energy distributions, such as for isochrones and for composite colors of galaxies can be synthesized for any passband. However, the rich empirical legacy of $BVRI$ observations—for instance of Period-Luminosity relations for Cepheids—will not be so easily transferred to a new photometric system, and so the problem of designing physical filters and calibrating photometry in this 'arcane' system will continue to be of importance.

REFERENCES

Bessell, M. S. 1990, PASP, 102, 1181

Casertano, S. & Mutchler, M. 1998, WFPC2 Instrument Sci. Rep. 98-02 (Baltimore: STScI)

Christian, C., Adams, M., Barnes, J., Hayes, D., Mould, J. & Siegel, M. 1985, PASP, 97, 363

Dolphin, A. E. 2000, PASP, 112, 1383

Dolphin, A. E. 2000, PASP, 112, 1397

Heyer, I., Richardson, M., Whitmore, B., & Lubin, L. 2004, WFPC2 Instrument Sci. Rep. 2004-01 (Baltimore: STScI)

Kelson, D. et al. 1996, ApJ, 463, 26

Landolt, A. 1983, AJ, 88, 439

Landolt, A, 1992, AJ, 104, 340

Saha, A. et al. 1996, ApJ, 466, 55

Saha, A., Armandroff, T., Sawyer, D. & Corson, C. 2000, SPIE 4008, 447

Schechter, P. L., Mateo, M. & Saha, A. 1993, PASP, 105, 1342

Sirianni et al. 2004, submitted

Stetson, P. B. 1998, PASP, 110, 1448

Stetson. P. B. 2000, PASP, 112, 925

Walker, A. R. 1994, PASP, 106, 828

Whitmore, B., Heyer, I. & Casertano, S. 1999, PASP, 111, 1559

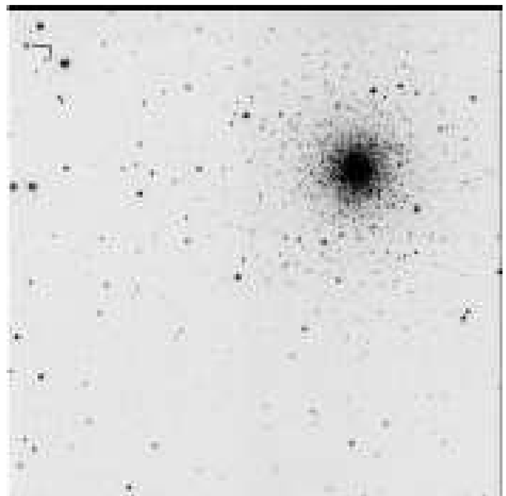

Fig. 1.— Chart of the target field for NGC 2419. North is to the left and East is down. A *FITS* file of this 4150 × 4100 pixel image is given in the electronic edition of the *PASP* and at ftp://taurus.tuc.noao.edu/pub/saha/Photseq/fg1_elec.fits. The positions in pixels in the FITS image correspond to the X and Y positions of given in the tables for NGC 2419 objects in this paper. The FITS image is also appointed with a world coordinate system (WCS) so that sky coordinates can be read directly from the image (using a suitable display program).

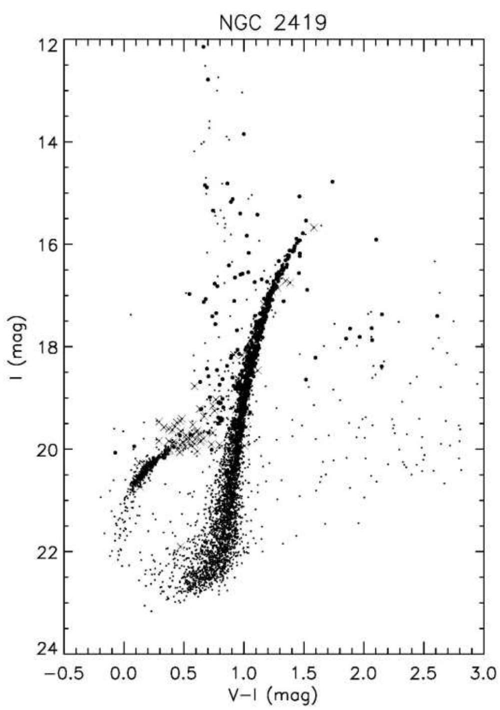

Fig. 2.— The color-magnitude diagram in V and I for the NGC 2419 field. Bold points mark objects with photometric uncertainty better than 0.015 mag in all passbands. Crosses mark variable stars. Note that the 'best' stars span a range of over 8 magnitudes, and a color range of over 3 mags in $V - I$.

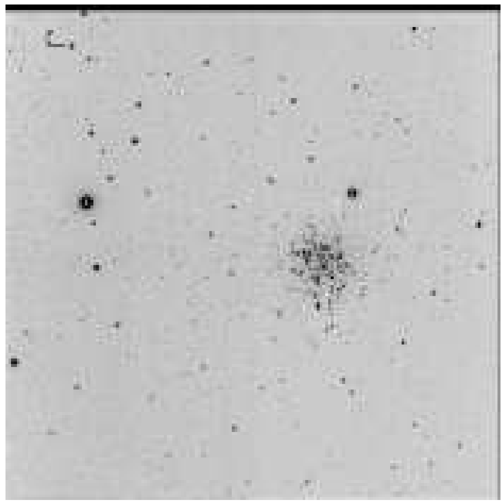

Fig. 3.— Chart of the target field for Pal 4. North is to the right and East is up. A *FITS* file of this 4150 × 4100 pixel image is given in the electronic edition of the *PASP* and at ftp://taurus.tuc.noao.edu/pub/saha/Photseq/fg3_elec.fits. The positions in pixels in the FITS image correspond to the X and Y positions of given in the tables for Pal 4 objects in this paper. The FITS image is also appointed with a world coordinate system (WCS) so that sky coordinates can be read directly from the image (using a suitable display program).

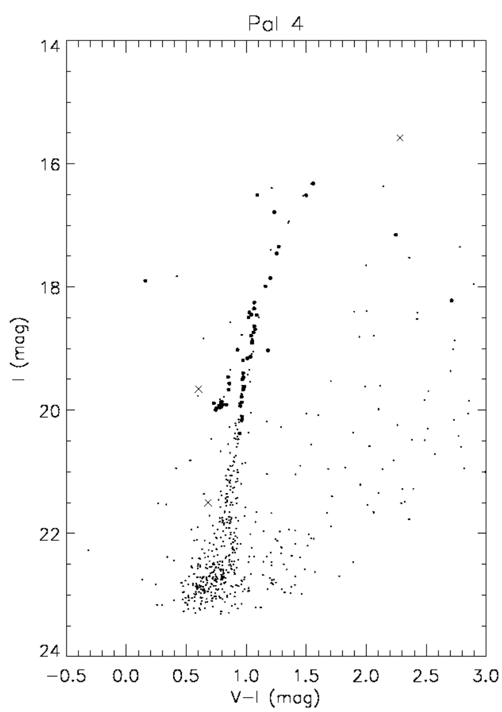

Fig. 4.— The color-magnitude diagram in V and I for the Pal 4 field. Bold points mark objects with photometric uncertainty better than 0.015 mag in all passbands. Crosses mark variable stars. Note that the 'best' stars span a range of nearly 5 magnitudes.

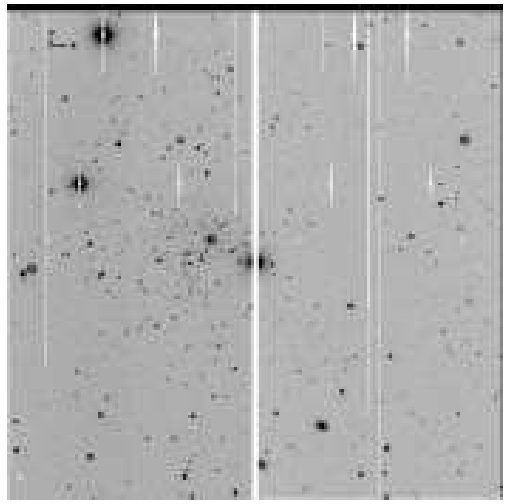

Fig. 5.— Chart of the target field for Pal 14. North is to the right and East is up. Due to the desire to position the bright star near the cluster between the two chips of MIMO, no dithering was done in the 'X' direction, and so this stacked deep retains the masked areas. A *FITS* file of this 4150×4100 pixel image is given in the electronic edition of the *PASP* and at ftp://taurus.tuc.noao.edu/pub/saha/Photseq/fg5_elec.fits. The positions in pixels in the FITS image correspond to the X and Y positions of given in the tables for Pal 14 objects in this paper. The FITS image is also appointed with a world coordinate system (WCS) so that sky coordinates can be read directly from the image (using a suitable display program).

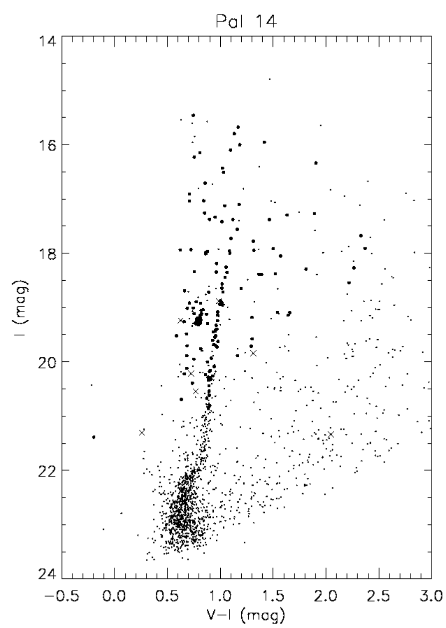

Fig. 6.— The color-magnitude diagram in V and I for the Pal 14 field. Bold points mark objects with photometric uncertainty better than 0.015 mag in all passbands. Crosses mark variable stars. Note that the 'best' stars span a range of over 5 magnitudes.

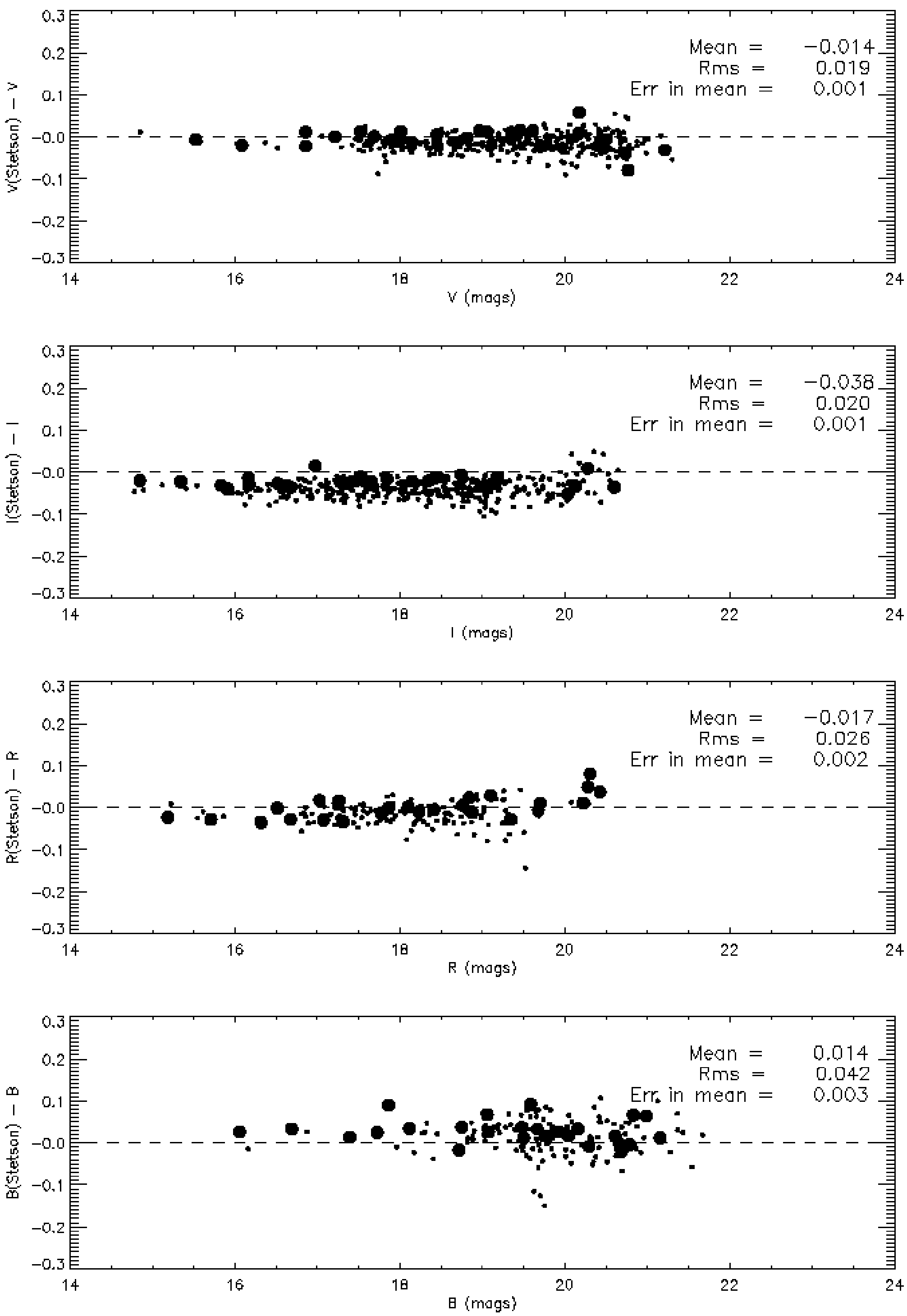

Fig. 7.— The star by star differences (shown as small dots) in all four passbands of the magnitudes of the 'best' stars from this study versus the magnitudes reported in Stetson (2000). The differences are shown as a function of object brightness. No obvious trends with brightness are seen. The unweighted mean differences with uncertainties are shown in the annotations. The large dots show the differences versus the Christian et al. (1985) sequence.

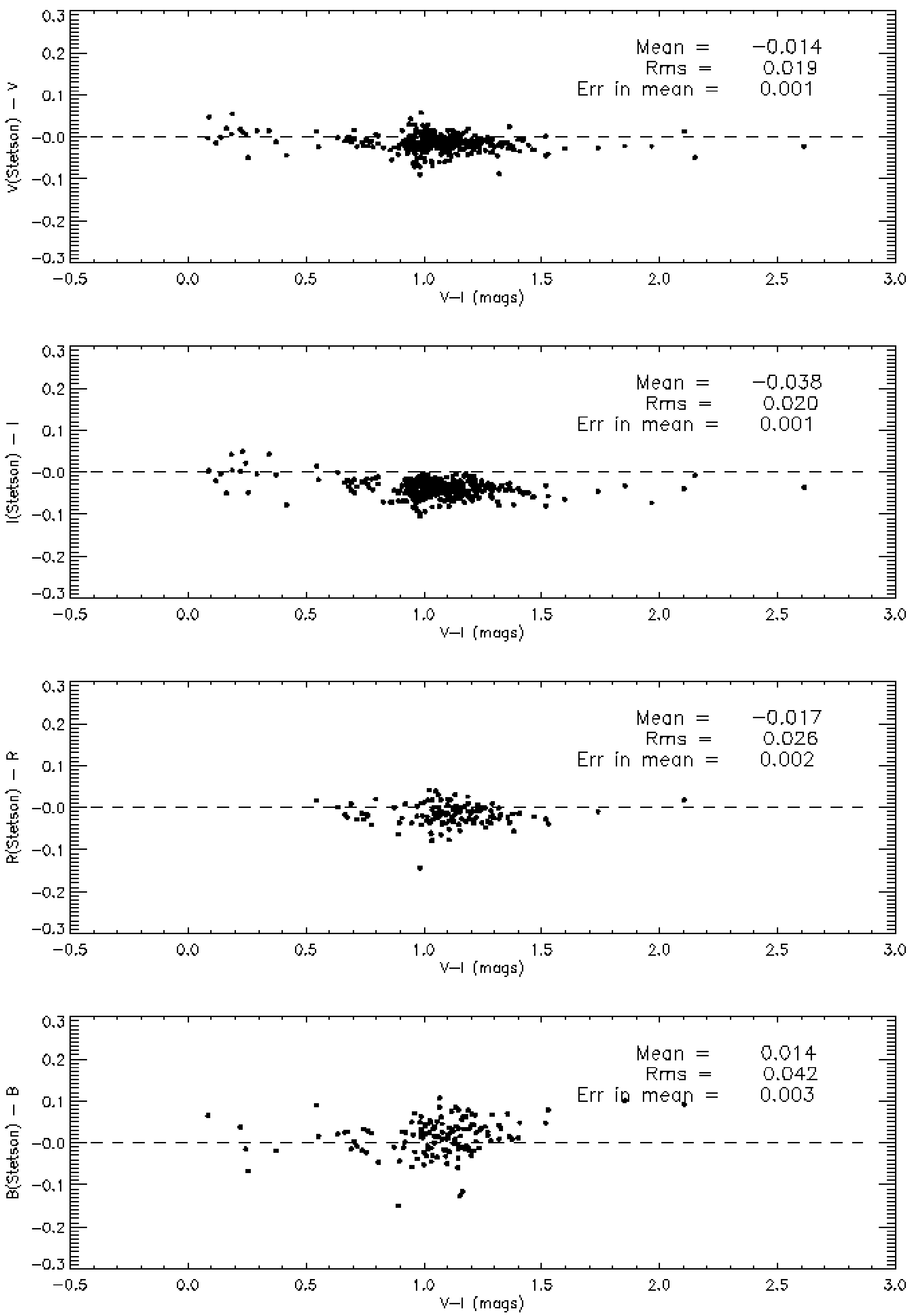

Fig. 8.— The star by star differences in all four passbands of the magnitudes of the 'best' stars from this study versus the magnitudes reported in Stetson (2000). The differences are shown as a function of object color. Clear trends are seen in V and I, especially in I, indicating that the source of the differences is likely in how well the two observation sets duplicate the original passband.

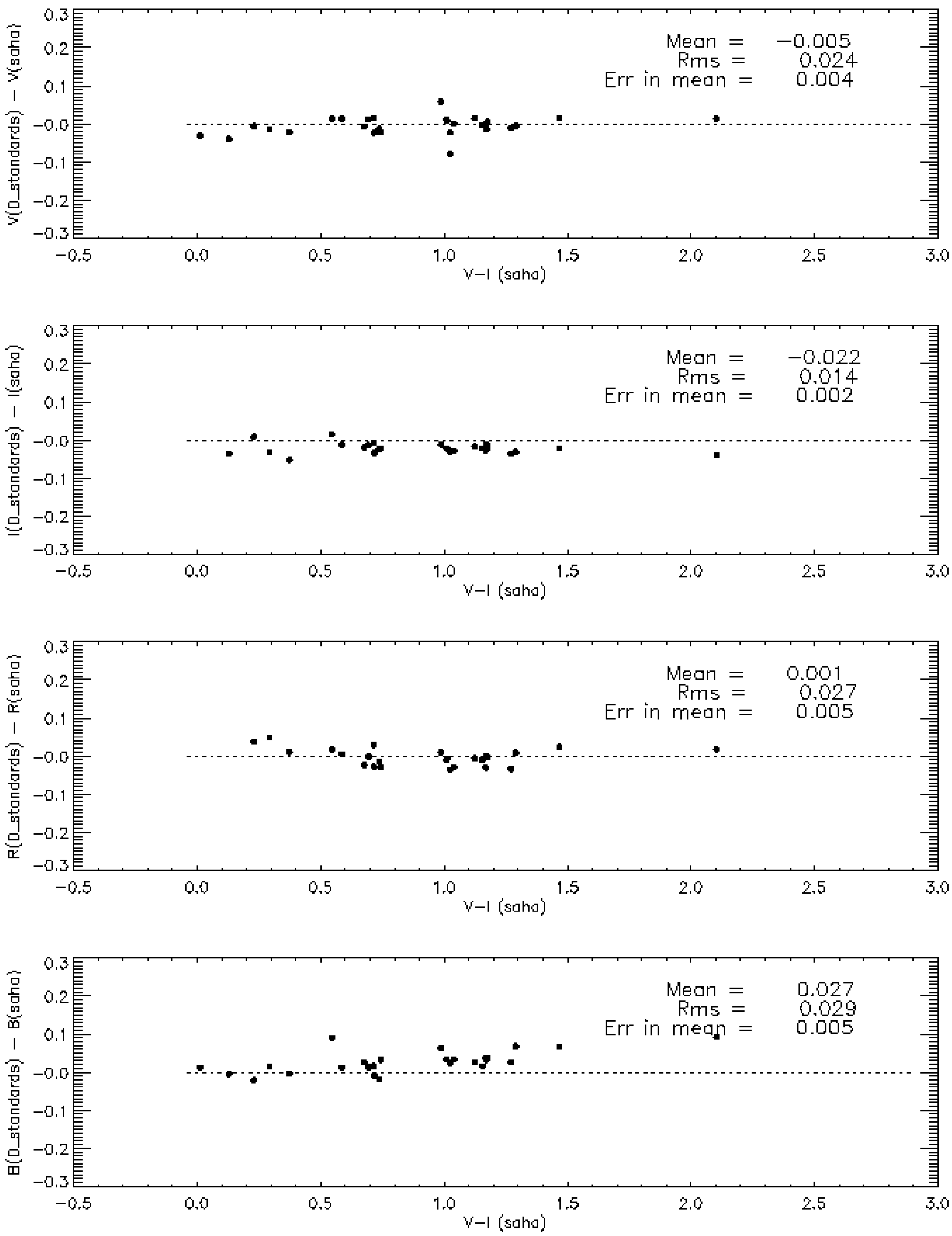

Fig. 9.— Same as Fig 8, but the comparison is against the unpublished sequence by Davis for the Kitt Peak consortium (see text). The trends seen for V and I in Fig. 8 are not seen here, but a trend appears for the B band.

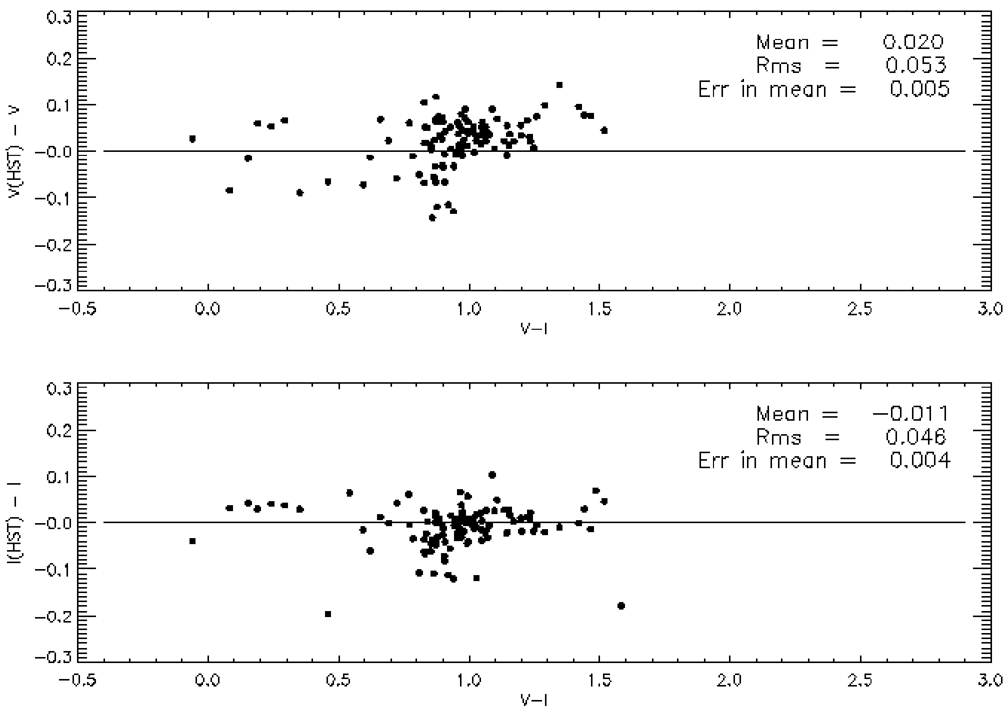

Fig. 10.— Comparison of V and I magnitudes against photometry with WFPC2 of stars in an area just south of NGC 2419. The *HST*/WFPC2 data were reduced with HSTPHOT (see text for details) using independent zero-point and color terms. The color trends seen in Fig 8 are not discernible here.

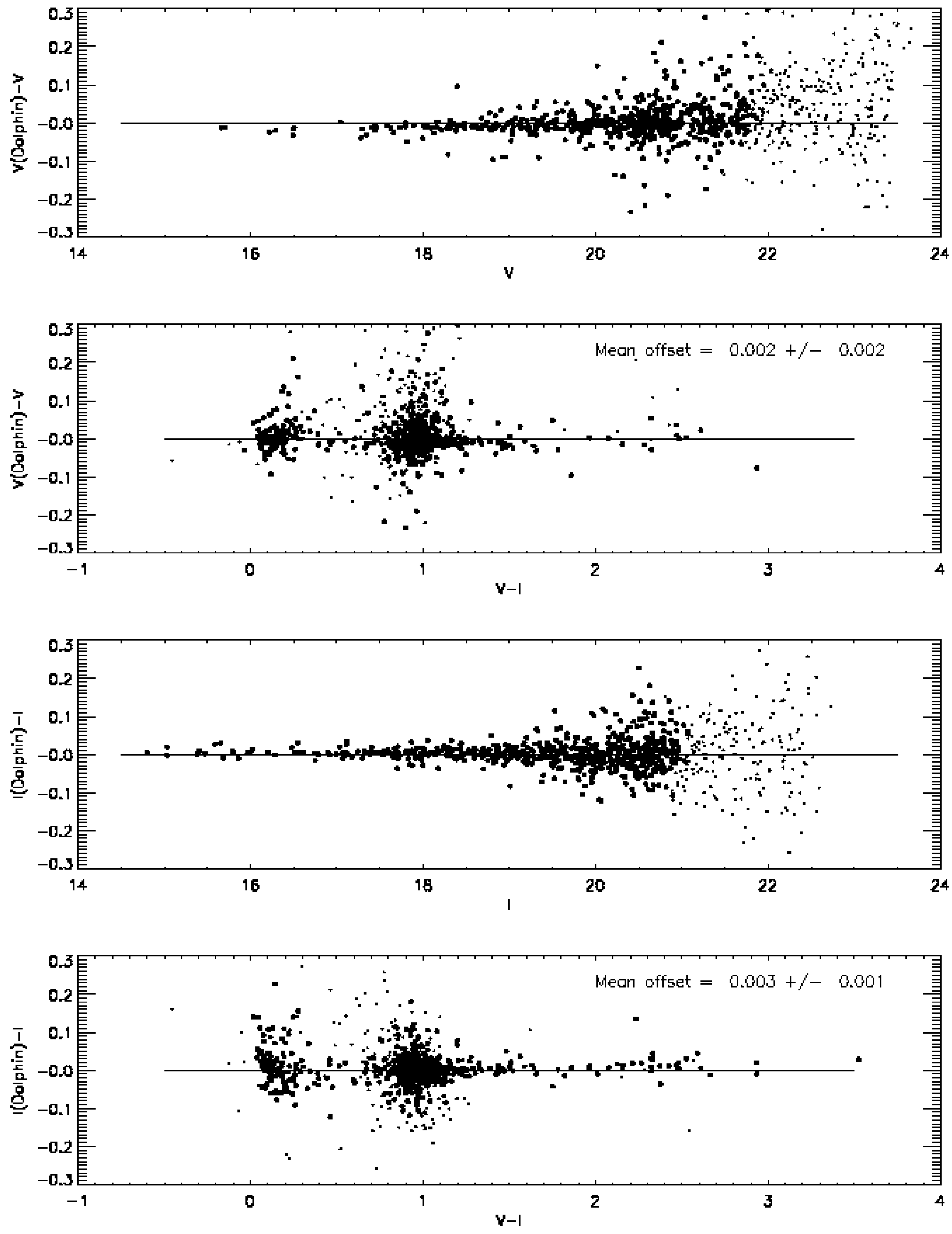

Fig. 11.— Comparison of V and I magnitudes from two different independent reduction methods applied to images obtained on 2003 Feb 09. V and I refer to magnitudes obtained with the methods described in this paper, whereas $V(Dolphin)$ and $I(Dolphin)$ are magnitudes derived using independent methods of PSF fitting, atmospheric extinction estimation, and color equation determination by one of us (AED). The excellent agreement corroborates that systematic errors arising from differences in methodology are insignificant.

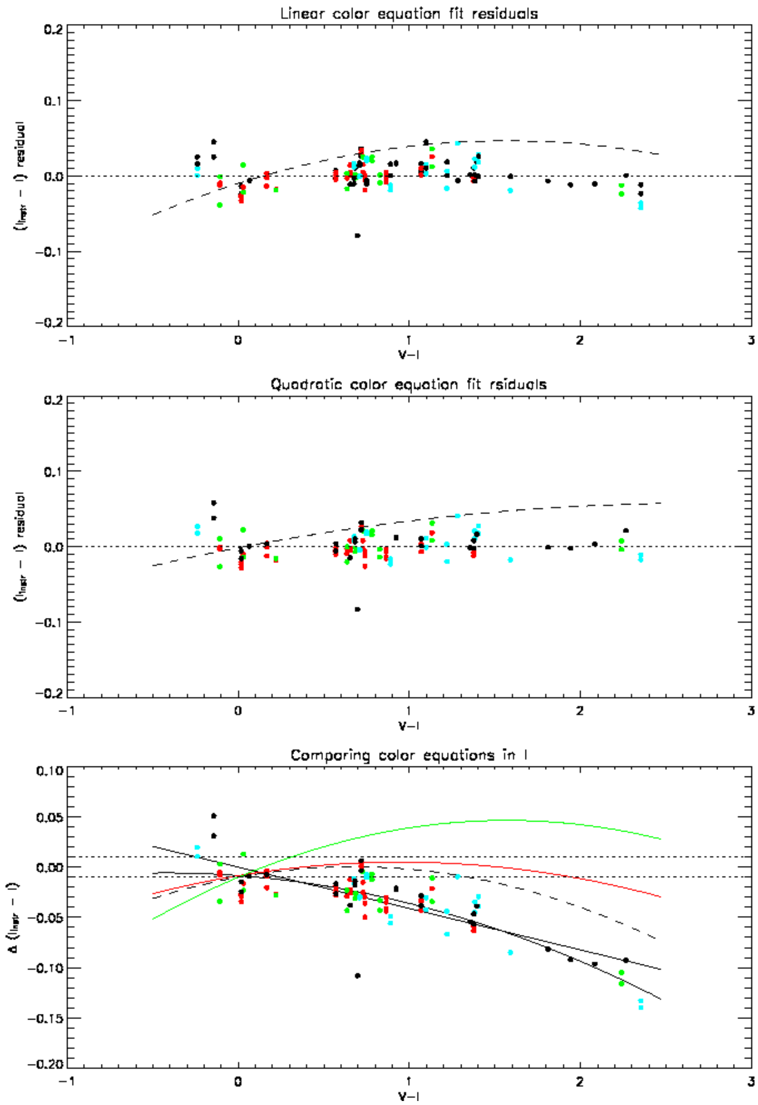

Fig. 12.— Residuals from simultaneously fitting the color equations to standard star data from 4 different nights in the manner described in §7 are shown in the first two panels: the top panel shows the case for a linear fit, and the second panel for a quadratic fit. The various colors mark data from different nights. The dashed line in the first two panels show how much the fit residuals would have to change systematically with color to produce concordance with Stetson's sequence in NGC 2419. The scatter in the standard star data is sufficiently small to rule out the possibility that the discrepancy is due to uncertainties in our determination of the color correction. In the lowest panel, we show the color equations themselves: the straight and curved continuous lines are our best linear and quadratic solutions respectively; the dashed line is the color equation required to bring our I band observations in NGC 2419 into agreement with Stetson's sequence; the red line shows the difference between our quadratic and linear fits and shows that for $-0.1 < V - I < 2.0$ the difference is less than 0.01 mag, and the green line shows the difference required from our linear fit to match Stetson's NGC 2419 sequence. More details are in §7.

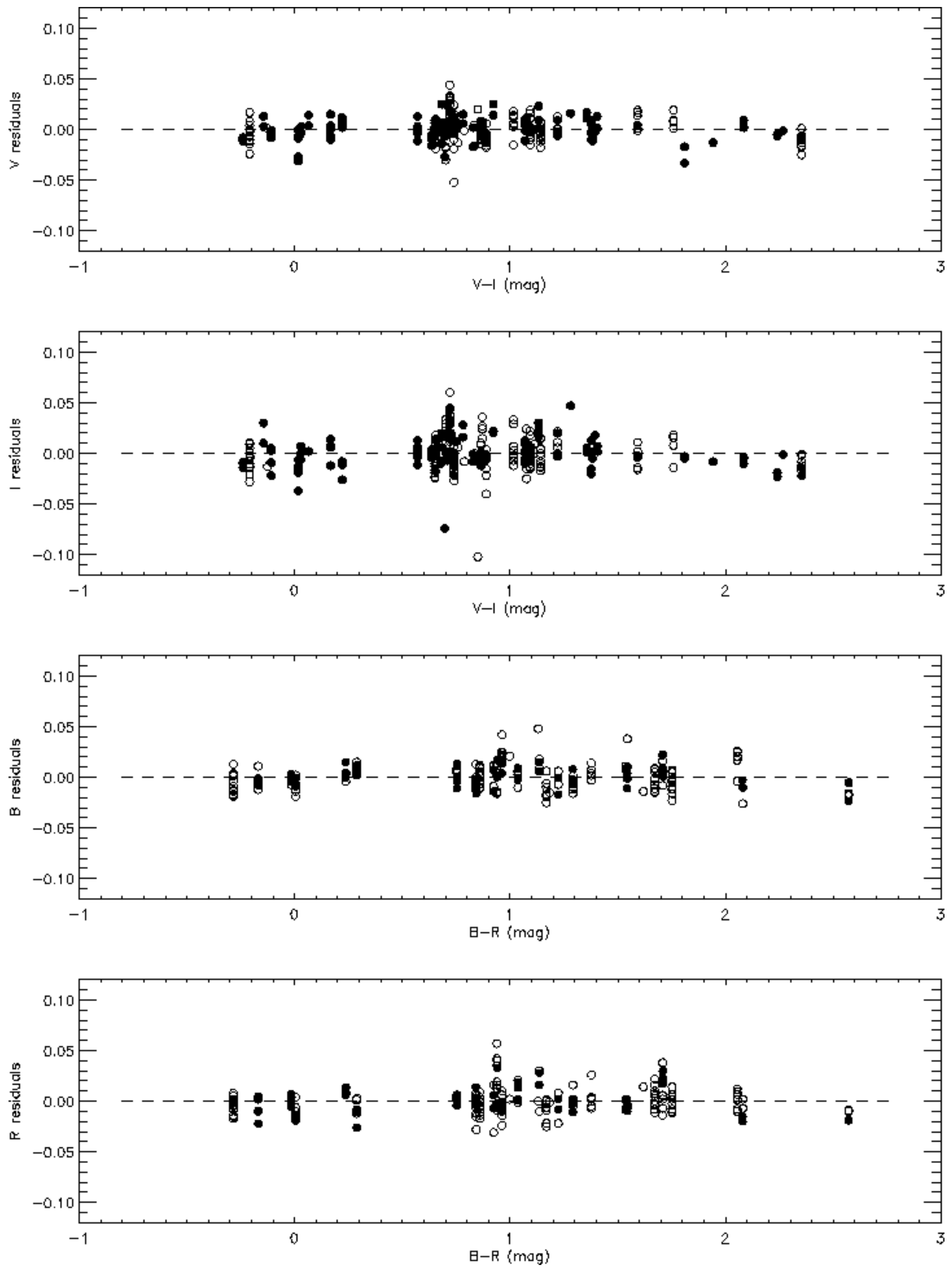

Fig. 13.— Residuals in all 4 passbands for the Landolt stars observed on all photometric nights are shown. The residuals are with respect to the predicted value using the photometric solution for the night in question. Filled circles show those observations that contribute specifically to the calibration of NGC 2419, while open circles contributed only to Pal 4 and/or Pal 14.

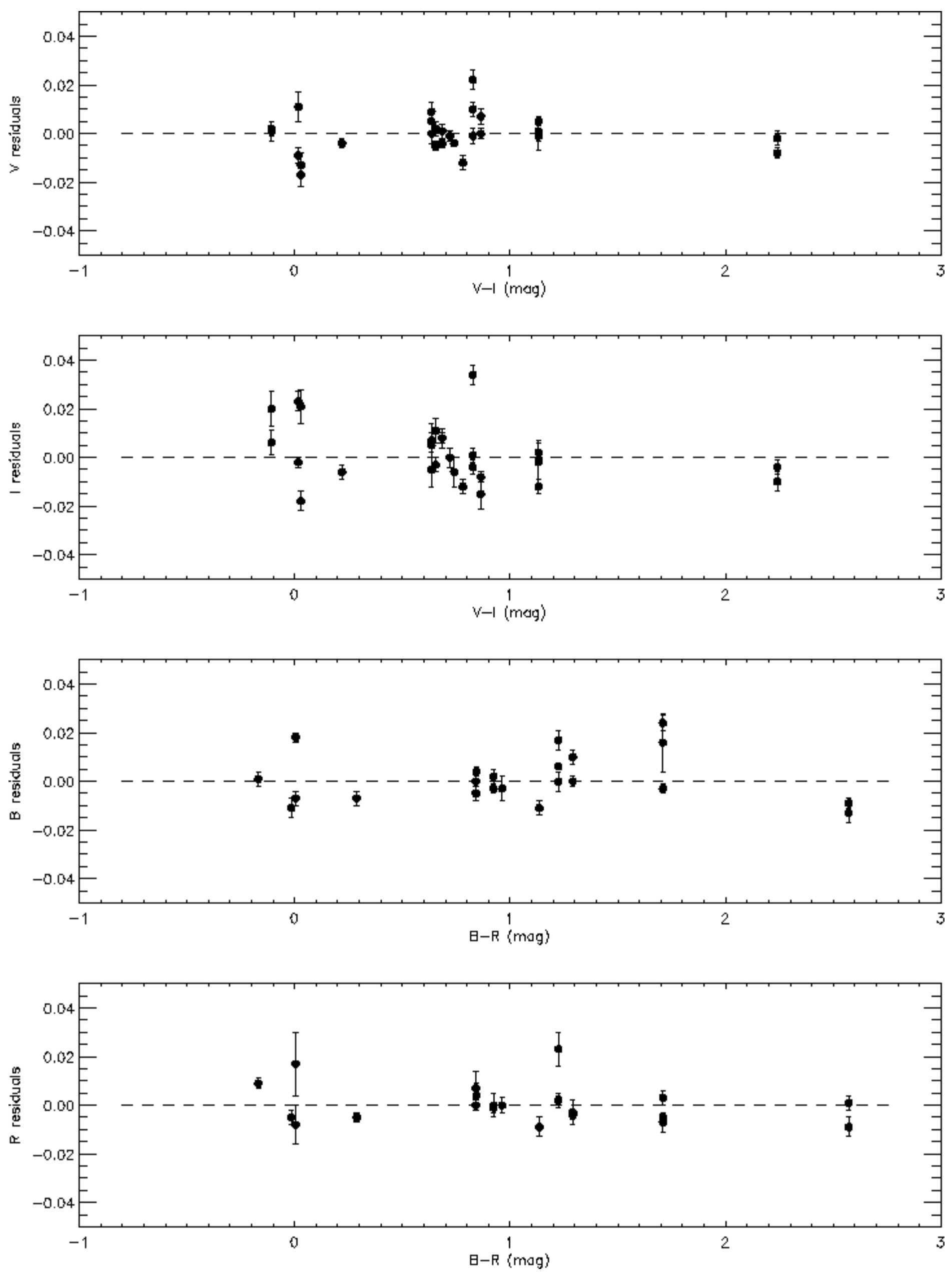

Fig. 14.— Same as Fig. 13, but showing the mean and standard errors in the residuals for only those Landolt standards observed thrice or more. Note the lack of any overall trends with color, although individual stars have mean residuals as large as 0.02 mag.

Table 1. Summary of Photometric Observations

UT Date	Telescope	Targets Observed[a]	Bandpasses	Landolt Fields[b]	Comment
2001 Feb 27	WIYN 3.5m	NGC 2419, Pal 4	*BVRI*	Rubin 149, SA101-326	–
2001 Apr 13	WIYN 3.5m	Pal 14	*VI*	PG1633+099	–
2001 Sep 21	WIYN 3.5m	NGC 2419	*VI*	SA92-430	–
2001 Dec 24	WIYN 3.5m	NGC 2419	*VI*	SA95-275, SA98-671	–
				Rubin 152	–
2002 Apr 12	WIYN 3.5m	Pal 3, Pal 14	*BVRI*	Rubin 149, PG0918+029	Photometric only in
				PG1633+099, SA110	2nd half of night
2002 Nov 13	WIYN 0.9m	NGC 2419, Pal 3, Pal 4	*BVRI*	SA92-A, Rubin 149	–
2002 Nov 14	WIYN 0.9m	NGC 2419, Pal 3, Pal 4	*BVRI*	SA92-A, SA98	–
				Rubin 149, PG1047+003	-
2002 Nov 15	WIYN 0.9m	NGC 2419, Pal 3, Pal 4	*BVRI*	SA92-A, SA98	–
				Rubin 149, PG1047+003	–
2003 Feb 09	WIYN 3.5m	NGC 2419, Pal 3, Pal 4	*BVRI*	SA98-671, Rubin 149	–
				SA104-334	–
2003 Jun 02	WIYN 3.5m	Pal 14	*BVRI*	PG1633+099, SA110-232	–
2003 Jun 03	WIYN 3.5m	Pal 3, Pal 4	*VI*	PG1633+099, SA110-232	–
2003 Jun 04	WIYN 3.5m	Pal 4	*BVRI*	PG1633+099, SA110-232	–
				SA104-336	–
2003 Jun 06	WIYN 3.5m	Pal 4, Pal 14	*BVRI*	SA104-336, PG1633+099	–

[a]Targets were often observed a multiple number of times, with varied positions on the field of view and/or at different air-masses

[b]Several stars around indicated object and within the field of view are Landolt standards. Each field may have multiple observations at different airmasses

Table 2. Summary of Photometric Observations

Target	Passband	ϵ_{sys} [a] (mags)	No. of stars [b]
NGC 2419	V	0.0032	74
	I	0.0058	43
	R	0.0043	87
	B	0.0203	25
Pal 14	V	0.0050	153
	I	0.0057	158
	R	0.0106	262
	B	0.0046	248
Pal 4	V	0.0123	122
	I	0.0072	114
	R	0.0070	122
	B	0.0061	91

[a] See §4 for details

[b] This is the number of objects that have measured magnitudes in this passband for *all* exposures of this target: see §4

Table 3. Stars in the NGC2419 Field with best Photometry

Star ID	X (pix)	Y (pix)	R.A. (J2000)	Decl. (J2000)	$< V >$	$\epsilon(V)$	n_V	$< I >$	$\epsilon(I)$	n_I	$< R >$	$\epsilon(R)$	n_R	$< B >$	$\epsilon(B)$	n_B
1	266.104	3962.359	7:37:53.69	38:59:07.0	12.808	0.008	4	12.146	0.012	4	12.447	0.005	4	13.291	0.013	3
2	447.962	3334.508	7:38:01.27	38:58:41.6	16.065	0.007	5	15.173	0.007	5	15.608	0.006	4	16.810	0.010	4
3	764.747	1553.491	7:38:22.74	38:57:57.4	17.518	0.005	6	16.972	0.012	5	17.258	0.010	3	17.860	0.010	5
4	960.799	2767.838	7:38:08.13	38:57:29.7	17.209	0.007	7	16.169	0.006	6	16.671	0.008	5	18.113	0.013	8
5	1068.558	2806.926	7:38:07.67	38:57:14.5	17.792	0.007	8	17.126	0.008	7	17.455	0.011	6	18.300	0.007	7
6	1094.433	2071.915	7:38:16.52	38:57:11.0	18.012	0.008	8	15.909	0.012	7	17.024	0.012	6	19.581	0.004	8
7	1103.414	2972.147	7:38:05.69	38:57:09.6	16.857	0.009	7	15.833	0.006	6	16.316	0.009	5	17.724	0.005	8
8	1204.976	2728.613	7:38:08.63	38:56:55.4	16.084	0.014	5	15.341	0.006	5	15.708	0.009	6	16.685	0.011	6
9	1226.861	2145.816	7:38:15.64	38:56:52.4	18.966	0.005	7	17.843	0.007	9	18.412	0.010	7	19.919	0.006	7
10	1275.468	1691.690	7:38:21.12	38:56:45.6	19.703	0.005	11	18.987	0.005	12	19.344	0.009	11	20.291	0.014	9
11	1286.337	2255.745	7:38:14.33	38:56:44.0	20.170	0.011	5	19.184	0.010	9	19.698	0.009	7	20.984	0.013	6
12	1392.309	2648.210	7:38:09.61	38:56:29.0	17.944	0.009	4	16.674	0.009	4	17.311	0.009	4	19.075	0.004	8
13	1412.083	1335.779	7:38:25.41	38:56:26.4	18.692	0.005	12	17.522	0.004	13	18.098	0.007	10	19.664	0.009	12
14	1446.808	1403.007	7:38:24.60	38:56:21.5	17.920	0.005	12	16.630	0.005	13	17.252	0.006	11	19.057	0.006	13
15	1498.800	2352.686	7:38:13.18	38:56:14.1	17.055	0.011	6	15.538	0.010	6	16.266	0.010	6	18.325	0.008	9
16	1501.779	1879.013	7:38:18.88	38:56:13.8	21.215	0.009	8	20.288	0.013	9	20.766	0.008	9	21.925	0.014	9
17	1504.341	2157.158	7:38:15.53	38:56:13.4	15.523	0.009	7	14.847	0.005	6	15.184	0.009	6	16.051	0.009	7
18	1576.518	2128.411	7:38:15.88	38:56:03.2	20.731	0.010	9	19.808	0.006	9	20.280	0.009	8	21.429	0.012	8
19	1687.761	2211.658	7:38:14.89	38:55:47.6	20.389	0.010	8	20.016	0.011	9	20.236	0.012	9	20.641	0.013	7
20	1734.892	1375.164	7:38:24.96	38:55:41.0	20.334	0.012	12	19.283	0.006	11	19.782	0.009	11	21.227	0.006	10
21	1743.864	2392.363	7:38:12.72	38:55:39.7	19.831	0.005	9	18.786	0.005	9	19.316	0.012	6	20.662	0.008	6
22	1788.466	1492.431	7:38:23.55	38:55:33.5	20.936	0.012	8	19.982	0.009	8	20.462	0.009	8	21.664	0.011	10
23	1798.831	1814.972	7:38:19.67	38:55:32.0	20.171	0.008	11	19.179	0.007	11	19.688	0.009	12	20.956	0.006	10
24	1809.749	2737.932	7:38:08.56	38:55:30.4	19.560	0.011	5	18.572	0.010	4	19.074	0.012	5	20.401	0.007	5
25	1829.164	867.028	7:38:31.08	38:55:27.8	20.740	0.011	6	20.009	0.008	7	20.360	0.014	5	21.298	0.011	11
26	1843.285	2287.826	7:38:13.98	38:55:25.7	18.805	0.004	13	17.651	0.005	13	18.227	0.008	12	19.761	0.005	14
27	1865.708	1230.949	7:38:26.71	38:55:22.7	19.456	0.005	12	18.396	0.005	13	18.927	0.006	12	20.303	0.010	14
28	1869.803	2161.703	7:38:15.50	38:55:22.0	20.086	0.007	11	19.082	0.012	11	19.584	0.010	12	20.873	0.011	10
29	1872.237	3139.232	7:38:03.74	38:55:21.5	19.110	0.007	5	18.016	0.010	4	18.549	0.008	4	20.011	0.006	5
30	1878.443	3155.894	7:38:03.54	38:55:20.6	18.321	0.008	4	17.559	0.011	6	17.943	0.013	3	18.896	0.006	8
31	1901.913	3225.322	7:38:02.70	38:55:17.3	17.896	0.013	6	16.600	0.008	6	17.242	0.006	5	19.062	0.007	8
32	1926.995	3331.367	7:38:01.43	38:55:13.8	17.837	0.005	7	16.511	0.009	7	17.164	0.013	6	19.009	0.007	7
33	1940.382	2264.015	7:38:14.28	38:55:12.1	19.098	0.005	12	17.981	0.005	13	18.541	0.006	12	20.009	0.008	12
34	1972.592	2002.898	7:38:17.42	38:55:07.6	17.526	0.004	13	16.770	0.005	13	17.153	0.005	13	18.168	0.009	16
35	1993.210	1441.337	7:38:24.18	38:55:04.7	19.693	0.007	14	17.841	0.005	13	18.743	0.006	12	21.125	0.014	11
36	1996.492	3211.583	7:38:02.88	38:55:04.0	13.484	0.004	4	12.784	0.007	4	13.103	0.010	4	13.983	0.007	4
37	1999.439	2395.075	7:38:12.70	38:55:03.8	19.468	0.004	13	18.382	0.005	13	18.928	0.007	11	20.345	0.011	11
38	2008.798	3663.678	7:37:57.44	38:55:02.2	18.319	0.009	7	17.108	0.009	7	17.715	0.010	4	19.339	0.013	8
39	2042.909	2239.537	7:38:14.58	38:54:57.7	18.144	0.004	13	17.407	0.005	13	17.778	0.004	13	18.716	0.009	14
40	2049.803	2181.065	7:38:15.28	38:54:56.7	20.560	0.011	10	19.578	0.009	9	20.077	0.009	10	21.303	0.008	10
41	2068.109	2383.915	7:38:12.84	38:54:54.1	20.212	0.009	10	19.194	0.008	9	19.709	0.007	10	21.017	0.011	10
42	2092.316	2037.521	7:38:17.01	38:54:50.8	19.455	0.005	10	18.378	0.005	10	18.922	0.005	11	20.323	0.009	13
43	2107.310	1409.056	7:38:24.58	38:54:48.7	20.552	0.009	11	19.552	0.006	10	20.076	0.005	12	21.338	0.008	11
44	2112.620	2418.211	7:38:12.43	38:54:47.8	20.211	0.009	11	19.217	0.006	11	19.730	0.007	11	20.998	0.010	12
45	2114.004	2542.434	7:38:10.94	38:54:47.6	17.598	0.004	14	16.820	0.003	12	17.212	0.003	13	18.264	0.007	16
46	2114.363	2488.552	7:38:11.59	38:54:47.6	20.734	0.011	10	19.761	0.011	9	20.282	0.010	10	21.465	0.009	10
47	2121.238	3119.545	7:38:04.00	38:54:46.5	19.793	0.006	10	18.756	0.003	11	19.282	0.008	11	20.618	0.013	13
48	2123.898	2500.391	7:38:11.45	38:54:46.2	20.532	0.011	11	20.278	0.011	9	20.443	0.010	11	20.710	0.015	10
49	2132.332	2311.292	7:38:13.72	38:54:45.1	20.257	0.006	12	19.451	0.009	10	19.879	0.011	11	20.844	0.012	14
50	2134.935	3106.176	7:38:04.16	38:54:44.6	17.648	0.006	13	16.282	0.004	13	16.956	0.006	10	18.880	0.013	16
51	2144.865	3174.639	7:38:03.33	38:54:43.2	20.403	0.009	8	19.484	0.010	4	19.961	0.009	5	21.089	0.007	4
52	2148.404	2924.532	7:38:06.34	38:54:42.7	19.367	0.005	12	18.290	0.003	12	18.845	0.010	9	20.240	0.010	8
53	2152.884	1773.820	7:38:20.19	38:54:42.3	20.331	0.004	12	19.329	0.005	10	19.846	0.009	13	21.097	0.007	12
54	2160.502	772.610	7:38:32.24	38:54:41.3	18.258	0.005	12	17.038	0.004	14	17.646	0.008	8	19.323	0.004	14
55	2176.744	3414.857	7:38:00.45	38:54:38.6	19.947	0.005	9	18.926	0.007	7	19.444	0.006	9	20.721	0.013	5
56	2185.126	2654.870	7:38:09.59	38:54:37.6	20.652	0.006	10	20.469	0.014	8	20.602	0.012	10	20.781	0.015	13
57	2187.905	2796.392	7:38:07.89	38:54:37.2	19.820	0.005	13	18.789	0.005	13	19.329	0.006	9	20.650	0.009	14
58	2213.646	3062.630	7:38:04.69	38:54:33.5	19.150	0.006	10	18.057	0.005	11	18.619	0.004	9	20.018	0.008	12
59	2214.949	3937.503	7:37:54.16	38:54:33.1	18.150	0.007	8	16.905	0.008	8	17.529	0.010	9	19.216	0.007	8

Table 3—Continued

Star ID	X (pix)	Y (pix)	R.A. (J2000)	Decl. (J2000)	< V >	$\epsilon(V)$	n_V	< I >	$\epsilon(I)$	n_I	< R >	$\epsilon(R)$	n_R	< B >	$\epsilon(B)$	n_B
60	2228.013	2236.002	7:38:14.64	38:54:31.7	19.565	0.008	13	18.490	0.003	12	19.036	0.009	13	20.420	0.007	15
61	2232.025	2934.270	7:38:06.23	38:54:31.0	19.424	0.004	14	18.404	0.005	12	18.931	0.004	10	20.202	0.007	15
62	2234.584	3076.783	7:38:04.52	38:54:30.6	18.917	0.003	14	17.789	0.002	12	18.359	0.006	10	19.843	0.005	16
63	2238.330	2602.637	7:38:10.23	38:54:30.1	19.901	0.007	12	18.871	0.008	12	19.391	0.006	13	20.739	0.007	13
64	2249.610	2721.846	7:38:08.79	38:54:28.5	19.349	0.005	14	18.306	0.004	12	18.841	0.004	12	20.165	0.006	15
65	2275.162	2723.589	7:38:08.77	38:54:25.0	20.211	0.005	13	19.188	0.007	12	19.710	0.010	13	21.003	0.009	12
66	2280.434	2253.823	7:38:14.43	38:54:24.3	21.012	0.006	9	20.043	0.006	9	20.536	0.010	9	21.721	0.011	11
67	2281.646	2045.889	7:38:16.93	38:54:24.1	18.095	0.003	14	16.851	0.002	13	17.460	0.005	14	19.174	0.009	17
68	2285.438	3217.877	7:38:02.83	38:54:23.4	16.370	0.004	11	15.401	0.005	11	15.862	0.004	9	17.246	0.006	15
69	2287.856	2848.153	7:38:07.27	38:54:23.1	19.702	0.005	13	17.637	0.006	13	18.728	0.009	9	21.088	0.012	11
70	2291.173	2922.450	7:38:06.38	38:54:22.7	19.072	0.003	14	18.021	0.007	14	18.550	0.004	12	19.885	0.005	14
71	2299.345	2514.331	7:38:11.29	38:54:21.6	20.454	0.010	10	20.128	0.010	9	20.337	0.013	13	20.707	0.012	14
72	2301.759	3090.451	7:38:04.36	38:54:21.1	19.398	0.003	13	18.320	0.003	14	18.866	0.011	10	20.244	0.007	15
73	2303.756	2158.034	7:38:15.58	38:54:21.0	19.386	0.012	10	18.320	0.007	9	18.846	0.003	12	20.261	0.006	15
74	2309.882	2835.765	7:38:07.43	38:54:20.1	20.926	0.006	10	19.958	0.010	9	20.483	0.009	8	21.673	0.011	11
75	2312.551	1931.802	7:38:18.30	38:54:19.8	20.231	0.009	11	19.207	0.011	10	19.733	0.012	12	21.012	0.008	11
76	2319.674	2461.688	7:38:11.93	38:54:18.7	19.003	0.003	14	17.896	0.003	13	18.449	0.005	14	19.917	0.005	15
77	2320.837	3488.532	7:37:59.57	38:54:18.4	18.416	0.003	14	16.889	0.003	13	17.611	0.007	10	19.682	0.010	13
78	2322.372	2339.749	7:38:13.40	38:54:18.4	20.628	0.012	12	19.641	0.007	10	20.146	0.008	13	21.367	0.012	12
79	2325.505	2974.937	7:38:05.75	38:54:17.8	19.421	0.005	11	18.348	0.007	13	18.896	0.004	11	20.288	0.009	14
80	2327.571	3045.183	7:38:04.91	38:54:17.5	21.035	0.010	10	20.087	0.010	9	20.593	0.011	7	21.729	0.013	10
81	2329.630	2190.310	7:38:15.19	38:54:17.4	16.517	0.005	9	14.780	0.006	10	15.611	0.006	11	17.890	0.008	13
82	2353.735	3138.141	7:38:03.79	38:54:13.8	19.371	0.005	13	18.351	0.007	13	18.870	0.005	13	20.151	0.007	16
83	2366.222	3163.677	7:38:03.48	38:54:12.1	17.645	0.004	13	16.180	0.004	13	16.855	0.004	13	18.883	0.008	16
84	2374.578	2109.229	7:38:16.17	38:54:11.1	20.581	0.013	11	19.612	0.009	12	20.115	0.008	12	21.313	0.012	12
85	2374.848	2766.292	7:38:08.27	38:54:10.9	19.937	0.004	11	18.931	0.006	12	19.435	0.006	12	20.725	0.008	12
86	2377.731	1191.951	7:38:27.21	38:54:10.7	17.287	0.004	14	16.413	0.004	13	16.851	0.003	14	17.960	0.009	16
87	2378.570	3009.122	7:38:05.35	38:54:10.4	19.187	0.004	13	18.075	0.004	13	18.632	0.004	12	20.075	0.005	15
88	2379.723	3078.292	7:38:04.51	38:54:10.2	19.340	0.006	14	18.259	0.009	14	18.808	0.005	12	20.199	0.009	15
89	2391.720	2690.272	7:38:09.18	38:54:08.6	20.054	0.004	13	19.038	0.006	11	19.559	0.005	13	20.865	0.010	13
90	2398.046	3007.961	7:38:05.36	38:54:07.6	20.173	0.009	12	19.222	0.005	13	19.705	0.005	12	20.895	0.006	12
91	2399.085	3107.489	7:38:04.16	38:54:07.5	19.561	0.005	13	18.530	0.005	13	19.059	0.007	12	20.345	0.008	15
92	2417.265	3217.786	7:38:02.84	38:54:04.9	18.927	0.003	14	17.792	0.005	13	18.364	0.003	13	19.853	0.007	16
93	2417.445	2759.273	7:38:08.35	38:54:04.9	19.994	0.005	13	18.964	0.012	11	19.502	0.007	13	20.816	0.005	13
94	2417.596	1974.431	7:38:17.80	38:54:05.0	18.241	0.002	14	17.044	0.006	13	17.602	0.003	14	19.278	0.006	17
95	2417.879	3108.652	7:38:04.15	38:54:04.8	19.306	0.004	13	18.211	0.006	13	18.769	0.008	12	20.187	0.007	14
96	2424.783	3066.262	7:38:04.66	38:54:03.9	19.515	0.005	14	18.448	0.003	14	18.981	0.007	14	20.358	0.005	15
97	2427.414	2579.219	7:38:10.52	38:54:03.6	20.582	0.009	10	20.352	0.014	9	20.499	0.011	11	20.769	0.010	12
98	2429.338	3949.739	7:37:54.03	38:54:03.0	19.721	0.012	7	18.664	0.006	9	19.219	0.013	9	20.519	0.007	6
99	2431.089	2977.750	7:38:05.73	38:54:03.0	20.215	0.004	12	19.194	0.009	12	19.707	0.006	13	21.011	0.009	12
100	2434.010	2788.141	7:38:08.01	38:54:02.6	20.263	0.006	11	19.269	0.010	12	19.797	0.008	13	21.015	0.007	13
101	2436.030	3156.224	7:38:03.58	38:54:02.3	18.754	0.004	14	17.637	0.003	14	18.194	0.007	13	19.650	0.006	15
102	2439.690	2168.900	7:38:15.46	38:54:01.9	16.026	0.003	10	15.120	0.004	11	15.542	0.002	11	16.867	0.006	15
103	2440.039	3218.018	7:38:02.84	38:54:01.7	18.628	0.004	14	17.489	0.005	14	18.057	0.003	12	19.548	0.006	17
104	2446.043	2622.227	7:38:10.01	38:54:01.0	17.800	0.004	14	16.445	0.004	13	17.105	0.003	14	18.998	0.007	17
105	2449.863	3908.386	7:37:54.53	38:54:00.1	20.233	0.012	7	19.414	0.006	9	19.849	0.007	8	20.774	0.015	6
106	2449.883	2760.686	7:38:08.34	38:54:00.4	19.195	0.004	13	18.147	0.007	13	18.680	0.004	13	20.027	0.007	15
107	2450.932	2448.210	7:38:12.10	38:54:00.3	20.869	0.009	10	19.922	0.013	9	20.448	0.011	9	21.613	0.013	11
108	2451.796	2936.814	7:38:06.22	38:54:00.1	19.564	0.006	12	18.521	0.005	11	19.057	0.006	12	20.392	0.005	13
109	2456.560	2273.740	7:38:14.20	38:53:59.5	21.008	0.009	10	20.059	0.014	9	20.579	0.008	10	21.728	0.010	12
110	2459.864	3367.865	7:38:01.04	38:53:58.9	18.807	0.004	14	17.647	0.002	14	18.224	0.004	11	19.741	0.005	15
111	2460.816	2814.438	7:38:07.69	38:53:58.8	18.944	0.003	14	17.837	0.005	13	18.395	0.007	14	19.842	0.006	15
112	2463.200	3020.818	7:38:05.21	38:53:58.5	19.706	0.005	13	18.758	0.005	13	19.245	0.006	13	20.421	0.007	14
113	2467.500	2107.033	7:38:16.21	38:53:58.0	19.322	0.004	12	18.687	0.004	12	19.014	0.007	12	19.813	0.010	16
114	2472.359	2642.431	7:38:09.77	38:53:57.2	19.192	0.004	11	18.084	0.006	12	18.650	0.004	13	20.095	0.007	12
115	2473.097	3547.327	7:37:58.88	38:53:57.0	18.891	0.004	13	17.813	0.003	13	18.330	0.004	9	19.814	0.005	15
116	2474.585	2270.797	7:38:14.24	38:53:57.0	19.421	0.005	14	18.323	0.005	12	18.880	0.005	14	20.270	0.008	14
117	2475.989	2321.107	7:38:13.63	38:53:56.8	20.270	0.008	10	19.717	0.007	10	20.030	0.006	12	20.566	0.012	15
118	2479.719	3070.977	7:38:04.61	38:53:56.1	20.426	0.006	10	20.082	0.012	9	20.296	0.008	12	20.652	0.011	12
119	2482.429	2873.986	7:38:06.98	38:53:55.8	17.895	0.004	14	16.578	0.003	13	17.215	0.004	14	19.040	0.009	17

Table 3—Continued

Star ID	X (pix)	Y (pix)	R.A. (J2000)	Decl. (J2000)	$< V >$	$\epsilon(V)$	n_V	$< I >$	$\epsilon(I)$	n_I	$< R >$	$\epsilon(R)$	n_R	$< B >$	$\epsilon(B)$	n_B
120	2483.309	1423.919	7:38:24.43	38:53:55.9	15.580	0.005	10	14.889	0.005	10	15.224	0.004	12	16.161	0.014	13
121	2484.829	2555.925	7:38:10.81	38:53:55.5	19.609	0.007	12	18.550	0.004	11	19.089	0.005	13	20.475	0.009	12
122	2486.269	2511.346	7:38:11.34	38:53:55.3	20.282	0.010	11	19.284	0.007	8	19.808	0.005	11	21.079	0.010	12
123	2486.349	3536.041	7:37:59.01	38:53:55.1	19.392	0.006	13	18.354	0.005	13	18.884	0.004	9	20.172	0.008	15
124	2488.481	916.662	7:38:30.53	38:53:55.2	20.529	0.015	10	20.275	0.014	10	20.432	0.009	10	20.692	0.015	12
125	2489.259	3728.784	7:37:56.70	38:53:54.6	18.328	0.003	13	17.126	0.003	13	17.724	0.004	10	19.319	0.010	14
126	2489.804	2672.893	7:38:09.40	38:53:54.8	18.845	0.004	13	17.718	0.004	12	18.282	0.004	14	19.783	0.006	15
127	2495.564	2549.440	7:38:10.89	38:53:54.0	18.916	0.004	11	17.781	0.004	11	18.345	0.004	12	19.852	0.004	13
128	2501.391	3361.089	7:38:01.12	38:53:53.0	19.977	0.005	12	18.971	0.006	12	19.480	0.008	12	20.749	0.007	12
129	2508.663	3099.488	7:38:04.27	38:53:52.1	20.082	0.013	9	19.113	0.009	9	19.609	0.013	9	20.841	0.015	9
130	2511.689	3275.640	7:38:02.15	38:53:51.6	19.838	0.007	13	19.017	0.010	13	19.445	0.004	13	20.401	0.009	13
131	2512.125	2792.529	7:38:07.96	38:53:51.6	17.931	0.005	13	16.648	0.004	12	17.273	0.003	14	19.030	0.006	16
132	2516.746	2602.092	7:38:10.25	38:53:51.0	19.573	0.004	12	18.574	0.008	11	19.081	0.006	13	20.334	0.005	15
133	2517.868	1906.957	7:38:18.62	38:53:51.0	18.601	0.005	14	17.414	0.006	13	18.005	0.004	14	19.580	0.003	16
134	2519.295	2960.380	7:38:05.94	38:53:50.6	17.979	0.005	13	16.694	0.004	13	17.314	0.004	14	19.083	0.014	17
135	2519.789	3346.043	7:38:01.30	38:53:50.4	19.819	0.004	12	18.783	0.004	13	19.307	0.008	9	20.610	0.012	10
136	2531.008	3366.707	7:38:01.06	38:53:48.9	19.263	0.005	13	18.198	0.004	13	18.741	0.003	13	20.098	0.009	14
137	2533.457	3012.958	7:38:05.31	38:53:48.6	20.631	0.007	8	20.460	0.014	7	20.595	0.010	10	20.763	0.013	12
138	2534.028	3830.719	7:37:55.47	38:53:48.3	19.749	0.007	11	18.767	0.007	12	19.274	0.004	8	20.438	0.010	10
139	2534.200	3533.141	7:37:59.05	38:53:48.4	20.115	0.006	13	19.107	0.009	12	19.629	0.006	11	20.879	0.008	12
140	2546.851	2872.559	7:38:07.00	38:53:46.7	19.252	0.007	12	18.196	0.007	11	18.740	0.005	13	20.083	0.004	13
141	2548.360	2972.657	7:38:05.80	38:53:46.5	19.967	0.005	9	18.963	0.008	11	19.461	0.009	13	20.761	0.009	12
142	2549.698	2337.690	7:38:13.44	38:53:46.4	19.783	0.006	10	18.755	0.004	10	19.279	0.004	11	20.599	0.010	13
143	2550.837	727.737	7:38:32.81	38:53:46.4	18.026	0.006	12	17.106	0.005	12	17.558	0.006	10	18.814	0.008	14
144	2563.462	2770.691	7:38:08.23	38:53:44.4	19.222	0.006	11	18.119	0.004	10	18.695	0.011	9	20.118	0.007	9
145	2568.879	2707.501	7:38:08.99	38:53:43.7	18.439	0.003	11	17.240	0.005	11	17.841	0.005	10	19.482	0.005	11
146	2573.222	3087.975	7:38:04.41	38:53:43.0	19.596	0.005	11	18.530	0.007	11	19.077	0.006	9	20.436	0.009	10
147	2574.486	714.423	7:38:32.97	38:53:43.1	17.737	0.007	11	16.418	0.007	12	17.034	0.005	7	18.883	0.015	9
148	2575.514	3219.493	7:38:02.83	38:53:42.6	20.372	0.008	9	20.027	0.011	8	20.228	0.010	8	20.572	0.008	9
149	2575.735	1717.153	7:38:20.91	38:53:42.8	19.953	0.013	11	18.930	0.010	10	19.462	0.008	9	20.773	0.013	9
150	2581.182	3486.587	7:37:59.62	38:53:41.8	20.032	0.010	9	19.946	0.011	8	20.013	0.009	9	20.045	0.014	10
151	2587.637	2243.073	7:38:14.58	38:53:41.1	18.836	0.008	12	17.701	0.005	11	18.278	0.011	10	19.771	0.013	11
152	2590.294	1557.072	7:38:22.83	38:53:40.8	18.489	0.004	12	17.327	0.004	11	17.914	0.006	10	19.473	0.010	10
153	2590.719	3013.585	7:38:05.31	38:53:40.5	18.379	0.003	12	17.189	0.004	12	17.781	0.007	10	19.409	0.005	10
154	2597.544	3142.151	7:38:03.76	38:53:39.6	18.733	0.004	13	17.585	0.003	13	18.165	0.007	9	19.678	0.005	10
155	2607.045	2659.605	7:38:09.57	38:53:38.3	17.527	0.008	12	16.127	0.006	11	16.807	0.008	10	18.824	0.010	12
156	2612.898	3526.640	7:37:59.14	38:53:37.3	20.980	0.008	10	20.033	0.009	10	20.526	0.008	6	21.656	0.013	7
157	2613.248	3132.959	7:38:03.87	38:53:37.4	19.777	0.003	13	18.740	0.004	13	19.281	0.012	9	20.585	0.010	8
158	2622.410	2728.487	7:38:08.74	38:53:36.1	18.700	0.003	13	17.556	0.004	12	18.139	0.003	12	19.676	0.006	15
159	2627.427	2395.273	7:38:12.75	38:53:35.5	17.550	0.005	13	16.143	0.005	12	16.836	0.004	14	18.863	0.005	17
160	2628.817	2622.162	7:38:10.02	38:53:35.3	19.048	0.010	12	17.971	0.007	12	18.511	0.009	13	19.945	0.011	14
161	2630.391	3120.647	7:38:04.02	38:53:34.9	19.220	0.007	12	18.182	0.009	13	18.731	0.005	13	20.048	0.012	14
162	2630.474	1668.352	7:38:21.50	38:53:35.2	20.473	0.008	11	19.496	0.006	11	20.018	0.006	12	21.272	0.012	12
163	2631.303	3611.097	7:37:58.12	38:53:34.7	19.152	0.006	12	18.026	0.004	12	18.609	0.006	13	20.070	0.011	13
164	2631.922	2978.520	7:38:05.73	38:53:34.8	18.466	0.006	11	17.288	0.008	10	17.886	0.004	13	19.495	0.006	16
165	2637.372	2050.045	7:38:16.91	38:53:34.1	17.623	0.004	13	16.249	0.006	12	16.930	0.003	14	18.881	0.005	17
166	2638.737	2823.540	7:38:07.60	38:53:33.8	17.501	0.013	13	16.121	0.009	12	16.803	0.008	14	18.831	0.011	16
167	2640.199	2701.366	7:38:09.07	38:53:33.6	20.076	0.010	10	19.088	0.010	10	19.594	0.006	9	20.876	0.009	8
168	2642.671	2882.730	7:38:06.89	38:53:33.3	17.394	0.006	13	15.939	0.008	12	16.651	0.007	13	18.738	0.012	15
169	2647.442	3040.151	7:38:04.99	38:53:32.6	20.126	0.005	12	19.137	0.008	12	19.647	0.009	13	20.960	0.009	12
170	2648.555	3883.611	7:37:54.85	38:53:32.2	17.563	0.004	13	16.574	0.003	13	17.064	0.004	13	18.451	0.009	15
171	2651.040	2931.875	7:38:06.30	38:53:32.1	19.987	0.007	9	18.971	0.009	9	19.485	0.009	10	20.816	0.011	9
172	2652.426	3440.039	7:38:00.18	38:53:31.8	20.071	0.007	12	19.079	0.010	12	19.589	0.008	12	20.823	0.011	12
173	2654.873	2712.201	7:38:08.94	38:53:31.6	18.361	0.005	14	17.175	0.003	13	17.780	0.003	14	19.383	0.006	15
174	2659.999	3142.509	7:38:03.76	38:53:30.8	19.997	0.008	9	20.069	0.008	10	20.050	0.009	10	19.980	0.015	13
175	2660.697	2975.521	7:38:05.77	38:53:30.7	20.199	0.008	9	19.732	0.011	8	20.017	0.006	10	20.501	0.014	14
176	2665.516	2580.770	7:38:10.52	38:53:30.1	20.475	0.012	9	19.597	0.013	8	20.068	0.010	9	21.151	0.014	9
177	2666.709	3640.719	7:37:57.77	38:53:29.7	18.166	0.006	13	16.963	0.005	13	17.559	0.003	13	19.196	0.008	14
178	2670.236	3492.958	7:37:59.55	38:53:29.3	18.043	0.003	13	16.783	0.004	13	17.410	0.003	13	19.147	0.008	14
179	2672.025	2541.543	7:38:11.00	38:53:29.2	18.366	0.004	12	17.158	0.003	13	17.765	0.004	13	19.425	0.008	11

Table 3—Continued

Star ID	X (pix)	Y (pix)	R.A. (J2000)	Decl. (J2000)	$< V >$	$\epsilon(V)$	n_V	$< I >$	$\epsilon(I)$	n_I	$< R >$	$\epsilon(R)$	n_R	$< B >$	$\epsilon(B)$	n_B
180	2674.746	1887.958	7:38:18.86	38:53:28.9	19.501	0.004	11	18.444	0.003	13	18.985	0.004	12	20.373	0.011	13
181	2676.287	3753.412	7:37:56.42	38:53:28.4	18.324	0.004	13	17.086	0.002	13	17.709	0.005	13	19.392	0.011	12
182	2678.671	3025.896	7:38:05.17	38:53:28.2	17.916	0.003	12	16.624	0.004	13	17.267	0.005	13	19.097	0.006	11
183	2678.972	2842.786	7:38:07.37	38:53:28.2	18.068	0.007	11	16.822	0.005	12	17.434	0.005	12	19.183	0.005	13
184	2679.626	2385.952	7:38:12.87	38:53:28.2	20.505	0.006	10	20.167	0.014	9	20.401	0.010	10	20.760	0.010	11
185	2680.717	3342.758	7:38:01.36	38:53:27.8	19.767	0.005	12	18.732	0.007	11	19.262	0.005	12	20.601	0.011	13
186	2688.889	3452.160	7:38:00.04	38:53:26.7	20.226	0.006	11	19.231	0.005	11	19.748	0.005	9	21.040	0.014	10
187	2691.077	3236.220	7:38:02.64	38:53:26.4	19.768	0.005	12	18.718	0.011	12	19.259	0.006	12	20.605	0.012	12
188	2694.087	2002.625	7:38:17.48	38:53:26.2	18.615	0.005	13	17.470	0.004	13	18.048	0.002	13	19.575	0.013	12
189	2699.374	3067.135	7:38:04.67	38:53:25.3	19.323	0.003	12	18.250	0.011	12	18.811	0.005	12	20.234	0.012	13
190	2701.270	3392.282	7:38:00.76	38:53:24.9	19.539	0.005	10	18.742	0.007	10	19.163	0.007	11	20.144	0.014	10
191	2701.385	3033.684	7:38:05.08	38:53:25.0	19.243	0.005	13	18.183	0.014	13	18.729	0.004	12	20.131	0.010	12
192	2701.590	3145.675	7:38:03.73	38:53:24.9	18.142	0.005	13	16.922	0.006	13	17.532	0.006	13	19.206	0.011	11
193	2705.275	2136.064	7:38:15.88	38:53:24.6	20.015	0.006	9	19.001	0.012	10	19.516	0.004	11	20.864	0.011	8
194	2708.017	2646.198	7:38:09.74	38:53:24.1	18.233	0.008	12	17.024	0.006	12	17.642	0.009	11	19.309	0.015	6
195	2710.932	2872.107	7:38:07.02	38:53:23.7	18.628	0.006	12	17.485	0.005	12	18.057	0.004	11	19.627	0.011	11
196	2713.363	3385.599	7:38:00.84	38:53:23.2	20.006	0.003	10	18.997	0.010	10	19.508	0.009	11	20.884	0.010	10
197	2714.352	3431.102	7:38:00.30	38:53:23.1	19.533	0.005	11	18.469	0.006	11	19.018	0.007	12	20.414	0.009	8
198	2716.347	2684.610	7:38:09.28	38:53:22.9	19.407	0.012	11	18.329	0.011	11	18.900	0.008	11	20.320	0.012	4
199	2723.051	2325.599	7:38:13.60	38:53:22.1	19.771	0.008	13	18.765	0.013	11	19.286	0.010	13	20.592	0.013	11
200	2728.731	2922.500	7:38:06.42	38:53:21.2	18.694	0.004	13	17.542	0.005	13	18.135	0.004	13	19.705	0.010	12
201	2731.518	2289.717	7:38:14.03	38:53:20.9	20.003	0.006	13	19.021	0.014	12	19.518	0.008	13	20.757	0.014	11
202	2732.225	2199.723	7:38:15.11	38:53:20.8	20.436	0.011	11	19.506	0.006	9	19.991	0.009	13	21.160	0.009	12
203	2732.971	2359.786	7:38:13.19	38:53:20.7	18.504	0.006	14	17.316	0.007	13	17.913	0.003	14	19.538	0.006	14
204	2735.226	3190.969	7:38:03.19	38:53:20.2	19.906	0.007	12	18.876	0.005	13	19.414	0.008	13	20.747	0.011	12
205	2736.227	3429.187	7:38:00.32	38:53:20.0	19.073	0.003	13	18.062	0.003	13	18.586	0.005	13	19.866	0.010	15
206	2736.286	2963.487	7:38:05.92	38:53:20.1	19.299	0.008	13	18.272	0.010	13	18.810	0.008	13	20.138	0.012	13
207	2738.229	2762.438	7:38:08.34	38:53:19.9	17.781	0.007	13	16.459	0.003	14	17.110	0.008	13	18.980	0.011	6
208	2740.960	3280.778	7:38:02.11	38:53:19.4	19.394	0.005	12	18.380	0.006	11	18.902	0.004	13	20.203	0.013	14
209	2742.266	2166.611	7:38:15.51	38:53:19.4	19.346	0.006	13	18.273	0.005	12	18.823	0.003	14	20.235	0.011	14
210	2745.635	3215.007	7:38:02.90	38:53:18.7	19.732	0.009	13	18.703	0.008	12	19.230	0.005	12	20.554	0.009	13
211	2750.395	3035.862	7:38:05.05	38:53:18.1	19.127	0.005	13	18.026	0.005	13	18.598	0.005	13	20.039	0.013	13
212	2756.171	3106.604	7:38:04.20	38:53:17.3	19.073	0.005	14	18.177	0.004	13	18.652	0.006	13	19.729	0.011	15
213	2757.296	2973.804	7:38:05.80	38:53:17.1	18.881	0.006	12	17.758	0.007	13	18.335	0.004	13	19.830	0.007	14
214	2758.048	1993.214	7:38:17.60	38:53:17.2	19.156	0.003	14	18.058	0.004	13	18.620	0.005	14	20.075	0.014	16
215	2758.217	2708.870	7:38:08.99	38:53:17.1	18.290	0.004	13	17.106	0.010	12	17.706	0.006	13	19.318	0.013	13
216	2759.170	1836.778	7:38:19.48	38:53:17.0	17.562	0.002	13	16.591	0.004	12	17.076	0.003	14	18.406	0.012	17
217	2760.295	2073.314	7:38:16.63	38:53:16.9	19.918	0.006	12	18.911	0.006	10	19.432	0.009	13	20.731	0.011	13
218	2761.806	3279.408	7:38:02.13	38:53:16.4	18.609	0.005	12	17.509	0.005	10	18.056	0.004	12	19.512	0.015	15
219	2765.559	3208.918	7:38:02.97	38:53:15.9	20.615	0.010	10	19.653	0.006	11	20.155	0.005	11	21.370	0.014	12
220	2766.428	3325.039	7:38:01.58	38:53:15.8	19.197	0.003	12	18.112	0.005	12	18.669	0.003	14	20.083	0.010	14
221	2767.260	2909.479	7:38:06.58	38:53:15.8	18.192	0.006	13	16.991	0.006	13	17.596	0.012	13	19.230	0.010	11
222	2768.448	3295.853	7:38:01.93	38:53:15.5	17.275	0.010	13	15.783	0.007	12	16.499	0.007	14	18.639	0.009	17
223	2770.745	2702.362	7:38:09.07	38:53:15.3	18.845	0.006	13	17.708	0.009	12	18.293	0.008	13	19.789	0.014	11
224	2773.920	2397.246	7:38:12.74	38:53:14.9	17.852	0.004	13	16.581	0.005	13	17.220	0.005	13	19.016	0.012	13
225	2775.105	2223.713	7:38:14.83	38:53:14.8	19.179	0.004	13	18.094	0.003	12	18.646	0.005	13	20.081	0.011	15
226	2779.800	2205.141	7:38:15.05	38:53:14.1	18.862	0.003	12	17.716	0.007	11	18.294	0.003	12	19.838	0.012	14
227	2782.583	3463.544	7:37:59.91	38:53:13.5	20.109	0.006	12	19.113	0.008	13	19.624	0.004	13	20.868	0.009	10
228	2783.781	2177.397	7:38:15.38	38:53:13.5	20.532	0.006	11	19.609	0.007	9	20.096	0.014	12	21.250	0.012	12
229	2785.031	2330.499	7:38:13.54	38:53:13.4	19.405	0.004	12	18.357	0.006	13	18.901	0.014	13	20.247	0.011	10
230	2789.770	2514.874	7:38:11.33	38:53:12.7	17.755	0.005	14	16.397	0.005	13	17.067	0.003	14	18.995	0.004	17
231	2791.982	3007.196	7:38:05.40	38:53:12.3	19.108	0.007	11	18.217	0.006	12	18.696	0.004	13	19.757	0.007	13
232	2804.908	2662.471	7:38:09.55	38:53:10.5	18.229	0.005	12	17.062	0.010	11	17.650	0.006	10	19.222	0.012	8
233	2805.166	2371.923	7:38:13.05	38:53:10.5	18.644	0.005	14	17.466	0.008	13	18.062	0.005	14	19.653	0.015	14
234	2805.923	2215.874	7:38:14.92	38:53:10.4	18.118	0.003	13	16.857	0.005	12	17.488	0.003	13	19.238	0.012	14
235	2806.198	2283.526	7:38:14.11	38:53:10.4	19.091	0.004	12	17.969	0.007	12	18.534	0.003	13	20.030	0.009	15
236	2806.999	2906.035	7:38:06.62	38:53:10.2	19.135	0.008	12	18.097	0.006	11	18.627	0.009	11	19.970	0.005	11
237	2808.084	3408.422	7:38:00.58	38:53:09.9	20.341	0.007	10	19.416	0.005	10	19.883	0.005	13	21.043	0.010	12
238	2809.008	3550.632	7:37:58.87	38:53:09.7	20.421	0.005	12	19.517	0.006	12	19.976	0.008	12	21.174	0.011	12
239	2810.015	3527.414	7:37:59.15	38:53:09.6	19.760	0.010	12	18.724	0.006	12	19.250	0.005	14	20.575	0.011	13

Table 3—Continued

Star ID	X (pix)	Y (pix)	R.A. (J2000)	Decl. (J2000)	< V >	$\epsilon(V)$	n_V	< I >	$\epsilon(I)$	n_I	< R >	$\epsilon(R)$	n_R	< B >	$\epsilon(B)$	n_B
240	2812.261	2204.503	7:38:15.06	38:53:09.5	19.412	0.006	12	18.367	0.005	12	18.892	0.008	12	20.268	0.013	11
241	2814.347	2610.236	7:38:10.18	38:53:09.2	17.389	0.006	13	15.923	0.005	12	16.637	0.004	14	18.755	0.009	16
242	2816.702	2793.309	7:38:07.98	38:53:08.8	17.618	0.005	10	16.327	0.007	12	16.969	0.008	10	18.774	0.007	8
243	2821.010	3307.463	7:38:01.79	38:53:08.1	20.145	0.013	11	19.164	0.010	11	19.654	0.010	13	20.892	0.009	13
244	2824.955	2629.140	7:38:09.95	38:53:07.7	19.005	0.011	11	18.059	0.006	9	18.567	0.011	13	19.750	0.014	14
245	2826.870	2596.069	7:38:10.35	38:53:07.4	18.602	0.008	13	17.438	0.010	12	18.029	0.005	13	19.623	0.014	13
246	2828.896	1859.012	7:38:19.22	38:53:07.2	20.204	0.005	12	19.201	0.007	11	19.706	0.007	13	21.015	0.011	12
247	2833.396	2518.093	7:38:11.29	38:53:06.5	18.903	0.006	10	17.798	0.006	9	18.355	0.005	12	19.825	0.010	13
248	2836.067	3634.760	7:37:57.86	38:53:05.9	18.424	0.007	13	17.208	0.002	12	17.823	0.004	13	19.466	0.012	15
249	2836.936	3600.481	7:37:58.27	38:53:05.8	20.144	0.008	12	19.139	0.008	11	19.646	0.005	13	20.920	0.012	13
250	2840.201	2361.167	7:38:13.18	38:53:05.6	18.008	0.003	14	16.723	0.005	13	17.358	0.002	14	19.146	0.006	17
251	2842.929	1750.939	7:38:20.52	38:53:05.3	20.799	0.006	11	19.845	0.015	9	20.344	0.007	11	21.539	0.013	12
252	2844.810	3766.540	7:37:56.27	38:53:04.7	20.500	0.008	7	19.530	0.006	7	20.040	0.005	12	21.267	0.014	13
253	2845.892	833.868	7:38:31.55	38:53:04.9	19.519	0.008	12	17.368	0.009	11	18.488	0.012	8	20.993	0.011	7
254	2847.015	2721.644	7:38:08.84	38:53:04.6	18.728	0.013	10	17.594	0.014	10	18.183	0.007	11	19.767	0.012	12
255	2848.076	1671.619	7:38:21.47	38:53:04.6	20.711	0.005	11	19.734	0.012	9	20.240	0.005	12	21.493	0.012	11
256	2849.273	1356.499	7:38:25.26	38:53:04.4	18.445	0.003	14	17.235	0.005	14	17.839	0.004	14	19.484	0.006	17
257	2850.395	3054.536	7:38:04.84	38:53:04.0	18.871	0.010	11	17.735	0.008	11	18.321	0.008	14	19.882	0.011	15
258	2851.586	1993.210	7:38:17.61	38:53:04.0	19.328	0.005	12	18.250	0.006	12	18.795	0.005	12	20.198	0.014	15
259	2853.189	3282.014	7:38:02.10	38:53:03.6	17.831	0.004	11	16.685	0.003	11	17.258	0.003	14	18.830	0.006	16
260	2854.042	2970.296	7:38:05.85	38:53:03.5	19.531	0.008	8	18.500	0.007	8	19.027	0.006	11	20.405	0.010	12
261	2858.010	2125.578	7:38:16.01	38:53:03.1	20.296	0.010	10	19.296	0.008	10	19.811	0.005	13	21.095	0.012	12
262	2858.083	2956.932	7:38:06.01	38:53:03.0	19.076	0.008	9	18.006	0.009	7	18.551	0.006	12	19.994	0.009	10
263	2865.388	2503.563	7:38:11.47	38:53:02.0	18.516	0.012	10	17.370	0.011	9	17.949	0.005	13	19.461	0.009	15
264	2867.423	2820.190	7:38:07.66	38:53:01.7	18.204	0.006	10	16.980	0.010	9	17.605	0.005	13	19.328	0.014	12
265	2869.052	2966.097	7:38:05.90	38:53:01.4	19.271	0.008	8	18.226	0.005	8	18.754	0.004	11	20.181	0.008	12
266	2869.516	3510.324	7:37:59.36	38:53:01.3	19.641	0.006	11	18.677	0.004	11	19.181	0.007	14	20.387	0.010	15
267	2870.070	2182.560	7:38:15.33	38:53:01.4	20.417	0.011	7	20.172	0.015	6	20.329	0.009	11	20.620	0.013	15
268	2870.935	3269.245	7:38:02.26	38:53:01.1	19.282	0.007	10	18.579	0.012	10	18.953	0.005	13	19.815	0.009	15
269	2871.056	2767.975	7:38:08.29	38:53:01.2	18.180	0.009	10	16.941	0.010	10	17.575	0.008	13	19.296	0.011	12
270	2872.935	2904.213	7:38:06.65	38:53:00.9	17.969	0.003	7	16.722	0.007	9	17.343	0.007	12	19.072	0.013	10
271	2873.311	3080.400	7:38:04.53	38:53:00.8	20.084	0.009	8	19.110	0.013	8	19.604	0.009	12	20.856	0.008	12
272	2874.409	3027.719	7:38:05.16	38:53:00.7	18.616	0.004	10	17.509	0.008	10	18.081	0.005	13	19.555	0.012	15
273	2889.153	3682.562	7:37:57.29	38:52:58.5	18.957	0.006	10	17.855	0.005	11	18.417	0.005	14	19.852	0.008	15
274	2890.369	2483.948	7:38:11.71	38:52:58.5	18.559	0.007	10	17.378	0.008	9	17.975	0.003	13	19.613	0.010	14
275	2891.123	3392.102	7:38:00.78	38:52:58.2	18.577	0.004	11	17.412	0.005	10	17.995	0.005	14	19.579	0.009	15
276	2891.803	1736.337	7:38:20.70	38:52:58.4	19.656	0.004	10	18.629	0.006	9	19.152	0.004	14	20.513	0.012	15
277	2901.860	2336.179	7:38:13.48	38:52:56.9	17.576	0.008	11	16.214	0.006	10	16.886	0.005	14	18.879	0.010	17
278	2901.941	3336.619	7:38:01.45	38:52:56.7	20.008	0.005	12	18.992	0.008	12	19.513	0.005	13	20.821	0.010	13
279	2905.639	2678.405	7:38:09.37	38:52:56.3	17.924	0.005	9	16.731	0.008	9	17.342	0.009	13	18.965	0.013	16
280	2908.754	2021.224	7:38:17.27	38:52:56.0	20.034	0.012	10	19.050	0.006	9	19.564	0.004	13	20.827	0.011	12
281	2908.966	1519.684	7:38:23.31	38:52:56.0	20.068	0.006	10	19.069	0.005	8	19.583	0.010	13	20.917	0.012	11
282	2913.894	3105.334	7:38:04.23	38:52:55.1	18.791	0.003	12	17.692	0.003	13	18.252	0.003	14	19.699	0.008	14
283	2917.205	3259.064	7:38:02.38	38:52:54.6	18.676	0.005	14	17.574	0.004	14	18.132	0.005	14	19.595	0.010	15
284	2918.155	2422.784	7:38:12.44	38:52:54.6	19.745	0.006	9	18.788	0.010	9	19.281	0.007	9	20.512	0.012	12
285	2918.821	2202.296	7:38:15.10	38:52:54.6	19.457	0.012	13	18.385	0.004	12	18.934	0.003	14	20.355	0.012	15
286	2919.350	3315.901	7:38:01.70	38:52:54.3	19.770	0.005	13	18.827	0.005	13	19.314	0.006	13	20.495	0.012	14
287	2921.061	3901.004	7:37:54.66	38:52:53.9	20.694	0.006	9	20.560	0.013	9	20.652	0.006	9	20.793	0.015	10
288	2926.912	2527.321	7:38:11.19	38:52:53.4	19.225	0.008	10	18.203	0.007	9	18.708	0.005	11	20.034	0.007	11
289	2927.776	3709.709	7:37:56.96	38:52:53.0	20.494	0.005	10	20.280	0.008	9	20.429	0.009	13	20.678	0.012	15
290	2941.608	3053.240	7:38:04.86	38:52:51.2	18.657	0.005	13	17.541	0.004	13	18.107	0.005	13	19.607	0.009	15
291	2942.946	3035.665	7:38:05.07	38:52:51.0	18.723	0.006	13	17.574	0.008	13	18.152	0.005	13	19.708	0.011	14
292	2946.402	2271.323	7:38:14.27	38:52:50.7	20.658	0.006	10	19.716	0.008	9	20.209	0.006	10	21.415	0.009	12
293	2948.401	2937.946	7:38:06.25	38:52:50.3	18.094	0.004	11	16.822	0.004	12	17.459	0.003	12	19.229	0.003	12
294	2950.221	2172.613	7:38:15.46	38:52:50.2	18.082	0.004	14	16.847	0.003	13	17.456	0.002	14	19.158	0.004	17
295	2952.372	2231.208	7:38:14.75	38:52:49.8	19.316	0.003	13	18.218	0.003	11	18.769	0.004	13	20.235	0.005	15
296	2952.772	2606.763	7:38:10.23	38:52:49.7	18.976	0.013	11	17.821	0.010	10	18.401	0.007	12	19.940	0.015	9
297	2959.064	3671.742	7:37:57.42	38:52:48.6	20.573	0.007	10	19.601	0.005	10	20.104	0.008	10	21.346	0.011	11
298	2962.317	3435.866	7:38:00.26	38:52:48.2	18.937	0.008	14	17.836	0.002	14	18.395	0.004	14	19.849	0.008	15
299	2963.968	3071.098	7:38:04.65	38:52:48.1	19.104	0.008	12	18.143	0.003	13	18.629	0.003	13	19.893	0.013	13

Table 3—Continued

Star ID	X (pix)	Y (pix)	R.A. (J2000)	Decl. (J2000)	$< V >$	$\epsilon(V)$	n_V	$< I >$	$\epsilon(I)$	n_I	$< R >$	$\epsilon(R)$	n_R	$< B >$	$\epsilon(B)$	n_B
300	2967.306	1795.477	7:38:19.99	38:52:47.8	19.092	0.003	14	18.008	0.002	12	18.554	0.003	14	20.011	0.014	15
301	2967.714	1485.821	7:38:23.72	38:52:47.8	19.801	0.008	13	18.769	0.003	12	19.299	0.003	13	20.634	0.013	14
302	2973.937	2049.969	7:38:16.93	38:52:46.8	20.521	0.011	9	19.582	0.006	8	20.068	0.005	9	21.294	0.014	11
303	2973.949	3838.618	7:37:55.42	38:52:46.5	20.284	0.006	10	19.272	0.011	10	19.791	0.004	11	21.072	0.013	12
304	2974.293	3327.998	7:38:01.56	38:52:46.6	19.607	0.006	13	18.560	0.005	13	19.101	0.005	13	20.453	0.007	14
305	2975.884	2064.633	7:38:16.76	38:52:46.6	20.492	0.009	10	20.229	0.011	9	20.401	0.009	12	20.708	0.015	12
306	2979.568	2865.794	7:38:07.12	38:52:45.9	18.611	0.007	12	17.446	0.006	13	18.037	0.006	12	19.631	0.012	12
307	2982.954	2352.608	7:38:13.29	38:52:45.5	20.629	0.007	10	19.689	0.010	9	20.182	0.008	10	21.388	0.011	10
308	2983.841	2820.725	7:38:07.66	38:52:45.3	17.814	0.010	12	16.487	0.007	12	17.165	0.009	13	19.055	0.010	13
309	2986.198	3086.600	7:38:04.46	38:52:44.9	19.507	0.010	13	18.602	0.013	13	19.077	0.011	13	20.209	0.009	12
310	2991.501	3624.014	7:37:58.00	38:52:44.1	20.711	0.006	10	19.772	0.007	10	20.261	0.005	10	21.453	0.010	11
311	2992.191	2190.661	7:38:15.24	38:52:44.3	19.233	0.004	14	18.374	0.007	12	18.807	0.005	14	20.001	0.007	15
312	3001.796	2888.390	7:38:06.85	38:52:42.8	19.023	0.007	11	17.991	0.007	11	18.523	0.011	12	19.953	0.013	12
313	3003.017	3293.614	7:38:01.98	38:52:42.5	20.286	0.007	11	19.294	0.007	12	19.812	0.006	11	21.094	0.013	12
314	3003.901	2050.982	7:38:16.92	38:52:42.6	20.745	0.006	10	19.798	0.006	9	20.300	0.012	10	21.541	0.015	12
315	3007.856	1320.311	7:38:25.71	38:52:42.1	19.906	0.006	13	19.099	0.005	12	19.519	0.004	13	20.514	0.014	13
316	3011.689	3062.030	7:38:04.76	38:52:41.4	20.042	0.010	11	19.033	0.009	11	19.554	0.009	6	20.906	0.011	6
317	3011.819	2554.253	7:38:10.87	38:52:41.4	17.576	0.005	13	16.651	0.006	12	17.102	0.003	13	18.433	0.006	16
318	3014.501	2304.194	7:38:13.88	38:52:41.1	20.535	0.008	10	20.342	0.015	9	20.487	0.011	10	20.688	0.010	12
319	3017.881	1297.774	7:38:25.98	38:52:40.7	19.899	0.005	13	18.880	0.004	12	19.395	0.003	13	20.717	0.013	15
320	3018.067	2276.382	7:38:14.21	38:52:40.6	20.198	0.005	11	19.235	0.007	11	19.724	0.012	13	20.978	0.012	12
321	3019.947	3558.196	7:37:58.79	38:52:40.1	20.935	0.010	10	19.995	0.005	10	20.489	0.007	10	21.694	0.011	12
322	3020.606	3370.612	7:38:01.05	38:52:40.1	19.745	0.008	10	18.807	0.011	10	19.303	0.010	12	20.499	0.011	12
323	3026.708	2728.981	7:38:08.77	38:52:39.3	18.489	0.008	10	17.397	0.009	11	17.955	0.015	7	19.323	0.012	7
324	3042.431	3735.216	7:37:56.67	38:52:36.9	19.530	0.006	12	17.645	0.005	12	18.574	0.005	12	20.965	0.005	10
325	3047.406	2252.652	7:38:14.50	38:52:36.5	19.799	0.009	10	18.805	0.007	10	19.310	0.003	12	20.637	0.010	10
326	3048.083	2978.596	7:38:05.77	38:52:36.3	18.860	0.006	12	17.768	0.004	12	18.301	0.008	11	19.787	0.009	9
327	3050.733	2359.666	7:38:13.21	38:52:36.0	19.286	0.005	10	18.221	0.008	9	18.759	0.005	9	20.191	0.011	10
328	3052.344	2218.667	7:38:14.91	38:52:35.8	18.722	0.004	13	17.626	0.004	12	18.173	0.003	13	19.646	0.014	13
329	3054.844	2278.060	7:38:14.19	38:52:35.4	17.501	0.007	12	16.081	0.005	11	16.764	0.007	13	18.810	0.005	14
330	3055.063	3136.669	7:38:03.87	38:52:35.3	20.508	0.014	10	19.533	0.005	9	20.031	0.008	9	21.315	0.014	9
331	3055.134	3351.180	7:38:01.29	38:52:35.2	19.656	0.006	11	18.711	0.008	10	19.198	0.006	12	20.418	0.010	12
332	3056.110	2070.832	7:38:16.69	38:52:35.3	18.135	0.005	13	16.908	0.005	12	17.519	0.003	13	19.260	0.011	15
333	3061.978	3244.333	7:38:02.57	38:52:34.3	19.990	0.005	11	19.036	0.010	11	19.503	0.007	11	20.733	0.011	11
334	3063.053	3147.414	7:38:03.74	38:52:34.1	20.076	0.006	10	19.067	0.005	10	19.585	0.007	10	20.926	0.012	10
335	3067.059	2842.205	7:38:07.41	38:52:33.6	19.456	0.014	10	18.634	0.005	8	19.072	0.013	9	19.995	0.010	6
336	3067.862	2936.308	7:38:06.28	38:52:33.5	18.468	0.004	12	17.295	0.002	12	17.875	0.004	12	19.485	0.006	12
337	3069.227	2882.365	7:38:06.93	38:52:33.3	19.565	0.005	8	18.535	0.006	7	19.058	0.009	9	20.443	0.012	9
338	3071.794	2781.315	7:38:08.14	38:52:33.0	18.410	0.009	12	17.213	0.011	12	17.822	0.012	11	19.425	0.006	12
339	3074.105	2962.633	7:38:05.96	38:52:32.6	17.911	0.003	12	16.636	0.003	13	17.266	0.002	12	19.061	0.004	13
340	3075.888	2271.980	7:38:14.27	38:52:32.5	18.489	0.005	12	17.288	0.007	11	17.883	0.004	13	19.530	0.005	14
341	3080.605	3214.583	7:38:02.93	38:52:31.7	20.487	0.008	10	19.496	0.005	10	20.001	0.009	11	21.274	0.008	10
342	3081.979	3051.287	7:38:04.90	38:52:31.5	17.814	0.002	13	16.501	0.003	13	17.149	0.007	13	19.002	0.009	12
343	3083.601	3304.854	7:38:01.85	38:52:31.2	18.484	0.004	13	17.351	0.003	13	17.914	0.003	13	19.437	0.005	13
344	3087.927	1889.154	7:38:18.88	38:52:30.8	18.447	0.005	13	17.261	0.004	12	17.847	0.003	13	19.472	0.008	13
345	3090.723	3007.347	7:38:05.43	38:52:30.3	19.877	0.008	11	19.090	0.006	10	19.512	0.007	11	20.480	0.011	10
346	3093.933	2966.412	7:38:05.92	38:52:29.8	18.688	0.006	12	17.575	0.005	12	18.129	0.003	12	19.646	0.010	9
347	3096.643	2544.414	7:38:10.99	38:52:29.5	18.029	0.005	12	16.783	0.003	11	17.394	0.004	11	19.158	0.009	11
348	3096.915	3540.762	7:37:59.01	38:52:29.3	19.909	0.003	13	18.876	0.003	13	19.406	0.005	13	20.724	0.011	14
349	3097.657	1497.181	7:38:23.59	38:52:29.5	20.804	0.007	10	19.855	0.006	10	20.341	0.006	10	21.581	0.011	10
350	3098.659	2798.733	7:38:07.94	38:52:29.2	19.360	0.011	12	18.309	0.005	12	18.847	0.009	11	20.295	0.014	11
351	3100.491	2560.971	7:38:10.80	38:52:29.0	18.295	0.006	11	17.096	0.002	11	17.694	0.004	11	19.351	0.005	12
352	3101.944	1984.826	7:38:17.73	38:52:28.9	21.191	0.009	10	20.246	0.011	9	20.731	0.006	9	21.914	0.013	11
353	3102.581	2444.051	7:38:12.20	38:52:28.7	18.143	0.005	14	16.911	0.004	13	17.520	0.004	14	19.244	0.003	16
354	3115.450	3339.923	7:38:01.43	38:52:26.7	19.670	0.004	12	18.716	0.004	12	19.207	0.003	13	20.418	0.010	14
355	3115.695	1565.116	7:38:22.77	38:52:27.0	18.650	0.002	14	17.483	0.004	14	18.070	0.003	14	19.668	0.011	16
356	3117.494	3123.754	7:38:04.03	38:52:26.5	19.686	0.009	12	18.719	0.007	12	19.224	0.007	11	20.441	0.010	9
357	3119.168	2242.232	7:38:14.63	38:52:26.4	19.111	0.014	14	18.066	0.005	13	18.599	0.006	14	19.988	0.006	15
358	3123.868	2357.159	7:38:13.25	38:52:25.7	18.846	0.004	14	17.699	0.003	13	18.275	0.005	14	19.840	0.005	15
359	3127.605	2603.009	7:38:10.29	38:52:25.2	19.886	0.013	7	18.918	0.012	8	19.388	0.007	9	20.695	0.015	12

Table 3—Continued

Star ID	X (pix)	Y (pix)	R.A. (J2000)	Decl. (J2000)	$< V >$	$\epsilon(V)$	n_V	$< I >$	$\epsilon(I)$	n_I	$< R >$	$\epsilon(R)$	n_R	$< B >$	$\epsilon(B)$	n_B
360	3133.160	3220.208	7:38:02.87	38:52:24.3	17.590	0.004	12	16.215	0.004	12	16.887	0.003	14	18.860	0.003	15
361	3139.373	50.249	7:38:41.00	38:52:23.7	18.941	0.015	9	17.881	0.007	11	18.417	0.013	7	19.748	0.015	15
362	3142.445	2997.206	7:38:05.55	38:52:23.0	19.734	0.005	13	18.746	0.009	12	19.256	0.009	13	20.544	0.011	13
363	3143.178	1988.872	7:38:17.68	38:52:23.1	19.585	0.005	13	18.596	0.008	12	19.102	0.004	13	20.407	0.011	13
364	3146.317	2782.474	7:38:08.13	38:52:22.5	19.293	0.010	11	18.269	0.008	11	18.792	0.005	9	20.136	0.010	10
365	3147.579	2798.402	7:38:07.94	38:52:22.3	19.829	0.012	10	18.818	0.010	9	19.338	0.012	11	20.654	0.014	10
366	3153.592	3676.313	7:37:57.38	38:52:21.3	20.342	0.008	13	19.360	0.004	13	19.858	0.004	13	21.137	0.014	12
367	3157.935	3361.478	7:38:01.17	38:52:20.8	18.597	0.005	11	17.426	0.003	11	18.017	0.005	12	19.606	0.009	15
368	3159.102	2680.336	7:38:09.36	38:52:20.7	19.231	0.007	13	18.456	0.004	12	18.869	0.007	13	19.774	0.013	15
369	3159.171	3377.250	7:38:00.98	38:52:20.6	18.860	0.004	13	17.713	0.003	13	18.289	0.004	13	19.824	0.008	14
370	3163.851	3110.609	7:38:04.19	38:52:20.0	19.806	0.004	13	18.776	0.004	13	19.299	0.004	13	20.638	0.007	13
371	3166.580	2978.253	7:38:05.78	38:52:19.6	18.150	0.003	13	16.922	0.002	14	17.530	0.002	13	19.240	0.004	15
372	3168.437	2015.647	7:38:17.36	38:52:19.5	21.135	0.006	10	20.181	0.009	9	20.665	0.007	10	21.875	0.012	12
373	3176.177	3128.124	7:38:03.98	38:52:18.2	19.841	0.005	12	18.862	0.010	13	19.357	0.006	13	20.646	0.007	13
374	3176.820	3446.142	7:38:00.16	38:52:18.1	19.316	0.005	13	18.273	0.004	14	18.792	0.008	11	20.130	0.012	8
375	3179.443	2632.629	7:38:09.94	38:52:17.9	19.274	0.006	13	18.160	0.004	12	18.696	0.006	13	20.281	0.010	14
376	3179.744	3071.282	7:38:04.66	38:52:17.7	20.716	0.008	10	20.620	0.013	10	20.694	0.011	10	20.851	0.013	13
377	3180.482	2274.335	7:38:14.25	38:52:17.8	19.536	0.008	13	18.489	0.004	13	19.016	0.005	13	20.449	0.009	15
378	3181.480	2056.199	7:38:16.87	38:52:17.7	17.695	0.003	13	16.230	0.003	12	16.918	0.004	14	18.948	0.006	17
379	3182.509	2919.201	7:38:06.49	38:52:17.4	20.184	0.009	10	19.249	0.008	9	19.722	0.004	11	20.912	0.011	11
380	3183.262	2788.148	7:38:08.07	38:52:17.3	19.582	0.008	11	18.556	0.006	11	19.075	0.004	10	20.450	0.011	11
381	3186.132	2467.876	7:38:11.92	38:52:17.0	19.466	0.004	12	18.403	0.005	10	18.945	0.005	11	20.376	0.014	12
382	3186.323	2876.995	7:38:07.00	38:52:16.9	19.119	0.003	11	18.023	0.003	12	18.572	0.003	11	20.051	0.010	11
383	3188.869	2436.286	7:38:12.30	38:52:16.6	20.069	0.013	10	19.103	0.009	11	19.586	0.014	12	20.836	0.010	9
384	3188.980	2120.872	7:38:16.10	38:52:16.6	20.671	0.006	10	19.696	0.006	9	20.202	0.007	10	21.458	0.014	10
385	3189.907	3470.957	7:37:59.86	38:52:16.2	20.605	0.008	10	20.417	0.012	10	20.548	0.010	10	20.767	0.015	11
386	3190.399	2773.991	7:38:08.24	38:52:16.3	20.203	0.008	10	19.256	0.006	11	19.739	0.006	11	21.000	0.012	11
387	3190.603	2078.092	7:38:16.61	38:52:16.4	19.857	0.006	12	18.831	0.005	11	19.346	0.005	13	20.710	0.010	13
388	3192.855	2398.324	7:38:12.76	38:52:16.0	20.751	0.007	10	19.785	0.006	9	20.289	0.012	10	21.540	0.014	12
389	3195.396	2787.325	7:38:08.08	38:52:15.6	19.679	0.006	11	18.664	0.007	10	19.180	0.005	11	20.508	0.014	11
390	3195.740	3022.010	7:38:05.26	38:52:15.5	20.201	0.009	11	19.393	0.010	10	19.815	0.009	11	20.844	0.014	13
391	3196.490	2660.127	7:38:09.61	38:52:15.5	19.526	0.008	11	18.486	0.009	11	19.021	0.007	12	20.407	0.015	10
392	3199.758	1949.838	7:38:18.15	38:52:15.1	18.701	0.004	13	17.568	0.004	12	18.137	0.003	13	19.668	0.006	16
393	3202.393	3231.250	7:38:02.74	38:52:14.5	18.331	0.004	14	17.118	0.002	14	17.718	0.003	14	19.391	0.006	16
394	3205.035	3808.105	7:37:55.80	38:52:14.0	18.980	0.004	14	17.859	0.004	14	18.429	0.003	14	19.914	0.008	15
395	3205.749	2148.105	7:38:15.77	38:52:14.2	20.489	0.010	10	20.268	0.011	9	20.402	0.009	11	20.687	0.014	14
396	3213.020	2584.794	7:38:10.52	38:52:13.2	17.904	0.004	14	16.614	0.003	14	17.257	0.004	14	19.097	0.007	17
397	3213.787	3189.384	7:38:03.25	38:52:12.9	20.451	0.008	12	19.479	0.006	12	19.976	0.005	12	21.234	0.008	12
398	3215.248	2965.570	7:38:05.94	38:52:12.8	18.475	0.004	13	17.317	0.002	14	17.896	0.003	13	19.478	0.009	15
399	3215.927	2937.227	7:38:06.28	38:52:12.7	18.681	0.003	13	17.533	0.002	13	18.110	0.004	13	19.680	0.007	16
400	3220.536	2553.040	7:38:10.90	38:52:12.1	19.031	0.003	13	18.011	0.004	12	18.530	0.004	13	19.867	0.008	15
401	3222.814	2532.239	7:38:11.15	38:52:11.8	19.470	0.004	13	18.413	0.005	12	18.950	0.005	13	20.351	0.010	14
402	3223.533	2904.757	7:38:06.67	38:52:11.6	20.876	0.008	11	20.001	0.009	11	20.473	0.010	11	21.613	0.009	12
403	3223.601	2747.895	7:38:08.56	38:52:11.6	19.330	0.005	12	18.329	0.007	12	18.839	0.005	12	20.107	0.012	11
404	3224.303	3068.328	7:38:04.70	38:52:11.5	20.140	0.010	12	19.139	0.009	12	19.645	0.005	13	20.963	0.009	12
405	3224.345	3032.891	7:38:05.13	38:52:11.5	19.058	0.006	13	17.992	0.003	13	18.530	0.004	13	19.955	0.012	14
406	3224.423	2450.041	7:38:12.14	38:52:11.6	19.285	0.010	11	18.222	0.008	10	18.765	0.005	13	20.184	0.011	13
407	3227.030	2169.593	7:38:15.51	38:52:11.3	20.623	0.009	10	19.662	0.010	10	20.145	0.010	11	21.364	0.015	12
408	3228.631	1779.511	7:38:20.20	38:52:11.1	18.999	0.002	14	17.888	0.004	13	18.441	0.003	14	19.950	0.013	15
409	3229.784	3113.417	7:38:04.16	38:52:10.7	18.811	0.004	14	17.671	0.003	14	18.233	0.003	14	19.781	0.006	15
410	3231.408	2464.203	7:38:11.97	38:52:10.6	17.660	0.003	13	16.313	0.004	12	16.975	0.005	14	18.924	0.005	15
411	3236.898	1812.871	7:38:19.80	38:52:09.9	20.972	0.006	10	20.034	0.010	9	20.541	0.008	10	21.747	0.014	12
412	3237.095	2681.370	7:38:09.36	38:52:09.8	17.459	0.003	13	16.036	0.004	12	16.729	0.003	14	18.787	0.006	17
413	3238.990	2930.642	7:38:06.36	38:52:09.4	19.083	0.008	12	17.981	0.004	11	18.536	0.005	13	20.003	0.006	14
414	3241.470	2437.097	7:38:12.30	38:52:09.2	18.686	0.004	12	17.541	0.004	12	18.108	0.004	14	19.678	0.006	15
415	3250.175	3338.639	7:38:01.45	38:52:07.8	19.624	0.004	13	18.613	0.004	13	19.136	0.006	13	20.432	0.010	15
416	3252.558	2049.310	7:38:16.96	38:52:07.7	20.161	0.004	12	18.643	0.005	11	19.354	0.005	13	21.461	0.011	12
417	3255.282	3605.440	7:37:58.25	38:52:07.0	19.490	0.004	13	18.444	0.003	13	18.975	0.004	13	20.342	0.010	15
418	3259.775	2922.670	7:38:06.46	38:52:06.5	17.829	0.007	12	16.739	0.003	12	17.246	0.004	13	18.799	0.008	15
419	3262.256	1820.257	7:38:19.72	38:52:06.3	18.113	0.004	14	17.344	0.004	13	17.729	0.003	14	18.798	0.011	16

Table 3—Continued

Star ID	X (pix)	Y (pix)	R.A. (J2000)	Decl. (J2000)	< V >	ϵ(V)	n_V	< I >	ϵ(I)	n_I	< R >	ϵ(R)	n_R	< B >	ϵ(B)	n_B
420	3262.477	3003.032	7:38:05.49	38:52:06.1	20.472	0.010	12	19.522	0.011	10	20.002	0.007	12	21.235	0.012	12
421	3262.875	3179.564	7:38:03.37	38:52:06.0	20.640	0.013	11	19.733	0.005	10	20.207	0.005	12	21.389	0.010	12
422	3263.067	3674.759	7:37:57.41	38:52:05.9	20.036	0.010	13	19.022	0.004	13	19.548	0.009	13	20.837	0.010	15
423	3266.277	2961.234	7:38:05.99	38:52:05.6	17.329	0.005	13	15.891	0.004	12	16.585	0.006	13	18.616	0.014	16
424	3274.426	3262.074	7:38:02.38	38:52:04.4	19.151	0.008	13	18.049	0.004	13	18.601	0.004	12	20.059	0.008	14
425	3277.520	2307.849	7:38:13.85	38:52:04.1	20.533	0.006	10	19.571	0.010	10	20.063	0.012	8	21.275	0.014	9
426	3281.087	2010.215	7:38:17.43	38:52:03.7	18.410	0.005	14	17.250	0.004	13	17.829	0.002	13	19.395	0.008	15
427	3284.513	2894.454	7:38:06.80	38:52:03.1	18.499	0.003	14	17.327	0.004	14	17.913	0.004	13	19.515	0.011	15
428	3289.469	2808.364	7:38:07.84	38:52:02.4	16.528	0.005	11	15.065	0.004	11	15.766	0.005	11	17.727	0.006	14
429	3291.666	2429.411	7:38:12.39	38:52:02.1	18.841	0.004	13	17.735	0.003	13	18.294	0.003	13	19.786	0.006	14
430	3292.397	3463.910	7:37:59.95	38:52:01.8	14.847	0.005	6	13.848	0.006	7	14.330	0.005	7	15.793	0.012	10
431	3296.462	1979.241	7:38:17.81	38:52:01.5	21.010	0.006	10	20.057	0.009	9	20.554	0.006	9	21.778	0.012	11
432	3302.711	2529.669	7:38:11.19	38:52:00.6	20.149	0.010	10	19.181	0.008	10	19.662	0.008	11	20.966	0.010	11
433	3305.412	2878.102	7:38:07.00	38:52:00.1	19.676	0.005	11	18.764	0.004	12	19.230	0.004	12	20.410	0.014	12
434	3307.879	2941.804	7:38:06.23	38:51:59.8	18.815	0.004	13	17.681	0.005	12	18.250	0.004	13	19.776	0.009	14
435	3310.099	3661.845	7:37:57.57	38:51:59.3	20.245	0.006	13	19.255	0.008	13	19.762	0.010	11	21.029	0.013	12
436	3313.317	2915.406	7:38:06.55	38:51:59.0	18.167	0.003	14	16.933	0.002	13	17.544	0.003	13	19.265	0.007	15
437	3316.413	3963.476	7:37:53.95	38:51:58.3	19.121	0.004	12	18.430	0.004	12	18.783	0.006	12	19.699	0.014	14
438	3316.840	2539.620	7:38:11.07	38:51:58.6	19.840	0.008	11	18.818	0.008	12	19.327	0.004	11	20.656	0.013	12
439	3321.182	3804.009	7:37:55.86	38:51:57.7	19.713	0.006	13	18.683	0.003	14	19.208	0.011	13	20.543	0.012	13
440	3322.678	3394.985	7:38:00.78	38:51:57.6	19.331	0.005	12	18.285	0.004	13	18.807	0.004	13	20.182	0.014	14
441	3324.329	3636.132	7:37:57.88	38:51:57.3	17.905	0.003	14	16.612	0.004	14	17.244	0.003	13	19.073	0.003	15
442	3325.038	3186.676	7:38:03.29	38:51:57.3	18.319	0.004	14	17.111	0.002	14	17.705	0.004	13	19.383	0.006	16
443	3329.701	2041.349	7:38:17.06	38:51:56.8	17.750	0.002	14	17.069	0.004	13	17.426	0.003	14	18.299	0.015	17
444	3333.956	1418.470	7:38:24.55	38:51:56.3	18.659	0.003	13	17.493	0.003	13	18.077	0.005	14	19.655	0.008	15
445	3344.448	2958.720	7:38:06.03	38:51:54.6	19.903	0.004	13	18.884	0.003	13	19.400	0.004	13	20.748	0.012	15
446	3348.958	3752.227	7:37:56.49	38:51:53.8	18.866	0.003	14	17.729	0.003	14	18.298	0.005	13	19.824	0.009	14
447	3355.365	2821.642	7:38:07.68	38:51:53.1	19.450	0.003	13	18.386	0.004	13	18.931	0.005	13	20.342	0.012	14
448	3356.492	2534.205	7:38:11.14	38:51:53.0	18.057	0.003	14	16.799	0.004	13	17.418	0.003	14	19.188	0.007	15
449	3356.962	2891.644	7:38:06.84	38:51:52.9	19.756	0.006	13	18.753	0.005	13	19.264	0.009	12	20.592	0.014	13
450	3358.266	3954.271	7:37:54.06	38:51:52.5	20.029	0.010	12	19.026	0.005	12	19.539	0.010	11	20.821	0.013	11
451	3358.314	3393.559	7:38:00.80	38:51:52.6	20.734	0.006	10	20.643	0.011	9	20.702	0.006	10	20.837	0.015	12
452	3358.560	2835.960	7:38:07.51	38:51:52.7	18.785	0.004	11	17.721	0.002	10	18.254	0.005	11	19.665	0.010	14
453	3360.019	3245.638	7:38:02.58	38:51:52.4	20.484	0.009	11	19.573	0.007	11	20.037	0.005	11	21.209	0.012	12
454	3362.510	3165.936	7:38:03.54	38:51:52.0	18.313	0.004	14	17.121	0.002	14	17.716	0.005	14	19.368	0.008	17
455	3371.265	2217.988	7:38:14.94	38:51:51.0	17.416	0.005	12	15.975	0.005	11	16.670	0.005	13	18.753	0.010	15
456	3373.440	2464.810	7:38:11.97	38:51:50.6	20.167	0.009	7	19.382	0.012	7	19.778	0.007	10	20.817	0.014	8
457	3377.530	3122.740	7:38:04.06	38:51:49.9	20.278	0.005	12	19.280	0.010	13	19.787	0.007	13	21.064	0.011	12
458	3379.954	2926.900	7:38:06.42	38:51:49.6	20.674	0.006	10	19.781	0.010	10	20.221	0.009	9	21.388	0.013	11
459	3380.020	1722.359	7:38:20.90	38:51:49.8	17.831	0.005	14	16.541	0.005	14	17.189	0.005	14	19.009	0.010	17
460	3380.095	1996.080	7:38:17.61	38:51:49.8	20.078	0.007	13	19.083	0.006	12	19.591	0.005	13	20.897	0.008	12
461	3383.994	2138.620	7:38:15.90	38:51:49.2	20.137	0.007	13	19.142	0.006	12	19.654	0.006	13	20.948	0.008	11
462	3386.680	3597.665	7:37:58.35	38:51:48.5	19.246	0.003	14	18.167	0.004	14	18.712	0.005	14	20.148	0.013	15
463	3389.527	3850.351	7:37:55.31	38:51:48.1	20.387	0.007	11	19.682	0.015	10	20.028	0.004	11	20.998	0.014	12
464	3391.235	2285.126	7:38:14.14	38:51:48.2	20.461	0.005	12	19.499	0.010	12	19.987	0.005	12	21.238	0.012	12
465	3397.201	537.513	7:38:35.15	38:51:47.4	20.534	0.009	8	18.385	0.007	11	19.512	0.011	9	21.918	0.014	10
466	3407.440	2785.303	7:38:08.12	38:51:45.8	19.860	0.007	13	19.215	0.008	12	19.581	0.006	12	20.300	0.013	14
467	3407.513	2736.060	7:38:08.71	38:51:45.8	19.532	0.006	13	18.479	0.005	13	19.015	0.007	13	20.419	0.011	13
468	3407.514	2525.170	7:38:11.25	38:51:45.8	19.454	0.003	14	18.470	0.004	12	18.968	0.005	11	20.241	0.011	14
469	3411.869	3011.800	7:38:05.40	38:51:45.1	19.661	0.004	12	18.581	0.004	13	19.081	0.006	11	20.954	0.005	11
470	3419.604	3499.736	7:37:59.53	38:51:43.9	20.409	0.008	12	19.441	0.006	12	19.935	0.007	12	21.189	0.010	12
471	3420.473	3769.030	7:37:56.29	38:51:43.8	21.164	0.009	9	20.225	0.013	10	20.691	0.013	7	21.884	0.013	9
472	3423.807	3402.715	7:38:00.70	38:51:43.4	16.535	0.004	11	15.423	0.003	11	15.938	0.005	12	17.548	0.008	15
473	3446.804	2876.539	7:38:07.03	38:51:40.3	18.486	0.004	14	17.333	0.003	14	17.911	0.005	14	19.486	0.009	17
474	3449.775	2672.440	7:38:09.48	38:51:39.9	20.314	0.005	11	19.334	0.005	12	19.836	0.009	13	21.121	0.011	12
475	3456.607	1905.227	7:38:18.71	38:51:39.0	20.983	0.006	10	20.023	0.008	9	20.517	0.008	10	21.745	0.013	11
476	3458.663	2595.381	7:38:10.41	38:51:38.6	19.056	0.009	14	17.986	0.005	13	18.518	0.005	13	19.947	0.012	16
477	3459.074	3097.171	7:38:04.38	38:51:38.5	20.375	0.011	11	19.958	0.009	10	20.214	0.012	13	20.631	0.015	13
478	3467.856	2678.430	7:38:09.41	38:51:37.3	20.372	0.004	10	19.412	0.007	10	19.871	0.008	11	21.541	0.014	11
479	3482.534	2302.878	7:38:13.93	38:51:35.3	20.766	0.007	10	19.822	0.009	10	20.323	0.007	10	21.513	0.015	12

Table 3—Continued

Star ID	X (pix)	Y (pix)	R.A. (J2000)	Decl. (J2000)	$< V >$	$\epsilon(V)$	n_V	$< I >$	$\epsilon(I)$	n_I	$< R >$	$\epsilon(R)$	n_R	$< B >$	$\epsilon(B)$	n_B
480	3491.913	2338.089	7:38:13.51	38:51:34.0	20.664	0.012	10	20.525	0.012	10	20.637	0.011	10	20.807	0.015	13
481	3502.707	2704.295	7:38:09.10	38:51:32.4	20.188	0.006	12	19.193	0.006	11	19.692	0.004	12	21.013	0.010	12
482	3505.578	3091.578	7:38:04.45	38:51:31.9	20.773	0.005	10	19.821	0.010	10	20.306	0.008	10	21.569	0.013	12
483	3506.453	3740.622	7:37:56.64	38:51:31.7	21.229	0.008	10	20.280	0.010	10	20.759	0.006	8	21.976	0.014	10
484	3510.641	3268.118	7:38:02.32	38:51:31.2	18.504	0.004	14	17.325	0.002	14	17.911	0.003	14	19.520	0.010	16
485	3511.110	2320.721	7:38:13.72	38:51:31.3	20.434	0.006	10	20.142	0.012	10	20.326	0.009	10	20.685	0.014	14
486	3511.962	2497.393	7:38:11.59	38:51:31.2	19.450	0.003	13	18.403	0.005	13	18.932	0.004	13	20.331	0.011	14
487	3512.468	3986.610	7:37:53.68	38:51:30.8	19.378	0.007	13	18.315	0.007	12	18.865	0.006	12	20.258	0.014	14
488	3522.185	2437.460	7:38:12.31	38:51:29.7	19.215	0.003	13	18.138	0.004	14	18.687	0.004	13	20.138	0.010	13
489	3523.719	2835.585	7:38:07.53	38:51:29.4	20.778	0.008	10	19.857	0.008	10	20.319	0.007	10	21.474	0.015	11
490	3536.560	2168.291	7:38:15.55	38:51:27.7	19.705	0.006	13	18.761	0.005	11	19.243	0.006	14	20.469	0.011	15
491	3539.080	2647.656	7:38:09.79	38:51:27.3	20.033	0.006	13	19.035	0.004	13	19.542	0.005	12	20.877	0.011	13
492	3541.979	1756.339	7:38:20.51	38:51:27.0	19.964	0.007	13	18.987	0.007	12	19.493	0.005	13	20.778	0.012	14
493	3556.348	2764.937	7:38:08.38	38:51:24.9	19.931	0.005	11	18.915	0.005	11	19.422	0.008	12	20.763	0.011	11
494	3557.394	1573.663	7:38:22.70	38:51:24.9	19.510	0.004	12	18.543	0.005	12	19.037	0.003	13	20.281	0.011	15
495	3557.745	2214.687	7:38:15.00	38:51:24.8	18.818	0.004	14	17.683	0.007	14	18.244	0.003	13	19.803	0.009	16
496	3558.359	3332.381	7:38:01.56	38:51:24.5	19.773	0.008	13	17.808	0.004	13	18.794	0.005	13	21.273	0.008	11
497	3564.144	2754.216	7:38:08.51	38:51:23.8	19.884	0.003	12	18.871	0.005	11	19.385	0.004	12	20.727	0.010	12
498	3564.828	2039.171	7:38:17.11	38:51:23.8	20.100	0.007	13	19.104	0.007	13	19.614	0.004	13	20.930	0.009	13
499	3564.833	3757.060	7:37:56.45	38:51:23.5	17.808	0.004	14	16.476	0.004	14	17.127	0.006	13	19.007	0.005	17
500	3568.368	3398.458	7:38:00.76	38:51:23.1	18.712	0.003	14	17.560	0.003	14	18.132	0.004	14	19.698	0.009	14
501	3568.820	2575.494	7:38:10.66	38:51:23.2	20.333	0.013	12	19.361	0.008	12	19.853	0.004	13	21.122	0.012	12
502	3572.065	2551.771	7:38:10.94	38:51:22.7	20.038	0.003	12	19.042	0.008	13	19.549	0.004	13	20.880	0.014	12
503	3575.671	1965.409	7:38:17.99	38:51:22.3	19.241	0.003	14	18.158	0.004	13	18.708	0.004	13	20.157	0.011	15
504	3578.740	2069.396	7:38:16.74	38:51:21.8	20.363	0.009	13	19.379	0.005	13	19.883	0.008	13	21.165	0.014	12
505	3579.675	2867.614	7:38:07.15	38:51:21.6	21.243	0.008	10	20.346	0.014	10	20.791	0.008	7	21.932	0.012	8
506	3580.038	2663.849	7:38:09.60	38:51:21.6	20.270	0.004	13	19.300	0.006	11	19.788	0.005	12	21.065	0.013	13
507	3586.251	1418.205	7:38:24.58	38:51:20.8	20.012	0.009	12	17.400	0.005	13	18.827	0.007	12	21.695	0.013	9
508	3606.912	3303.829	7:38:01.90	38:51:17.7	19.856	0.003	12	18.844	0.010	13	19.363	0.004	13	20.708	0.008	13
509	3613.539	2583.701	7:38:10.56	38:51:16.9	19.748	0.004	13	18.820	0.005	13	19.290	0.004	13	20.497	0.014	13
510	3616.687	2351.450	7:38:13.36	38:51:16.5	19.383	0.004	14	18.321	0.005	13	18.856	0.007	14	20.274	0.010	15
511	3623.589	3098.395	7:38:04.37	38:51:15.4	15.674	0.003	10	14.812	0.003	10	15.227	0.004	12	16.466	0.012	13
512	3633.465	3256.831	7:38:02.47	38:51:13.9	18.624	0.002	14	17.495	0.003	14	18.068	0.006	14	19.571	0.008	16
513	3642.306	2171.332	7:38:15.52	38:51:12.9	18.402	0.002	14	17.197	0.004	14	17.798	0.005	14	19.482	0.009	16
514	3645.034	1948.764	7:38:18.20	38:51:12.5	19.810	0.003	12	18.213	0.006	13	18.964	0.004	12	21.180	0.011	10
515	3650.779	2688.512	7:38:09.31	38:51:11.6	20.012	0.005	12	19.184	0.009	12	19.595	0.005	13	20.700	0.012	13
516	3657.473	464.290	7:38:36.05	38:51:10.9	17.583	0.006	9	16.547	0.005	11	17.044	0.007	10	18.461	0.011	15
517	3659.829	3214.535	7:38:02.98	38:51:10.2	20.523	0.005	10	20.360	0.010	10	20.446	0.009	11	20.698	0.015	13
518	3659.866	2524.074	7:38:11.28	38:51:10.4	19.706	0.003	14	18.696	0.005	14	19.208	0.004	14	20.529	0.010	14
519	3660.621	849.026	7:38:31.43	38:51:10.4	18.770	0.007	11	17.617	0.004	12	18.182	0.006	13	19.761	0.012	14
520	3660.730	3552.735	7:37:58.91	38:51:10.0	19.915	0.003	13	18.900	0.004	13	19.405	0.007	12	20.737	0.009	12
521	3661.421	3807.505	7:37:55.85	38:51:09.9	19.469	0.006	13	18.459	0.007	13	18.969	0.007	14	20.299	0.012	13
522	3668.701	2966.834	7:38:05.96	38:51:09.0	19.365	0.002	13	18.296	0.003	13	18.832	0.004	14	20.256	0.008	15
523	3669.749	2896.507	7:38:06.81	38:51:08.9	19.430	0.003	12	18.367	0.003	12	18.898	0.006	13	20.306	0.010	13
524	3671.374	2914.734	7:38:06.59	38:51:08.7	20.401	0.014	11	19.436	0.008	13	19.900	0.009	12	21.143	0.007	12
525	3673.633	3116.477	7:38:04.16	38:51:08.3	18.333	0.005	13	17.146	0.003	12	17.735	0.005	14	19.360	0.008	16
526	3678.053	3058.650	7:38:04.86	38:51:07.7	19.193	0.006	13	18.103	0.005	12	18.650	0.004	14	20.108	0.008	15
527	3710.714	1548.674	7:38:23.02	38:51:03.3	19.563	0.008	12	18.542	0.004	12	19.052	0.004	12	20.393	0.014	14
528	3728.458	3114.041	7:38:04.20	38:51:00.6	18.734	0.004	13	17.614	0.003	14	18.173	0.004	14	19.686	0.006	15
529	3729.187	2046.919	7:38:17.03	38:51:00.7	21.302	0.010	10	20.436	0.012	9	20.891	0.008	10	21.990	0.013	11
530	3732.074	1890.151	7:38:18.91	38:51:00.3	19.838	0.004	13	18.819	0.006	13	19.332	0.008	13	20.691	0.010	13
531	3732.144	3040.024	7:38:05.09	38:51:00.1	20.144	0.006	13	19.137	0.006	13	19.638	0.008	13	20.947	0.009	13
532	3749.829	2830.588	7:38:07.61	38:50:57.7	19.441	0.003	14	18.391	0.006	13	18.914	0.004	13	20.304	0.010	15
533	3750.719	2990.539	7:38:05.68	38:50:57.5	19.843	0.008	13	18.838	0.009	13	19.347	0.008	13	20.659	0.013	13
534	3754.940	2448.574	7:38:12.20	38:50:57.0	20.670	0.011	10	20.550	0.012	10	20.623	0.007	11	20.788	0.015	13
535	3763.097	2683.004	7:38:09.38	38:50:55.8	20.003	0.006	12	19.039	0.009	12	19.530	0.006	12	20.817	0.013	13
536	3773.028	3087.080	7:38:04.52	38:50:54.4	20.670	0.007	11	19.728	0.006	11	20.202	0.008	10	21.465	0.015	12
537	3788.455	2949.087	7:38:06.18	38:50:52.2	20.284	0.009	11	19.500	0.007	12	19.894	0.005	12	20.864	0.014	11
538	3788.976	2502.864	7:38:11.55	38:50:52.2	19.817	0.004	12	18.843	0.006	13	19.333	0.005	12	20.645	0.011	12
539	3791.276	3894.140	7:37:54.82	38:50:51.6	19.005	0.004	13	17.941	0.005	13	18.481	0.006	12	19.915	0.013	14

Table 3—Continued

Star ID	X (pix)	Y (pix)	R.A. (J2000)	Decl. (J2000)	$< V >$	$\epsilon(V)$	n_V	$< I >$	$\epsilon(I)$	n_I	$< R >$	$\epsilon(R)$	n_R	$< B >$	$\epsilon(B)$	n_B
540	3820.864	3265.129	7:38:02.39	38:50:47.6	19.784	0.004	12	18.761	0.005	13	19.276	0.004	12	20.636	0.011	14
541	3834.022	2872.601	7:38:07.11	38:50:45.8	19.832	0.006	12	18.826	0.008	11	19.321	0.005	12	20.652	0.009	13
542	3837.032	3014.499	7:38:05.40	38:50:45.4	18.022	0.003	14	16.564	0.003	14	17.230	0.006	13	19.296	0.005	16
543	3851.007	2900.919	7:38:06.77	38:50:43.4	19.125	0.005	14	18.031	0.003	14	18.578	0.003	13	20.052	0.011	14
544	3872.051	3510.678	7:37:59.44	38:50:40.4	20.048	0.009	13	19.046	0.008	13	19.554	0.005	12	20.861	0.012	12
545	3881.709	3948.466	7:37:54.18	38:50:38.9	19.966	0.008	12	18.953	0.006	11	19.470	0.005	10	20.783	0.014	12
546	3883.491	3185.726	7:38:03.35	38:50:38.8	19.940	0.005	14	17.871	0.004	14	18.939	0.006	12	21.471	0.011	10
547	3889.376	2959.990	7:38:06.06	38:50:38.0	20.747	0.005	10	19.777	0.010	10	20.250	0.006	12	21.514	0.007	12
548	3892.067	2162.206	7:38:15.65	38:50:37.8	20.872	0.006	8	19.925	0.007	11	20.420	0.007	10	21.648	0.010	11
549	3899.065	2573.272	7:38:10.71	38:50:36.7	20.053	0.007	12	19.054	0.006	11	19.556	0.004	12	20.881	0.014	13
550	3920.677	2215.085	7:38:15.02	38:50:33.8	20.524	0.007	10	19.556	0.005	13	20.045	0.005	11	21.308	0.012	10
551	3936.133	2672.994	7:38:09.52	38:50:31.5	18.228	0.003	12	17.004	0.004	14	17.607	0.005	13	19.309	0.008	16
552	3978.136	2954.566	7:38:06.13	38:50:25.6	20.335	0.008	10	19.371	0.006	11	19.849	0.005	11	21.092	0.014	13
553	4002.763	3596.358	7:37:58.42	38:50:22.0	20.416	0.012	12	19.459	0.007	9	19.940	0.007	10	21.185	0.012	11
554	4018.465	2750.180	7:38:08.59	38:50:19.9	18.444	0.003	11	17.114	0.004	12	17.735	0.005	11	19.567	0.005	15
555	4035.005	3960.235	7:37:54.05	38:50:17.3	19.730	0.004	11	18.703	0.007	9	19.235	0.007	9	20.569	0.008	11
556	4058.832	2722.466	7:38:08.93	38:50:14.3	19.511	0.007	11	18.467	0.006	12	18.990	0.004	10	20.380	0.008	14
557	4081.384	3073.213	7:38:04.72	38:50:11.0	20.210	0.005	10	19.209	0.008	10	19.709	0.007	10	21.012	0.009	10
558	4121.021	3384.559	7:38:00.98	38:50:05.4	20.965	0.009	8	20.039	0.008	7	20.504	0.007	8	21.703	0.013	11
559	4124.625	3577.061	7:37:58.66	38:50:04.8	18.621	0.003	10	17.680	0.006	11	18.138	0.007	9	19.487	0.008	13

Table 4. Stars in the NGC2419 Field with at least V and I Photometry[a]

X (pix)	Y (pix)	R.A. (J2000)	Decl. (J2000)	$< V >$	$\epsilon(V)$	n_V	$\chi^2_\nu(V)$	$< I >$	$\epsilon(I)$	n_I	$\chi^2_\nu(I)$	$< R >$	$\epsilon(R)$	n_R	$\chi^2_\nu(R)$	$< B >$	$\epsilon(B)$	n_B	$\chi^2_\nu(B)$
12.084	1063.137	7:38:28.60	38:59:43.2	16.207	0.021	2	21.37	15.446	0.004	2	0.13	—	—	0	—	16.812	0.034	2	49.13
42.603	2613.932	7:38:09.91	38:59:38.8	13.195	0.010	4	9.24	12.518	0.005	4	1.14	12.829	0.004	2	0.59	13.625	0.018	4	34.14
53.641	2073.155	7:38:16.43	38:59:37.3	19.744	0.010	4	1.09	18.686	0.019	4	0.27	—	—	0	—	20.553	0.048	2	2.64
70.817	1355.050	7:38:25.08	38:59:34.9	14.686	0.014	2	9.97	14.041	0.006	3	0.51	—	—	0	—	15.172	0.017	3	8.74
88.735	3234.700	7:38:02.44	38:59:32.2	18.979	0.013	4	2.06	18.279	0.036	4	1.57	18.582	0.032	3	1.26	19.410	0.146	2	6.96
94.668	1579.926	7:38:22.37	38:59:31.6	19.797	0.010	4	1.16	18.776	0.018	4	0.47	—	—	0	—	20.627	0.080	2	7.63
100.635	271.525	7:38:38.14	38:59:30.8	16.703	0.031	2	47.05	15.812	0.012	2	6.76	—	—	0	—	—	—	1	—
139.994	489.142	7:38:35.52	38:59:25.2	17.472	0.026	2	28.02	16.954	0.009	2	0.55	—	—	0	—	17.845	0.054	2	32.40
185.257	3910.766	7:37:54.30	38:59:18.4	19.308	0.035	4	13.61	17.553	0.022	3	1.30	18.389	0.018	4	1.00	—	—	0	—
185.263	1811.405	7:38:19.59	38:59:18.8	16.126	0.007	5	4.21	15.371	0.004	5	1.50	—	—	0	—	16.712	0.012	5	10.24
197.430	1536.490	7:38:22.91	38:59:17.1	20.455	0.020	2	0.03	18.287	0.015	2	2.34	—	—	0	—	—	—	1	—
201.919	2615.004	7:38:09.91	38:59:16.4	12.670	0.007	4	5.59	11.997	0.013	4	11.52	12.298	0.004	3	0.39	13.105	0.018	4	34.14
215.781	409.932	7:38:36.48	38:59:14.6	16.151	0.005	3	1.50	15.114	0.007	2	2.20	—	—	0	—	17.042	0.021	3	19.40
233.600	3577.413	7:37:58.32	38:59:11.7	17.245	0.004	5	0.60	16.344	0.007	4	1.25	16.737	0.015	3	4.77	18.107	0.021	5	6.94
235.884	714.516	7:38:32.81	38:59:11.8	19.952	0.141	2	200.34	18.771	0.018	4	0.51	—	—	0	—	—	—	1	—
248.231	1019.940	7:38:29.13	38:59:10.0	19.997	0.049	2	6.23	19.213	0.062	2	0.90	—	—	1	—	—	—	1	—
249.232	2071.773	7:38:16.46	38:59:09.8	20.384	0.020	2	0.71	19.453	0.037	2	1.57	20.039	0.092	2	0.14	—	—	1	—
266.104	3962.359	7:37:53.69	38:59:07.0	12.808	0.008	4	6.02	12.146	0.012	4	4.52	12.447	0.005	4	1.37	13.291	0.013	3	5.25
274.500	1018.282	7:38:29.15	38:59:06.3	14.442	0.013	4	11.69	13.730	0.006	4	1.30	—	—	0	—	15.011	0.010	4	4.38
278.044	3643.064	7:37:57.53	38:59:05.5	20.724	0.033	4	1.38	19.140	0.062	3	0.13	—	—	1	—	—	—	0	—
352.549	3504.873	7:37:59.21	38:58:55.0	19.396	0.010	4	0.76	17.360	0.015	3	0.23	18.391	0.022	3	0.14	—	—	1	—
371.947	2206.228	7:38:14.85	38:58:52.5	18.604	0.009	5	0.44	17.813	0.009	5	0.96	—	—	1	—	19.283	0.026	5	7.38
427.265	3369.039	7:38:00.85	38:58:44.5	16.103	0.006	5	3.19	15.038	0.012	4	4.99	15.539	0.009	4	2.91	17.026	0.025	5	34.99
447.962	3334.508	7:38:01.27	38:58:41.6	16.065	0.007	5	4.21	15.173	0.007	5	4.27	15.608	0.006	4	0.62	16.810	0.010	4	1.63
483.176	2766.121	7:38:08.12	38:58:36.8	16.448	0.014	4	10.26	15.602	0.009	2	0.30	15.970	0.030	3	13.64	17.157	0.033	5	49.58
486.780	2774.305	7:38:08.02	38:58:36.3	16.777	0.015	3	11.29	15.939	0.010	3	5.31	16.319	0.029	3	10.06	17.531	0.044	4	83.43
523.724	429.180	7:38:36.27	38:58:31.3	18.504	0.009	4	0.36	17.420	0.023	5	8.30	—	—	0	—	19.475	0.069	2	48.09
538.583	454.902	7:38:35.96	38:58:29.2	20.455	0.050	3	6.50	18.375	0.011	4	1.46	—	—	0	—	—	—	0	—
542.809	3768.269	7:37:56.05	38:58:28.2	19.225	0.010	3	0.02	18.315	0.042	2	0.56	18.759	0.036	3	1.73	—	—	1	—
560.880	1974.990	7:38:17.65	38:58:26.0	20.765	0.118	2	16.30	19.740	0.180	2	22.50	—	—	0	—	—	—	1	—
581.194	932.143	7:38:30.21	38:58:23.2	20.581	0.082	2	17.09	18.432	0.016	4	3.02	—	—	0	—	—	—	1	—
629.642	956.087	7:38:29.93	38:58:16.4	18.924	0.011	5	1.61	16.334	0.016	5	17.43	—	—	0	—	20.439	0.080	2	16.16
652.566	961.928	7:38:29.86	38:58:13.2	19.654	0.017	4	3.22	17.987	0.033	4	12.98	—	—	1	—	—	—	1	—
675.937	642.346	7:38:33.71	38:58:09.9	17.059	0.009	5	5.86	15.932	0.007	5	3.73	—	—	1	—	18.073	0.016	5	3.62
691.097	1275.763	7:38:26.08	38:58:07.8	20.197	0.024	3	1.45	19.630	0.092	3	6.06	—	—	1	—	20.627	0.165	2	32.30
764.747	1553.491	7:38:22.74	38:57:57.4	17.518	0.005	6	2.04	16.972	0.012	5	2.78	17.258	0.010	3	2.45	17.860	0.010	5	1.79
787.392	2177.741	7:38:15.23	38:57:54.1	17.687	0.004	6	0.65	16.519	0.004	6	1.10	17.074	0.007	3	0.93	18.747	0.020	6	4.62
792.681	1468.472	7:38:23.77	38:57:53.5	19.609	0.024	6	12.15	18.144	0.018	5	3.74	18.838	0.010	3	0.60	20.828	0.271	2	84.59
803.475	3814.560	7:37:55.51	38:57:51.6	17.407	0.009	5	4.53	16.625	0.022	4	4.65	16.997	0.006	4	1.03	18.077	0.038	5	64.88
820.872	1791.352	7:38:19.88	38:57:49.5	16.855	0.006	6	3.71	16.161	0.021	6	31.48	16.513	0.008	3	1.73	17.388	0.010	6	8.98
824.328	2129.482	7:38:15.81	38:57:49.0	22.641	0.062	2	0.34	20.756	0.020	2	0.63	—	—	1	—	—	—	0	—
829.624	2373.868	7:38:12.87	38:57:48.2	21.946	0.035	2	0.00	19.688	0.046	2	23.09	—	—	0	—	—	—	0	—
835.581	3576.812	7:37:58.38	38:57:47.1	18.661	0.019	5	4.79	17.416	0.028	4	2.86	18.016	0.029	4	3.43	19.571	0.051	2	0.49
866.516	2879.360	7:38:06.78	38:57:42.9	20.611	0.010	5	1.16	18.035	0.021	5	10.51	19.502	0.009	5	1.17	22.294	0.086	2	8.58
867.612	2188.686	7:38:15.10	38:57:42.9	20.421	0.015	4	2.83	20.128	0.032	3	10.40	20.278	0.010	4	0.18	20.608	0.023	5	6.37
874.267	2051.591	7:38:16.75	38:57:41.9	21.610	0.026	2	0.88	20.709	0.024	2	1.53	21.173	0.079	2	16.06	22.297	0.039	2	0.27
903.590	2958.527	7:38:05.83	38:57:37.7	19.926	0.015	7	5.00	17.984	0.009	7	1.90	18.980	0.010	6	1.33	21.418	0.041	3	17.88
922.200	2870.610	7:38:06.89	38:57:35.1	22.184	0.081	2	5.11	21.282	0.084	2	8.12	21.729	0.028	2	0.03	—	—	1	—
960.799	2767.838	7:38:08.13	38:57:29.7	17.209	0.007	7	4.67	16.169	0.006	6	3.11	16.671	0.008	5	6.58	18.113	0.013	8	11.33
960.814	1493.107	7:38:23.48	38:57:29.8	22.156	0.035	2	0.36	21.282	0.061	2	4.27	—	—	1	—	22.869	0.094	2	2.87
964.146	2328.920	7:38:13.42	38:57:29.3	20.247	0.017	4	3.77	19.277	0.013	4	2.00	19.770	0.021	3	4.96	21.006	0.010	3	0.48
975.263	2576.122	7:38:10.44	38:57:27.7	22.067	0.086	3	4.71	21.252	0.061	2	4.27	—	—	1	—	22.731	0.114	2	6.14
977.050	2833.150	7:38:07.35	38:57:27.4	20.995	0.020	3	1.55	20.040	0.015	3	2.39	20.507	0.088	2	9.20	21.657	0.052	3	7.70
991.308	988.753	7:38:29.56	38:57:25.6	20.642	0.047	3	5.74	18.545	0.013	4	1.98	19.626	0.026	3	6.86	22.126	0.066	2	5.21
1002.670	2917.050	7:38:06.34	38:57:23.8	21.320	0.053	3	9.08	20.407	0.019	3	3.58	20.866	0.028	4	9.61	22.023	0.046	3	2.74
1014.314	87.297	7:38:40.42	38:57:22.4	14.836	0.009	4	5.34	13.959	0.006	3	0.47	—	—	0	—	15.581	0.017	4	12.06
1027.600	2893.560	7:38:06.63	38:57:20.3	20.722	0.020	4	5.42	19.814	0.009	4	0.86	20.282	0.040	3	2.55	21.440	0.044	3	5.68
1045.245	1756.597	7:38:20.32	38:57:17.9	22.740	0.062	2	0.23	20.634	0.038	3	6.76	21.816	0.026	2	0.74	—	—	1	—

[a]The full text of this table may be found at: ftp://taurus.tuc.noao.edu/pub/saha/Photseq/table4.txt

Table 5. Likely Variable Stars in the NGC2419 Field

Star ID	X (pix)	Y (pix)	R.A. (J2000)	Decl. (J2000)	$< V >$	$\epsilon(V)$	n_V	$\chi^2_\nu(V)$	$< I >$	$\epsilon(I)$	n_I	$\chi^2_\nu(I)$	$< R >$	$\epsilon(R)$	n_R	$\chi^2_\nu(R)$	$< B >$	$\epsilon(B)$	n_B	$\chi^2_\nu(B)$
V1	1495.028	2459.969	7:38:11.88	38:56:14.6	20.410	0.030	5	20.50	20.037	0.063	6	52.35	20.217	0.036	5	30.42	20.665	0.028	5	18.48
V2	1829.114	2584.987	7:38:10.40	38:55:27.7	20.408	0.082	6	173.13	20.028	0.071	4	65.38	20.298	0.073	6	84.29	20.949	0.063	7	88.39
V3	1858.845	2224.339	7:38:14.75	38:55:23.5	21.204	0.023	7	5.23	20.381	0.092	7	41.93	20.831	0.070	6	36.61	21.722	0.031	3	1.32
V4	2171.801	1975.868	7:38:17.76	38:54:39.6	20.474	0.073	10	244.39	19.831	0.047	9	59.76	19.989	0.077	11	396.75	20.699	0.089	13	359.09
V5	2172.556	1806.291	7:38:19.80	38:54:39.5	19.922	0.123	11	1180.60	19.481	0.075	10	194.65	20.189	0.035	12	38.10	20.916	0.057	12	139.70
V6	2309.284	2978.859	7:38:05.70	38:54:20.1	20.485	0.064	11	168.63	19.895	0.060	10	41.90	20.269	0.041	7	27.07	21.039	0.040	8	50.80
V7	2328.558	2106.259	7:38:16.21	38:54:17.5	20.653	0.082	8	130.97	20.042	0.061	8	53.15	20.299	0.051	11	26.83	21.192	0.100	11	71.34
V8	2407.928	2585.301	7:38:10.45	38:54:06.3	20.767	0.026	6	3.71	19.864	0.053	4	34.73	20.357	0.058	7	62.93	21.389	0.020	10	2.71
V9	2436.533	2422.324	7:38:12.41	38:54:02.3	19.925	0.099	12	1075.24	19.454	0.057	10	121.09	20.178	0.029	13	35.94	20.950	0.048	13	79.48
V10	2534.180	2626.820	7:38:09.96	38:53:48.6	20.317	0.076	7	116.50	19.796	0.055	7	46.69	20.295	0.065	6	24.12	20.642	0.039	7	18.11
V11	2534.841	2870.485	7:38:07.03	38:53:48.4	20.489	0.011	8	3.31	20.277	0.017	7	2.34	20.514	0.060	8	94.78	20.685	0.026	10	22.37
V12	2536.237	2727.602	7:38:08.75	38:53:48.3	18.063	0.062	11	292.33	16.715	0.018	10	34.96	17.335	0.033	11	89.75	19.141	0.092	11	629.27
V13	2554.933	2747.249	7:38:08.51	38:53:45.6	20.100	0.046	7	23.50	19.525	0.024	6	3.00	19.806	0.059	7	30.83	20.380	0.270	4	261.50
V14	2588.772	2568.852	7:38:10.66	38:53:40.9	20.408	0.028	7	13.80	20.279	0.092	6	21.01	20.278	0.025	7	3.81	20.556	0.024	6	7.50
V15	2595.170	2893.369	7:38:06.76	38:53:39.9	19.760	0.153	7	345.61	19.466	0.046	5	4.11	19.754	0.083	8	70.55	20.053	0.089	10	206.19
V16	2610.606	2526.792	7:38:11.17	38:53:37.8	20.329	0.064	9	84.26	19.706	0.022	8	9.27	20.024	0.119	5	98.09	20.742	0.099	7	209.78
V17	2618.126	2566.919	7:38:10.69	38:53:36.8	19.847	0.057	8	63.08	19.216	0.036	8	20.45	19.611	0.026	11	17.19	20.360	0.043	12	68.51
V18	2631.240	2790.520	7:38:08.00	38:53:34.9	20.546	0.016	7	4.26	20.361	0.019	6	1.57	20.554	0.064	9	76.50	20.713	0.020	11	16.86
V19	2635.183	2596.511	7:38:10.33	38:53:34.4	20.458	0.028	9	23.13	19.795	0.020	8	10.42	19.979	0.054	9	77.54	20.690	0.076	11	173.14
V20	2646.380	2743.875	7:38:08.56	38:53:32.8	20.170	0.050	12	55.51	19.236	0.047	12	52.66	19.664	0.054	8	54.98	20.686	0.186	5	151.65
V21	2646.987	2743.378	7:38:08.56	38:53:32.7	20.170	0.050	12	55.51	19.236	0.047	12	52.66	19.664	0.054	8	54.98	20.686	0.186	5	151.65
V22	2650.017	2644.727	7:38:09.75	38:53:32.3	20.942	0.056	6	70.99	19.936	0.012	8	4.20	20.472	0.114	5	177.85	21.678	0.020	2	0.24
V23	2655.258	2632.282	7:38:09.90	38:53:31.5	19.721	0.031	8	90.88	18.736	0.012	11	16.99	19.315	0.059	9	300.94	20.603	0.035	4	13.90
V24	2659.349	3178.098	7:38:03.34	38:53:30.9	20.246	0.086	10	246.02	19.729	0.058	10	94.95	20.022	0.096	10	317.21	20.574	0.137	11	874.14
V25	2669.256	2318.538	7:38:13.68	38:53:29.6	20.254	0.060	9	104.82	19.642	0.060	8	95.77	20.083	0.117	9	407.18	21.053	0.068	13	132.39
V26	2693.468	2770.722	7:38:08.24	38:53:26.1	20.006	0.082	9	185.02	19.250	0.037	8	48.23	19.586	0.084	5	44.97	20.277	0.101	2	11.90
V27	2698.526	2737.359	7:38:08.64	38:53:25.4	20.265	0.054	8	24.81	19.278	0.031	7	15.43	19.761	0.018	6	5.75	20.974	0.075	3	17.75
V28	2715.674	3153.924	7:38:03.63	38:53:23.0	20.402	0.086	10	235.98	19.807	0.039	10	42.44	19.678	0.064	11	177.46	20.358	0.121	11	613.79
V29	2718.825	2541.976	7:38:10.99	38:53:22.6	20.527	0.051	7	69.66	20.062	0.048	6	16.71	20.118	0.049	6	23.68	20.542	0.178	3	74.89
V30	2719.000	2541.944	7:38:10.99	38:53:22.6	20.527	0.051	7	69.66	20.062	0.048	6	16.71	20.118	0.049	6	23.68	20.542	0.178	3	74.89
V31	2762.460	2806.540	7:38:07.81	38:53:16.4	20.029	0.102	6	59.08	19.361	0.217	3	69.30	19.686	0.093	5	108.05	20.510	0.107	4	129.87
V32	2769.459	2946.242	7:38:06.13	38:53:15.4	20.126	0.181	10	2199.17	19.652	0.172	9	520.69	20.066	0.094	11	295.41	20.329	0.150	11	718.75
V33	2780.933	2738.891	7:38:08.63	38:53:13.9	20.637	0.025	10	9.01	19.907	0.026	10	7.62	20.121	0.060	9	79.98	20.742	0.118	9	359.00
V34	2790.422	2912.685	7:38:06.54	38:53:12.5	19.076	0.042	5	60.61	18.158	0.053	7	81.05	18.542	0.009	4	2.62	-10.000	-1.000	1	-100.00
V35	2805.430	2712.900	7:38:08.94	38:53:10.4	20.660	0.031	8	10.18	20.516	0.048	6	4.43	20.697	0.089	6	35.54	20.923	0.016	6	1.67
V36	2811.797	2491.154	7:38:11.61	38:53:09.6	20.336	0.076	5	53.57	19.810	0.022	5	2.49	20.066	0.070	6	74.21	20.297	0.038	2	14.79
V37	2818.120	2587.710	7:38:10.45	38:53:08.7	20.422	0.073	7	142.87	19.681	0.058	6	29.67	20.171	0.034	6	29.81	21.065	0.040	4	32.25
V38	2819.130	3063.910	7:38:04.72	38:53:08.4	21.306	0.062	6	20.13	20.479	0.054	7	18.10	20.993	0.031	6	6.89	-10.000	-1.000	0	-100.00
V39	2821.657	2524.131	7:38:11.22	38:53:08.2	19.889	0.053	9	136.45	19.406	0.044	8	52.44	19.793	0.091	8	323.13	20.340	0.167	7	642.06
V40	2854.400	2537.640	7:38:11.06	38:53:03.6	20.966	0.068	6	58.84	20.011	0.063	3	40.91	20.518	0.033	5	16.14	21.593	0.065	2	10.95
V41	2857.460	2986.520	7:38:05.66	38:53:03.1	20.531	0.015	5	3.08	20.341	0.038	4	5.12	20.523	0.103	6	72.87	20.682	0.017	6	3.84
V42	2866.662	2885.897	7:38:06.87	38:53:01.8	19.578	0.042	7	66.90	18.461	0.022	7	20.50	19.057	0.051	8	161.45	20.374	0.016	6	5.75
V43	2883.480	2570.700	7:38:10.66	38:52:59.5	20.446	0.103	6	249.02	19.988	0.035	6	9.52	20.405	0.077	5	93.22	21.127	0.233	4	202.20
V44	2887.130	2457.720	7:38:12.02	38:52:59.0	20.032	0.144	6	510.62	19.628	0.082	5	32.81	20.075	0.095	9	250.14	20.706	0.189	12	1007.63
V45	2888.634	2769.028	7:38:08.28	38:52:58.7	19.416	0.028	6	21.15	18.390	0.051	6	160.04	18.911	0.020	5	13.53	20.258	0.036	2	0.02
V46	2911.720	2854.300	7:38:07.25	38:52:55.5	20.523	0.039	3	3.13	19.567	0.079	6	33.98	20.005	0.019	3	0.28	-10.000	-1.000	0	-100.00
V47	2916.920	2745.420	7:38:08.56	38:52:54.7	19.900	0.061	6	62.57	19.158	0.038	5	24.42	19.618	0.047	4	12.04	20.535	0.124	2	48.36
V48	2949.830	2917.970	7:38:06.49	38:52:50.1	20.460	0.023	10	10.52	19.948	0.029	9	7.46	20.181	0.059	8	61.93	20.758	0.044	7	32.92
V49	2952.837	3015.708	7:38:05.31	38:52:49.7	19.797	0.056	11	84.41	19.031	0.039	10	23.70	19.198	0.111	7	400.41	20.439	0.157	3	89.36
V50	2953.146	3015.792	7:38:05.31	38:52:49.6	19.797	0.056	11	84.41	19.031	0.039	10	23.70	19.198	0.111	7	400.41	20.439	0.157	3	89.36
V51	2964.081	2446.614	7:38:12.16	38:52:48.2	20.335	0.068	9	176.22	19.921	0.045	9	18.63	20.303	0.044	8	34.66	20.749	0.081	10	116.63
V52	2977.050	2492.955	7:38:11.60	38:52:46.3	20.586	0.090	8	109.70	19.565	0.049	6	8.34	20.153	0.063	7	51.85	-10.000	-1.000	1	-100.00
V53	2977.074	2368.874	7:38:13.10	38:52:46.4	20.483	0.063	9	38.69	19.923	0.062	8	18.70	20.157	0.037	5	10.54	20.864	0.150	4	178.36
V54	2977.483	3182.608	7:38:03.31	38:52:46.2	20.268	0.077	11	268.90	19.662	0.051	11	74.97	19.758	0.078	11	491.15	20.547	0.105	14	551.68
V55	2985.480	3815.062	7:37:55.70	38:52:44.9	20.345	0.133	11	774.19	19.855	0.091	11	329.46	20.238	0.071	12	178.34	20.926	0.086	13	278.87
V56	2991.779	3018.486	7:38:05.28	38:52:44.2	20.714	0.015	8	6.85	19.918	0.015	8	2.95	20.331	0.017	7	5.77	21.486	0.113	6	80.26
V57	2992.687	2564.797	7:38:10.74	38:52:44.1	19.205	0.018	7	14.56	18.180	0.008	7	3.59	18.726	0.076	6	180.11	19.886	0.065	2	15.35
V58	2998.635	1990.757	7:38:17.65	38:52:43.4	19.982	0.128	10	1413.04	19.608	0.072	9	141.08	19.914	0.121	10	1023.87	20.248	0.211	12	3698.43
V59	3009.614	3585.701	7:37:58.46	38:52:41.5	20.284	0.061	11	170.84	19.713	0.040	10	71.50	19.684	0.088	13	697.52	20.316	0.136	12	914.29
V60	3009.956	2788.906	7:38:08.05	38:52:41.7	19.233	0.082	7	187.59	18.190	0.080	7	131.79	18.767	0.057	6	56.15	19.860	0.083	4	159.05

Table 5—Continued

Star ID	X (pix)	Y (pix)	R.A. (J2000)	Decl. (J2000)	$< V >$	$\epsilon(V)$	n_V	$\chi^2_\nu(V)$	$< I >$	$\epsilon(I)$	n_I	$\chi^2_\nu(I)$	$< R >$	$\epsilon(R)$	n_R	$\chi^2_\nu(R)$	$< B >$	$\epsilon(B)$	n_B	$\chi^2_\nu(B)$
V61	3013.056	2092.584	7:38:16.42	38:52:41.3	20.128	0.114	10	1000.50	19.835	0.072	9	129.99	20.048	0.082	12	236.55	20.533	0.106	12	532.85
V62	3027.856	2051.110	7:38:16.92	38:52:39.3	20.332	0.070	11	229.27	19.690	0.052	9	94.66	19.848	0.066	11	319.95	20.590	0.096	13	457.67
V63	3030.575	2586.620	7:38:10.48	38:52:38.8	18.135	0.145	4	1266.44	16.750	0.144	3	282.33	17.379	0.056	6	100.40	19.143	0.029	6	46.90
V64	3042.306	2741.781	7:38:08.62	38:52:37.1	18.333	0.051	12	355.25	17.168	0.008	12	7.37	17.803	0.027	12	62.84	19.364	0.017	12	15.25
V65	3063.239	2200.710	7:38:15.13	38:52:34.3	20.278	0.066	9	197.23	19.863	0.028	9	13.68	19.988	0.031	11	33.88	20.433	0.024	11	22.24
V66	3069.523	2762.122	7:38:08.37	38:52:33.3	19.151	0.043	7	83.52	18.165	0.085	10	142.10	18.671	0.032	8	35.03	19.869	0.019	6	11.73
V67	3070.995	2437.930	7:38:12.27	38:52:33.1	20.357	0.070	10	223.45	19.809	0.042	9	31.06	20.073	0.053	10	101.32	20.521	0.042	10	50.83
V68	3072.023	2795.118	7:38:07.98	38:52:32.9	19.358	0.078	9	330.62	18.769	0.055	9	146.01	19.162	0.039	9	126.43	20.043	0.028	10	31.53
V69	3089.516	2754.098	7:38:08.47	38:52:30.5	19.824	0.030	9	32.00	18.796	0.020	10	18.36	19.449	0.076	6	90.33	20.391	0.180	2	49.07
V70	3093.714	2603.367	7:38:10.28	38:52:29.9	19.578	0.039	9	15.15	18.626	0.053	7	21.27	18.998	0.043	8	26.18	20.403	0.063	6	35.15
V71	3114.330	2578.930	7:38:10.58	38:52:27.0	18.140	0.090	6	230.45	16.855	0.026	5	12.54	17.488	0.051	8	182.79	19.082	0.047	14	188.94
V72	3117.580	2402.180	7:38:12.71	38:52:26.6	19.984	0.092	10	475.19	19.559	0.066	8	156.11	19.969	0.158	8	482.60	20.151	0.220	8	1121.65
V73	3119.460	2669.560	7:38:09.49	38:52:26.3	20.441	0.050	7	25.34	19.509	0.038	6	24.41	19.919	0.048	7	33.01	21.064	0.046	4	4.25
V74	3137.923	2793.357	7:38:08.00	38:52:23.7	19.907	0.081	7	241.95	19.574	0.056	4	48.08	19.800	0.094	4	60.02	19.805	0.042	5	7.68
V75	3138.039	2793.241	7:38:08.00	38:52:23.7	19.907	0.081	7	241.95	19.574	0.056	4	48.08	19.800	0.094	4	60.02	19.805	0.042	5	7.68
V76	3163.560	2694.838	7:38:09.19	38:52:20.1	20.489	0.054	7	29.29	19.561	0.054	8	35.65	20.044	0.046	3	9.91	-10.000	-1.000	0	-100.00
V77	3166.867	2777.204	7:38:08.20	38:52:19.6	20.389	0.051	10	87.63	19.401	0.016	11	10.84	19.853	0.013	7	3.95	21.028	0.026	6	5.74
V78	3179.280	2613.079	7:38:10.18	38:52:17.9	20.609	0.078	6	31.72	19.725	0.050	5	12.71	20.117	0.070	6	32.11	21.467	0.041	4	4.46
V79	3189.541	3144.189	7:38:03.79	38:52:16.4	20.868	0.054	7	80.14	20.733	0.029	7	4.99	20.912	0.044	6	30.86	20.946	0.038	8	50.39
V80	3202.909	3535.976	7:37:59.08	38:52:14.4	20.490	0.055	11	146.65	19.852	0.045	11	76.96	19.988	0.039	12	118.48	20.756	0.069	13	228.23
V81	3234.568	3285.348	7:38:02.09	38:52:10.0	20.839	0.037	4	10.11	19.976	0.050	6	39.39	20.462	0.032	7	20.70	21.496	0.028	6	2.78
V82	3249.691	2517.815	7:38:11.33	38:52:08.0	21.527	0.118	7	28.62	20.680	0.019	7	0.67	21.021	0.027	4	2.02	22.122	0.072	3	6.17
V83	3253.495	2367.815	7:38:13.13	38:52:07.5	20.422	0.062	11	154.01	19.917	0.041	9	30.66	20.167	0.050	11	84.08	20.714	0.066	12	197.09
V84	3282.462	2782.988	7:38:08.14	38:52:03.4	20.321	0.084	7	137.28	19.751	0.044	4	11.76	20.100	0.158	5	142.35	20.788	0.142	4	129.14
V85	3293.646	2360.733	7:38:13.22	38:52:01.9	21.937	0.069	7	21.18	21.178	0.024	6	0.65	21.570	0.024	5	2.00	22.528	0.025	5	1.41
V86	3312.624	2364.114	7:38:13.18	38:51:59.2	22.374	0.129	6	34.15	21.903	0.056	6	2.19	22.225	0.032	4	1.67	22.763	0.104	6	19.69
V87	3318.697	2495.017	7:38:11.61	38:51:58.3	17.257	0.057	12	966.25	15.673	0.036	11	331.44	16.369	0.057	12	892.09	18.807	0.097	14	1080.29
V88	3373.993	3053.476	7:38:04.89	38:51:50.5	18.172	0.137	6	514.47	16.937	0.144	5	570.21	17.559	0.163	5	728.20	19.244	0.095	9	323.26
V89	3374.806	2535.513	7:38:11.12	38:51:50.4	21.734	0.060	6	24.33	20.929	0.042	6	6.62	21.472	0.108	3	18.85	-10.000	-1.000	0	-100.00
V90	3405.096	3525.895	7:37:59.22	38:51:46.0	20.365	0.011	10	5.65	19.988	0.076	9	99.64	20.197	0.014	12	7.24	20.591	0.013	14	8.47
V91	3852.123	2395.051	7:38:12.85	38:50:43.4	20.397	0.068	12	221.54	19.927	0.043	10	70.54	20.138	0.049	12	93.62	20.740	0.051	13	120.08
V92	4002.830	1702.787	7:38:21.18	38:50:22.3	20.218	0.054	8	109.36	19.844	0.050	7	61.43	20.229	0.048	8	67.85	20.837	0.078	12	275.31

Table 6. Stars in the Pal 4 Field with best Photometry

Star ID	X (pix)	Y (pix)	R.A. (J2000)	Decl. (J2000)	$< V >$	$\epsilon(V)$	n_V	$< I >$	$\epsilon(I)$	n_I	$< R >$	$\epsilon(R)$	n_R	$< B >$	$\epsilon(B)$	n_B
1	1392.870	2104.530	11:29:17.58	28:55:22.7	21.322	0.014	5	20.378	0.013	5	20.859	0.010	5	22.090	0.009	5
2	1586.340	1492.180	11:29:11.00	28:55:49.7	20.930	0.008	6	18.218	0.013	6	19.728	0.014	5	22.421	0.010	5
3	1917.170	598.700	11:29:01.41	28:56:35.9	18.056	0.011	6	17.898	0.009	6	17.984	0.011	6	18.170	0.013	6
4	2124.650	2354.410	11:29:20.23	28:57:05.6	20.737	0.011	6	19.946	0.009	6	20.335	0.012	6	21.309	0.013	6
5	2246.010	2135.150	11:29:17.87	28:57:22.6	21.124	0.012	6	20.165	0.014	6	20.654	0.014	6	21.900	0.014	6
6	2306.050	1567.040	11:29:11.78	28:57:30.9	20.164	0.008	6	19.156	0.005	6	19.657	0.007	6	21.065	0.012	6
7	2406.070	2079.100	11:29:17.27	28:57:45.1	19.800	0.004	6	18.740	0.007	6	19.256	0.003	6	20.743	0.004	6
8	2410.330	2138.220	11:29:17.90	28:57:45.7	20.698	0.014	6	19.925	0.014	6	20.305	0.011	6	21.291	0.009	6
9	2412.700	3338.550	11:29:30.78	28:57:46.3	17.597	0.004	5	16.506	0.007	5	17.010	0.006	5	18.557	0.008	6
10	2462.690	1885.410	11:29:15.19	28:57:53.0	19.945	0.007	6	19.019	0.010	6	19.471	0.009	6	20.737	0.012	6
11	2476.860	1910.260	11:29:15.46	28:57:55.0	19.542	0.009	6	18.455	0.007	6	18.982	0.003	6	20.538	0.010	6
12	2502.650	2158.450	11:29:18.12	28:57:58.7	20.601	0.010	6	19.617	0.006	6	20.095	0.005	6	21.412	0.014	5
13	2544.180	2165.700	11:29:18.19	28:58:04.6	20.723	0.005	6	19.971	0.010	6	20.343	0.009	6	21.296	0.014	6
14	2545.310	1738.590	11:29:13.61	28:58:04.6	20.716	0.012	6	19.928	0.008	6	20.319	0.008	6	21.311	0.009	6
15	2551.320	2055.690	11:29:17.01	28:58:05.5	19.758	0.005	6	18.686	0.004	6	19.199	0.007	6	20.712	0.008	5
16	2555.840	2849.400	11:29:25.53	28:58:06.4	18.021	0.006	5	16.788	0.007	5	17.358	0.004	6	19.075	0.006	6
17	2560.230	1865.000	11:29:14.97	28:58:06.7	20.617	0.010	6	19.887	0.011	6	20.257	0.006	6	21.196	0.014	6
18	2560.670	2989.180	11:29:27.02	28:58:07.1	20.639	0.010	6	19.666	0.009	6	20.141	0.007	6	21.464	0.013	5
19	2599.850	1298.680	11:29:08.89	28:58:12.1	19.952	0.007	6	18.907	0.006	6	19.416	0.005	6	20.874	0.014	6
20	2600.730	1709.700	11:29:13.30	28:58:12.4	17.879	0.007	5	16.322	0.005	5	17.046	0.007	5	19.556	0.013	6
21	2601.810	2143.800	11:29:17.96	28:58:12.7	20.663	0.005	6	19.874	0.006	6	20.263	0.006	6	21.261	0.015	5
22	2608.490	3084.390	11:29:28.04	28:58:13.8	20.212	0.008	6	19.030	0.009	6	19.574	0.006	6	21.195	0.006	6
23	2616.170	1605.280	11:29:12.18	28:58:14.5	20.162	0.007	5	19.191	0.012	4	19.661	0.004	5	20.980	0.010	6
24	2636.270	2132.800	11:29:17.84	28:58:17.5	19.494	0.005	6	18.451	0.007	6	18.959	0.006	6	20.394	0.009	6
25	2636.700	2007.580	11:29:16.49	28:58:17.5	19.438	0.006	6	18.413	0.003	6	18.911	0.005	6	20.336	0.014	6
26	2656.350	2044.760	11:29:16.89	28:58:20.3	19.954	0.005	6	18.902	0.006	6	19.412	0.004	6	20.900	0.007	6
27	2671.740	1938.010	11:29:15.75	28:58:22.4	19.149	0.003	6	17.989	0.004	6	18.545	0.003	6	20.216	0.007	6
28	2676.510	2202.100	11:29:18.58	28:58:23.2	20.741	0.010	6	19.781	0.009	6	20.244	0.006	6	21.552	0.011	6
29	2678.190	1996.870	11:29:16.38	28:58:23.4	20.710	0.006	6	19.917	0.007	6	20.304	0.006	6	21.279	0.010	5
30	2688.490	1963.670	11:29:16.02	28:58:24.8	20.469	0.005	6	19.501	0.009	6	19.975	0.009	6	21.307	0.014	6
31	2699.390	1440.590	11:29:10.41	28:58:26.2	20.725	0.006	6	19.937	0.007	6	20.319	0.006	6	21.317	0.006	6
32	2703.490	1593.690	11:29:12.05	28:58:26.8	20.716	0.009	6	19.913	0.008	6	20.301	0.006	6	21.303	0.007	6
33	2715.680	1656.060	11:29:12.72	28:58:28.5	18.707	0.006	6	17.455	0.004	6	18.057	0.006	6	19.900	0.009	6
34	2733.520	1910.360	11:29:15.45	28:58:31.1	20.724	0.011	6	19.950	0.010	6	20.337	0.006	6	21.320	0.013	6
35	2735.220	1856.280	11:29:14.87	28:58:31.3	18.614	0.003	6	17.344	0.002	6	17.952	0.003	6	19.826	0.008	6
36	2736.200	1453.370	11:29:10.55	28:58:31.4	20.167	0.005	6	19.132	0.005	6	19.628	0.004	6	21.067	0.011	6
37	2741.990	1542.320	11:29:11.50	28:58:32.2	20.519	0.006	6	19.666	0.006	6	20.084	0.011	6	21.164	0.012	6
38	2775.890	2166.220	11:29:18.19	28:58:37.1	20.309	0.006	6	19.460	0.007	6	19.883	0.005	6	20.976	0.011	6
39	2777.060	1935.900	11:29:15.72	28:58:37.2	20.716	0.006	6	19.913	0.007	6	20.310	0.010	6	21.327	0.010	6
40	2787.270	2200.870	11:29:18.56	28:58:38.7	19.929	0.007	6	18.881	0.004	6	19.394	0.005	6	20.859	0.014	6
41	2791.260	1979.710	11:29:16.19	28:58:39.3	20.444	0.005	6	19.467	0.010	6	19.948	0.005	6	21.290	0.014	6
42	2793.750	1764.370	11:29:13.88	28:58:39.5	19.416	0.005	6	18.349	0.005	6	18.871	0.004	6	20.330	0.006	6
43	2799.890	2032.940	11:29:16.76	28:58:40.5	18.012	0.009	6	16.512	0.005	5	17.220	0.004	6	19.476	0.005	6
44	2804.090	2069.970	11:29:17.16	28:58:41.1	20.626	0.011	6	19.652	0.007	5	20.117	0.007	6	21.449	0.012	6
45	2824.410	1908.690	11:29:15.43	28:58:43.9	20.879	0.010	6	19.930	0.008	6	20.386	0.012	6	21.671	0.013	6
46	2828.840	1783.800	11:29:14.09	28:58:44.5	19.704	0.005	6	18.637	0.004	6	19.154	0.003	6	20.652	0.006	6
47	2834.590	999.330	11:29:05.67	28:58:45.1	19.396	0.005	6	17.151	0.007	6	18.332	0.010	6	20.881	0.010	6
48	2844.540	1963.230	11:29:16.01	28:58:46.7	19.510	0.005	6	18.492	0.004	6	18.985	0.004	6	20.383	0.011	5
49	2852.160	1969.390	11:29:16.08	28:58:47.8	19.832	0.013	6	18.791	0.011	6	19.296	0.007	6	20.757	0.005	5
50	2885.910	1413.350	11:29:10.11	28:58:52.4	20.739	0.010	6	19.994	0.014	6	20.357	0.006	6	21.267	0.007	6
51	2899.670	895.720	11:29:04.56	28:58:54.2	19.319	0.013	6	18.253	0.003	6	18.756	0.007	6	20.262	0.009	6
52	2899.810	1958.400	11:29:15.96	28:58:54.5	20.375	0.012	6	19.401	0.010	6	19.872	0.006	6	21.234	0.013	6
53	2948.870	3063.390	11:29:27.81	28:59:01.7	20.730	0.006	6	19.952	0.009	6	20.338	0.011	6	21.318	0.010	6
54	2961.120	2095.810	11:29:17.43	28:59:03.2	20.720	0.007	6	19.933	0.012	6	20.310	0.010	6	21.329	0.012	6
55	2985.730	1714.930	11:29:13.34	28:59:06.5	19.057	0.003	6	17.855	0.002	6	18.428	0.006	6	20.160	0.006	6
56	3017.660	1875.730	11:29:15.07	28:59:11.1	20.834	0.006	6	19.872	0.006	6	20.333	0.006	6	21.638	0.008	6
57	3108.690	2117.780	11:29:17.66	28:59:23.9	20.701	0.009	6	19.927	0.010	6	20.303	0.008	6	21.294	0.012	6
58	3176.920	1845.780	11:29:14.74	28:59:33.4	20.745	0.013	5	19.911	0.012	6	20.319	0.007	5	21.326	0.014	6
59	3201.140	2020.150	11:29:16.61	28:59:36.9	20.659	0.008	6	19.863	0.006	6	20.258	0.007	6	21.280	0.009	6
60	3316.500	2392.410	11:29:20.60	28:59:53.2	21.069	0.011	6	20.104	0.009	6	20.574	0.008	6	21.854	0.014	6
61	3682.630	2120.560	11:29:17.67	29:00:44.6	20.427	0.007	6	19.569	0.007	6	19.978	0.008	6	21.090	0.012	4

Table 7. Stars in the Pal 4 Field with at least V and I Photometry[a]

X (pix)	Y (pix)	R.A. (J2000)	Decl. (J2000)	$< V >$	$\epsilon(V)$	n_V	$\chi^2_\nu(V)$	$< I >$	$\epsilon(I)$	n_I	$\chi^2_\nu(I)$	$< R >$	$\epsilon(R)$	n_R	$\chi^2_\nu(R)$	$< B >$	$\epsilon(B)$	n_B	$\chi^2_\nu(B)$
108.190	1539.510	11:29:11.56	28:52:21.9	23.591	0.127	2	2.79	21.883	0.091	2	2.74	—	—	1	—	—	—	0	—
130.000	3599.400	11:29:33.64	28:52:25.4	21.775	0.074	3	18.02	21.510	0.341	2	32.58	21.393	0.056	3	10.16	—	—	1	—
235.250	3257.850	11:29:29.97	28:52:40.2	22.101	0.041	3	5.11	20.560	0.035	3	3.64	21.251	0.046	3	22.64	—	—	0	—
363.150	3061.880	11:29:27.87	28:52:58.1	22.006	0.084	3	21.22	21.360	0.042	3	1.36	21.681	0.080	3	18.09	—	—	1	—
420.510	3754.630	11:29:35.29	28:53:06.3	23.367	0.069	2	0.11	22.502	0.131	2	1.75	23.017	0.055	2	0.62	—	—	0	—
480.930	1991.220	11:29:16.39	28:53:14.4	22.905	0.044	2	0.24	20.055	0.031	2	10.87	21.669	0.019	2	0.21	—	—	0	—
487.270	2333.120	11:29:20.06	28:53:15.4	20.262	0.019	3	8.18	17.045	0.023	3	65.23	18.796	0.015	4	21.62	21.911	0.068	3	13.34
502.440	1326.380	11:29:09.27	28:53:17.3	23.835	0.104	2	0.61	22.388	0.083	2	0.85	—	—	1	—	—	—	0	—
596.690	943.350	11:29:05.16	28:53:30.4	18.603	0.014	3	16.53	17.400	0.019	2	28.06	17.879	0.022	2	37.89	19.903	0.050	2	12.55
640.170	2408.580	11:29:20.86	28:53:36.9	22.744	0.036	2	0.00	21.658	0.159	2	10.65	22.188	0.061	2	10.03	—	—	0	—
661.700	3654.830	11:29:34.22	28:53:40.2	22.205	0.078	3	9.87	19.689	0.042	3	23.16	21.012	0.015	3	2.61	—	—	1	—
669.420	3194.140	11:29:29.28	28:53:41.2	20.943	0.058	3	45.14	18.521	0.026	3	15.73	19.787	0.050	3	55.82	22.517	0.129	3	8.71
711.200	3392.980	11:29:31.41	28:53:47.1	23.812	0.098	2	0.04	22.500	0.221	2	5.40	—	—	1	—	—	—	1	—
740.030	2315.880	11:29:19.86	28:53:50.9	18.309	0.019	3	43.99	16.959	0.007	3	5.50	17.573	0.009	4	11.83	19.465	0.010	3	5.61
810.960	3253.050	11:29:29.91	28:54:01.1	22.910	0.044	2	0.07	22.180	0.094	2	1.53	22.500	0.028	2	0.02	—	—	1	—
873.670	2103.900	11:29:17.59	28:54:09.7	23.546	0.092	2	1.53	21.535	0.044	2	0.04	22.524	0.037	2	0.09	—	—	0	—
912.430	1995.380	11:29:16.42	28:54:15.1	20.131	0.019	3	18.53	17.352	0.014	3	11.15	18.866	0.015	4	14.82	21.734	0.044	2	5.15
962.260	1231.590	11:29:08.23	28:54:21.9	23.511	0.064	2	0.08	22.309	0.106	2	2.21	—	—	1	—	—	—	1	—
969.060	1592.090	11:29:12.10	28:54:22.9	22.882	0.217	2	32.57	21.672	0.046	2	0.33	22.206	0.180	2	38.82	—	—	1	—
979.240	2101.120	11:29:17.55	28:54:24.5	22.889	0.126	3	8.88	20.161	0.009	2	0.02	21.588	0.053	3	9.15	—	—	1	—
1016.770	293.110	11:28:58.17	28:54:29.2	23.286	0.055	2	0.00	20.712	0.019	2	0.04	—	—	1	—	—	—	0	—
1031.280	1217.030	11:29:08.07	28:54:31.6	21.552	0.022	3	5.68	20.053	0.026	2	0.11	20.644	0.026	3	7.92	—	—	1	—
1137.220	2128.740	11:29:17.84	28:54:46.7	21.453	0.023	3	5.97	20.668	0.031	3	3.15	21.078	0.022	3	5.61	21.963	0.035	3	3.27
1220.110	3564.800	11:29:33.24	28:54:58.7	20.840	0.043	3	39.74	18.415	0.028	3	23.56	19.712	0.026	3	15.05	22.429	0.159	2	17.47
1244.750	1342.260	11:29:09.41	28:55:01.6	23.190	0.060	3	1.79	20.421	0.032	3	14.16	21.974	0.032	3	4.00	—	—	1	—
1267.010	2898.000	11:29:26.09	28:55:05.2	23.508	0.072	2	0.77	22.221	0.073	2	0.70	22.899	0.179	2	11.49	24.398	0.140	3	5.32
1298.900	1314.460	11:29:09.11	28:55:09.2	23.341	0.118	3	3.70	21.671	0.169	3	20.16	22.543	0.154	2	29.89	—	—	1	—
1319.050	458.980	11:28:59.94	28:55:11.8	23.618	0.069	3	0.15	22.076	0.124	2	4.72	22.745	0.090	2	6.72	—	—	1	—
1343.620	1222.980	11:29:08.13	28:55:15.5	23.447	0.057	2	0.71	21.342	0.031	3	1.15	22.349	0.045	2	3.51	—	—	0	—
1346.690	1420.610	11:29:10.24	28:55:16.0	22.894	0.031	3	0.00	21.816	0.041	3	0.12	22.398	0.052	3	4.78	23.845	0.040	3	1.25
1365.750	3567.380	11:29:33.26	28:55:19.2	19.479	0.030	3	27.11	18.836	0.006	3	0.43	19.138	0.032	2	50.44	19.948	0.009	3	1.65
1383.060	2342.270	11:29:20.12	28:55:21.3	23.160	0.102	3	4.43	21.209	0.176	3	55.14	22.135	0.139	2	26.67	24.531	0.099	2	1.78
1389.430	2996.900	11:29:27.14	28:55:22.4	22.951	0.135	2	3.08	22.402	0.248	3	9.08	—	—	1	—	—	—	1	—
1392.870	2104.530	11:29:17.58	28:55:22.7	21.322	0.014	5	3.06	20.378	0.013	5	2.57	20.859	0.010	5	2.25	22.090	0.009	5	0.41
1410.940	1625.070	11:29:12.43	28:55:25.1	23.667	0.068	3	0.75	21.275	0.045	3	3.52	22.406	0.035	2	1.53	—	—	1	—
1418.430	3036.100	11:29:27.56	28:55:26.5	23.051	0.185	3	14.04	22.394	0.176	2	4.91	22.788	0.210	3	23.00	23.838	0.044	2	1.37
1437.740	2191.420	11:29:18.51	28:55:29.0	22.211	0.115	3	7.30	21.038	0.041	3	1.01	21.508	0.071	3	4.72	—	—	1	—
1442.270	1954.680	11:29:15.97	28:55:29.6	20.859	0.015	5	5.76	18.795	0.019	5	26.64	19.870	0.020	5	26.28	22.361	0.013	5	2.16
1448.690	2761.900	11:29:24.62	28:55:30.7	22.834	0.036	2	0.43	22.438	0.092	2	0.02	22.661	0.038	2	0.00	23.086	0.060	3	10.63
1469.320	1032.400	11:29:06.08	28:55:33.1	21.601	0.014	5	1.31	19.613	0.013	5	5.99	20.648	0.014	4	4.40	22.951	0.093	4	25.67
1496.670	2190.360	11:29:18.49	28:55:37.3	23.409	0.047	3	0.03	22.667	0.096	2	1.04	23.073	0.039	3	0.21	24.057	0.067	3	0.15
1519.990	1064.170	11:29:06.42	28:55:40.2	21.610	0.012	6	0.84	18.873	0.013	6	11.78	20.406	0.009	5	1.93	23.125	0.018	3	0.98
1531.760	814.200	11:29:03.74	28:55:41.8	24.242	0.116	2	0.14	22.836	0.108	2	0.56	23.525	0.065	2	0.10	—	—	1	—
1556.850	1443.540	11:29:10.48	28:55:45.5	23.284	0.118	3	5.77	22.238	0.135	3	5.06	22.872	0.060	2	2.44	23.589	0.155	3	31.41
1569.130	1731.110	11:29:13.57	28:55:47.3	23.774	0.080	3	0.34	23.053	0.132	2	0.21	23.424	0.053	3	0.75	24.380	0.068	2	1.12
1586.340	1492.180	11:29:11.00	28:55:49.7	20.930	0.008	6	1.86	18.218	0.013	6	21.27	19.728	0.014	5	11.76	22.421	0.010	5	1.24
1589.720	1045.420	11:29:06.21	28:55:50.0	22.857	0.053	4	2.90	22.162	0.055	3	0.13	22.600	0.050	2	2.57	23.287	0.062	3	5.90
1599.610	2237.880	11:29:19.00	28:55:51.8	23.764	0.070	3	0.15	20.948	0.029	3	3.27	22.533	0.031	3	1.56	—	—	1	—
1610.610	1707.770	11:29:13.31	28:55:53.2	23.439	0.052	3	0.57	22.694	0.181	3	3.49	23.076	0.082	3	3.58	23.960	0.043	3	0.72
1640.450	3646.020	11:29:34.09	28:55:57.8	22.758	0.180	2	4.11	20.933	0.055	2	2.07	—	—	0	—	—	—	1	—
1643.840	2321.600	11:29:19.89	28:55:58.0	23.648	0.217	2	8.18	22.087	0.054	3	0.03	22.758	0.072	3	4.00	24.289	0.052	3	0.26
1649.040	1811.510	11:29:14.42	28:55:58.6	23.694	0.092	2	0.88	22.709	0.296	2	7.59	23.225	0.377	3	29.94	24.535	0.204	3	7.18
1673.890	877.280	11:29:04.41	28:56:01.8	21.562	0.024	5	6.81	20.275	0.057	5	41.32	20.958	0.072	4	59.97	22.319	0.017	6	3.50
1674.880	1144.970	11:29:07.28	28:56:02.0	23.044	0.085	4	5.54	22.010	0.048	3	0.66	22.604	0.058	3	3.58	23.792	0.039	3	1.21
1679.990	1862.570	11:29:14.97	28:56:03.0	21.076	0.110	5	174.42	20.037	0.159	4	89.54	20.871	0.087	5	94.17	21.435	0.077	6	137.04
1715.990	2194.130	11:29:18.53	28:56:08.1	23.909	0.083	3	0.27	22.889	0.109	2	0.04	23.551	0.120	2	3.55	24.447	0.065	2	0.94
1727.150	1597.130	11:29:12.12	28:56:09.5	21.832	0.014	6	0.97	20.864	0.026	6	2.90	21.311	0.028	6	11.10	22.576	0.019	4	1.42
1728.900	2485.180	11:29:21.65	28:56:10.0	23.714	0.205	3	6.07	21.654	0.074	2	0.01	22.859	0.046	2	0.70	—	—	1	—
1757.760	1700.730	11:29:13.23	28:56:13.9	23.381	0.055	2	0.11	22.122	0.100	3	3.72	22.640	0.095	3	6.94	23.760	0.042	3	1.45

[a]The full text of this table may be found at: ftp://taurus.tuc.noao.edu/pub/saha/Photseq/table7.txt

Table 8. Likely Variable Stars in the Pal 4 Field

Star ID	X (pix)	Y (pix)	R.A. (J2000)	Decl. (J2000)	$< V >$	$\epsilon(V)$	n_V	$\chi^2_\nu(V)$	$< I >$	$\epsilon(I)$	n_I	$\chi^2_\nu(I)$	$< R >$	$\epsilon(R)$	n_R	$\chi^2_\nu(R)$	$< B >$	$\epsilon(B)$	n_B	$\chi^2_\nu(B)$
V1	2014.840	2730.520	11:29:24.27	28:56:50.3	22.185	0.190	5	94.03	21.503	0.142	6	25.96	21.824	0.168	5	135.51	22.697	0.200	5	152.63
V2	2609.960	1846.370	11:29:14.77	28:58:13.7	17.858	0.436	4	30355.61	15.580	0.204	4	6679.30	16.611	0.403	4	26047.48	19.840	0.383	6	17645.34
V3	2699.190	2092.920	11:29:17.41	28:58:26.3	20.258	0.075	5	228.70	19.657	0.061	6	98.17	19.823	0.076	5	374.85	20.641	0.096	6	582.93

Table 9. Stars in the Pal 14 Field with best Photometry

Star ID	X (pix)	Y (pix)	R.A. (J2000)	Decl. (J2000)	$< V >$	$\epsilon(V)$	n_V	$< I >$	$\epsilon(I)$	n_I	$< R >$	$\epsilon(R)$	n_R	$< B >$	$\epsilon(B)$	n_B
1	30.520	3272.550	16:11:11.10	14:53:54.2	19.754	0.008	3	18.389	0.004	3	19.012	0.015	4	20.821	0.009	4
2	52.970	3075.740	16:11:09.19	14:53:57.3	18.655	0.005	3	17.933	0.004	4	18.275	0.006	6	19.142	0.006	4
3	58.800	2045.850	16:10:59.18	14:53:57.7	20.697	0.008	4	19.728	0.010	4	20.203	0.009	6	21.462	0.012	5
4	65.000	653.680	16:10:45.66	14:53:58.1	18.282	0.003	3	17.332	0.005	3	17.773	0.006	4	19.144	0.006	3
5	257.770	2179.340	16:11:00.48	14:54:25.8	19.669	0.003	4	18.897	0.006	4	19.269	0.003	6	20.315	0.005	5
6	327.040	3781.770	16:11:16.04	14:54:36.1	20.099	0.006	3	19.292	0.007	3	19.663	0.014	4	20.666	0.006	3
7	372.780	2580.600	16:11:04.37	14:54:42.1	18.112	0.007	4	17.260	0.005	4	17.667	0.005	6	18.793	0.003	5
8	466.250	2052.810	16:10:59.24	14:54:55.0	19.091	0.005	4	18.337	0.007	4	18.711	0.004	6	19.676	0.004	5
9	510.820	2044.400	16:10:59.16	14:55:01.3	20.067	0.008	4	19.298	0.006	4	19.681	0.004	6	20.658	0.008	5
10	564.300	874.420	16:10:47.79	14:55:08.3	19.623	0.004	4	18.916	0.012	4	19.267	0.006	6	20.167	0.008	5
11	582.040	1069.570	16:10:49.69	14:55:10.9	19.582	0.003	4	18.565	0.007	4	19.066	0.007	6	20.464	0.009	5
12	687.190	2141.560	16:11:00.10	14:55:26.1	17.186	0.007	5	16.001	0.010	5	16.534	0.003	5	18.203	0.008	4
13	775.410	2751.950	16:11:06.02	14:55:38.7	19.313	0.011	6	18.257	0.008	6	18.795	0.003	4	20.276	0.007	3
14	799.810	2097.280	16:10:59.66	14:55:41.9	20.289	0.007	9	19.328	0.007	9	19.809	0.006	4	21.086	0.012	4
15	832.810	848.040	16:10:47.53	14:55:46.1	18.558	0.008	4	17.938	0.011	4	18.248	0.007	6	19.024	0.008	5
16	842.080	634.060	16:10:45.45	14:55:47.3	20.102	0.011	3	18.292	0.015	3	19.165	0.003	4	21.602	0.014	3
17	900.700	2324.250	16:11:01.87	14:55:56.2	20.384	0.007	9	19.434	0.005	9	19.912	0.005	6	21.339	0.012	5
18	950.890	2080.460	16:10:59.50	14:56:03.1	20.177	0.005	9	19.297	0.005	9	19.734	0.003	6	20.870	0.006	5
19	1027.950	2592.900	16:11:04.47	14:56:14.2	19.873	0.010	9	19.037	0.004	9	19.470	0.005	6	20.529	0.006	5
20	1079.810	2538.830	16:11:03.95	14:56:21.4	21.225	0.011	9	20.337	0.007	9	20.810	0.014	6	21.986	0.008	5
21	1090.370	1423.120	16:10:53.11	14:56:22.5	20.010	0.011	6	19.214	0.005	6	19.629	0.004	6	20.628	0.012	5
22	1110.000	1823.450	16:10:56.99	14:56:25.4	19.413	0.003	5	18.352	0.004	5	18.882	0.003	6	20.348	0.008	5
23	1112.680	3371.730	16:11:12.04	14:56:26.4	19.264	0.011	7	17.947	0.006	7	18.555	0.006	6	20.391	0.006	5
24	1169.820	2537.400	16:11:03.93	14:56:34.1	19.753	0.006	9	19.008	0.005	9	19.397	0.006	6	20.365	0.005	5
25	1185.650	2518.650	16:11:03.75	14:56:36.3	21.516	0.011	8	20.618	0.006	8	21.108	0.010	6	22.249	0.014	5
26	1218.400	2399.240	16:11:02.59	14:56:40.9	18.842	0.004	6	17.377	0.006	6	18.053	0.005	6	20.082	0.007	5
27	1222.780	2640.450	16:11:04.93	14:56:41.6	21.130	0.006	9	20.394	0.006	9	20.794	0.005	6	21.748	0.008	5
28	1278.860	2394.610	16:11:02.54	14:56:49.4	19.872	0.004	9	19.053	0.004	9	19.474	0.011	6	20.534	0.005	5
29	1297.450	2531.010	16:11:03.86	14:56:52.0	21.047	0.011	9	19.885	0.004	9	20.455	0.005	6	22.063	0.014	5
30	1304.430	2861.040	16:11:07.07	14:56:53.1	19.089	0.011	6	17.777	0.006	6	18.384	0.007	6	20.204	0.006	5
31	1316.780	3432.400	16:11:12.62	14:56:55.1	19.916	0.008	9	19.257	0.004	9	19.599	0.004	6	20.401	0.012	5
32	1345.400	998.100	16:10:48.97	14:56:58.2	21.003	0.014	4	19.711	0.013	4	20.300	0.004	6	22.089	0.008	5
33	1346.020	2194.810	16:11:00.60	14:56:58.7	19.735	0.008	9	18.711	0.004	9	19.218	0.003	6	20.617	0.007	5
34	1349.340	2936.350	16:11:07.80	14:56:59.5	18.844	0.011	7	17.981	0.003	7	18.419	0.006	6	19.550	0.003	5
35	1357.930	1132.820	16:10:50.28	14:57:00.0	20.479	0.005	6	19.179	0.006	6	19.788	0.007	6	21.608	0.014	5
36	1358.980	3829.150	16:11:16.47	14:57:01.1	20.783	0.011	9	19.141	0.006	9	19.930	0.008	6	22.119	0.014	5
37	1393.390	1521.670	16:10:54.05	14:57:05.1	18.719	0.005	6	17.560	0.005	6	18.120	0.003	6	19.772	0.005	5
38	1416.020	2427.320	16:11:02.85	14:57:08.7	20.055	0.006	9	19.274	0.004	9	19.679	0.004	6	20.658	0.005	5
39	1419.650	2308.450	16:11:01.70	14:57:09.1	21.431	0.007	9	20.537	0.006	9	21.013	0.010	6	22.182	0.013	5
40	1421.610	1693.050	16:10:55.72	14:57:09.2	20.701	0.008	9	19.951	0.008	9	20.322	0.005	6	21.265	0.009	5
41	1427.740	1820.410	16:10:56.96	14:57:10.1	20.604	0.010	9	19.626	0.006	9	20.109	0.005	6	21.369	0.005	5
42	1452.080	2058.560	16:10:59.27	14:57:13.6	20.095	0.009	9	19.282	0.006	9	19.691	0.003	6	20.666	0.007	5
43	1452.340	3006.270	16:11:08.48	14:57:14.0	16.204	0.013	3	15.460	0.006	3	15.812	0.005	3	16.818	0.010	3
44	1472.890	1962.220	16:10:58.33	14:57:16.5	19.089	0.007	7	17.998	0.005	7	18.539	0.003	6	20.054	0.004	5
45	1488.840	954.310	16:10:48.54	14:57:18.3	19.991	0.008	7	19.214	0.006	7	19.601	0.007	6	20.593	0.012	5
46	1492.080	1569.390	16:10:54.52	14:57:19.0	20.366	0.007	9	19.409	0.004	9	19.888	0.003	6	21.190	0.006	5
47	1492.880	2058.040	16:10:59.26	14:57:19.3	19.488	0.006	6	18.443	0.004	6	18.964	0.003	6	20.397	0.010	5
48	1495.540	1272.910	16:10:51.64	14:57:19.4	20.878	0.011	9	19.578	0.005	9	20.188	0.004	6	21.979	0.008	5
49	1495.630	2093.880	16:10:59.61	14:57:19.7	20.647	0.007	9	19.696	0.004	9	20.177	0.009	6	21.396	0.006	5
50	1513.040	2058.550	16:10:59.27	14:57:22.2	18.496	0.005	6	17.377	0.006	6	17.928	0.002	6	19.506	0.003	5
51	1518.170	1285.810	16:10:51.76	14:57:22.6	20.751	0.007	9	19.093	0.004	9	19.893	0.003	6	22.112	0.008	5
52	1531.690	1763.980	16:10:56.41	14:57:24.7	19.972	0.009	9	18.953	0.003	9	19.459	0.004	5	20.835	0.005	5
53	1534.940	1979.670	16:10:58.50	14:57:25.2	17.744	0.006	6	17.037	0.005	6	17.389	0.004	5	18.293	0.003	5
54	1537.930	2747.890	16:11:05.96	14:57:25.9	19.781	0.009	6	18.390	0.007	6	19.044	0.004	5	20.946	0.005	5
55	1551.650	1823.680	16:10:56.98	14:57:27.5	20.114	0.013	9	19.321	0.004	9	19.709	0.008	5	20.710	0.005	5
56	1555.430	697.820	16:10:46.05	14:57:27.6	17.565	0.003	3	16.708	0.003	3	17.134	0.003	3	18.290	0.007	3
57	1583.190	3689.560	16:11:15.11	14:57:32.6	20.884	0.007	9	20.224	0.008	9	20.569	0.009	5	21.332	0.008	5
58	1597.260	2945.690	16:11:07.88	14:57:34.3	16.981	0.004	6	16.228	0.003	6	16.604	0.004	5	17.627	0.006	4
59	1597.690	1744.100	16:10:56.21	14:57:33.9	20.012	0.010	9	19.202	0.004	9	19.609	0.005	6	20.607	0.005	5

Table 9—Continued

Star ID	X (pix)	Y (pix)	R.A. (J2000)	Decl. (J2000)	< V >	ϵ(V)	n_V	< I >	ϵ(I)	n_I	< R >	ϵ(R)	n_R	< B >	ϵ(B)	n_B
60	1603.430	2071.850	16:10:59.39	14:57:34.9	21.230	0.005	9	20.319	0.005	9	20.791	0.010	6	21.964	0.015	5
61	1615.010	2311.600	16:11:01.72	14:57:36.6	20.085	0.005	9	19.306	0.003	9	19.714	0.003	6	20.717	0.008	5
62	1617.380	3100.380	16:11:09.39	14:57:37.2	19.947	0.008	9	19.127	0.003	9	19.559	0.005	6	20.584	0.007	5
63	1622.820	2047.900	16:10:59.16	14:57:37.6	19.994	0.006	9	19.124	0.004	9	19.559	0.003	6	20.741	0.006	5
64	1626.360	2101.000	16:10:59.68	14:57:38.1	21.707	0.009	9	20.807	0.013	9	21.274	0.006	6	22.397	0.015	5
65	1629.710	1035.390	16:10:49.32	14:57:38.2	20.569	0.013	9	19.886	0.007	9	20.222	0.006	6	21.065	0.008	5
66	1638.960	2975.040	16:11:08.17	14:57:40.2	20.475	0.007	8	19.520	0.004	8	20.013	0.006	6	21.284	0.007	5
67	1638.980	1993.970	16:10:58.64	14:57:39.8	19.944	0.009	6	18.947	0.005	6	19.447	0.005	6	20.798	0.008	5
68	1641.890	2174.600	16:11:00.39	14:57:40.3	20.052	0.008	7	19.289	0.007	7	19.687	0.010	5	20.643	0.006	4
69	1654.220	3590.890	16:11:14.15	14:57:42.5	20.803	0.012	9	20.120	0.006	9	20.472	0.009	5	21.336	0.005	5
70	1658.290	2899.890	16:11:07.44	14:57:42.9	19.876	0.009	8	18.876	0.005	8	19.388	0.005	6	20.714	0.010	5
71	1661.320	1707.470	16:10:55.85	14:57:42.9	19.608	0.009	9	18.718	0.003	9	19.158	0.004	6	20.315	0.005	5
72	1662.130	2071.390	16:10:59.39	14:57:43.1	20.055	0.004	9	19.289	0.004	9	19.686	0.003	6	20.633	0.006	5
73	1668.040	1631.150	16:10:55.11	14:57:43.8	20.064	0.010	9	19.256	0.003	9	19.662	0.004	6	20.671	0.005	5
74	1671.310	2468.720	16:11:03.25	14:57:44.6	20.060	0.005	6	19.248	0.005	6	19.658	0.004	6	20.680	0.006	5
75	1672.020	2733.190	16:11:05.82	14:57:44.7	17.368	0.008	5	15.952	0.009	5	16.624	0.003	5	18.750	0.008	4
76	1672.460	1590.940	16:10:54.72	14:57:44.4	21.732	0.015	9	20.843	0.012	9	21.292	0.009	6	22.504	0.015	5
77	1676.640	2107.720	16:10:59.74	14:57:45.2	19.989	0.004	4	19.199	0.008	4	19.594	0.007	4	20.586	0.008	4
78	1710.430	1441.490	16:10:53.27	14:57:49.7	20.040	0.009	9	19.268	0.007	9	19.662	0.006	6	20.610	0.007	5
79	1714.550	3528.690	16:11:13.55	14:57:51.0	20.281	0.014	7	17.912	0.013	7	19.201	0.008	5	21.763	0.009	5
80	1724.110	863.920	16:10:47.65	14:57:51.4	19.415	0.012	7	17.915	0.007	7	18.613	0.006	6	20.724	0.012	5
81	1730.390	2333.240	16:11:01.93	14:57:52.8	20.111	0.009	9	19.138	0.006	9	19.634	0.005	6	20.993	0.010	5
82	1746.580	1174.210	16:10:50.67	14:57:54.6	19.701	0.007	9	19.014	0.003	9	19.367	0.007	6	20.191	0.005	5
83	1748.660	2840.810	16:11:06.86	14:57:55.6	19.897	0.007	8	18.377	0.007	8	19.097	0.005	6	21.162	0.007	5
84	1752.950	2313.800	16:11:01.74	14:57:56.0	21.542	0.011	9	20.670	0.007	9	21.120	0.009	6	22.308	0.014	5
85	1754.470	1816.800	16:10:56.91	14:57:56.0	18.829	0.006	6	17.728	0.003	6	18.267	0.003	6	19.823	0.005	5
86	1756.960	3400.640	16:11:12.30	14:57:56.9	18.845	0.010	7	17.966	0.004	7	18.382	0.008	6	19.631	0.008	5
87	1764.590	3532.300	16:11:13.58	14:57:58.0	19.927	0.009	9	18.911	0.007	9	19.419	0.011	5	20.778	0.007	5
88	1772.150	1293.960	16:10:51.83	14:57:58.3	18.272	0.014	6	17.375	0.003	6	17.815	0.004	6	19.019	0.009	5
89	1778.530	2279.970	16:11:01.41	14:57:59.6	19.044	0.006	7	17.959	0.005	7	18.495	0.004	6	20.014	0.004	5
90	1786.640	3820.900	16:11:16.38	14:58:01.2	21.187	0.009	9	20.260	0.005	9	20.717	0.005	5	21.925	0.015	5
91	1793.930	2082.640	16:10:59.49	14:58:01.6	20.215	0.005	9	19.242	0.004	9	19.726	0.005	6	21.081	0.006	5
92	1807.770	2473.470	16:11:03.29	14:58:03.7	20.533	0.004	9	19.606	0.004	9	20.074	0.006	6	21.305	0.005	5
93	1808.020	1462.950	16:10:53.47	14:58:03.4	19.155	0.010	7	18.190	0.002	7	18.669	0.005	6	19.978	0.008	5
94	1827.050	2318.130	16:11:01.78	14:58:06.4	19.981	0.004	9	19.198	0.005	9	19.597	0.004	6	20.581	0.006	5
95	1845.850	3312.210	16:11:11.44	14:58:09.4	20.621	0.009	9	19.681	0.008	9	20.147	0.007	6	21.430	0.010	5
96	1868.290	3604.610	16:11:14.28	14:58:12.6	17.541	0.005	6	16.510	0.010	6	17.001	0.007	4	18.410	0.008	4
97	1874.390	2079.350	16:10:59.46	14:58:12.9	17.616	0.011	6	16.909	0.005	6	17.259	0.008	6	18.163	0.007	5
98	1899.710	1094.550	16:10:49.89	14:58:16.1	18.166	0.005	6	17.125	0.006	6	17.615	0.005	6	19.050	0.008	5
99	1904.610	2866.980	16:11:07.11	14:58:17.5	20.848	0.010	9	19.934	0.005	9	20.404	0.005	6	21.630	0.011	5
100	1910.590	2101.350	16:10:59.67	14:58:18.0	20.361	0.006	8	19.394	0.004	8	19.861	0.004	6	21.194	0.014	5
101	1930.050	2346.970	16:11:02.06	14:58:20.9	21.168	0.005	9	20.284	0.005	9	20.738	0.007	6	21.923	0.014	5
102	1957.610	2368.650	16:11:02.27	14:58:24.8	21.094	0.005	9	20.234	0.008	9	20.671	0.006	6	21.797	0.014	5
103	1987.560	2134.190	16:10:59.99	14:58:28.9	18.240	0.015	6	16.335	0.010	6	17.268	0.005	6	19.687	0.011	5
104	1995.620	2903.010	16:11:07.46	14:58:30.3	20.499	0.008	9	19.550	0.005	9	20.040	0.007	6	21.314	0.013	5
105	2000.050	1561.260	16:10:54.42	14:58:30.4	21.033	0.006	9	20.091	0.004	9	20.561	0.007	6	21.788	0.008	5
106	2010.550	2243.620	16:11:01.05	14:58:32.1	20.385	0.007	9	19.451	0.005	9	19.906	0.003	6	21.180	0.012	5
107	2018.300	1528.510	16:10:54.10	14:58:33.0	21.069	0.006	9	20.162	0.006	9	20.599	0.005	6	21.773	0.015	5
108	2039.960	1611.840	16:10:54.91	14:58:36.0	18.279	0.008	6	17.100	0.005	6	17.673	0.006	6	19.348	0.010	5
109	2135.330	2233.710	16:11:00.95	14:58:49.7	20.108	0.009	9	19.521	0.004	9	19.830	0.010	6	20.507	0.011	5
110	2217.820	1971.080	16:10:58.40	14:59:01.2	17.876	0.003	5	17.034	0.006	5	17.453	0.006	5	18.612	0.005	4
111	2232.660	1885.740	16:10:57.57	14:59:03.2	20.057	0.010	9	19.080	0.005	9	19.566	0.007	6	20.894	0.009	5
112	2335.980	879.980	16:10:47.79	14:59:17.4	21.076	0.008	8	20.177	0.006	8	20.627	0.008	6	21.847	0.011	5
113	2348.120	1681.050	16:10:55.58	14:59:19.4	20.574	0.007	9	19.759	0.007	9	20.138	0.013	6	21.301	0.011	5
114	2348.440	2717.000	16:11:05.64	14:59:19.8	21.334	0.006	9	20.441	0.006	9	20.881	0.007	6	22.047	0.015	5
115	2359.250	1859.450	16:10:57.31	14:59:21.0	20.390	0.008	9	19.705	0.008	9	20.044	0.006	6	20.920	0.009	5
116	2360.620	3122.890	16:11:09.59	14:59:21.7	20.763	0.007	9	18.545	0.004	9	19.706	0.007	6	22.272	0.014	5
117	2364.570	2428.010	16:11:02.83	14:59:22.0	19.353	0.004	9	18.691	0.003	9	19.026	0.007	6	19.834	0.009	5
118	2388.920	1292.480	16:10:51.80	14:59:25.0	21.193	0.006	8	21.390	0.012	8	21.283	0.010	6	21.094	0.005	5
119	2438.160	1073.290	16:10:49.67	14:59:31.8	19.304	0.006	9	18.343	0.002	9	18.813	0.006	6	20.160	0.007	5

Table 9—Continued

Star ID	X (pix)	Y (pix)	R.A. (J2000)	Decl. (J2000)	$< V >$	$\epsilon(V)$	n_V	$< I >$	$\epsilon(I)$	n_I	$< R >$	$\epsilon(R)$	n_R	$< B >$	$\epsilon(B)$	n_B
120	2515.590	3116.880	16:11:09.52	14:59:43.4	20.048	0.005	9	19.232	0.005	9	19.647	0.014	6	20.663	0.011	5
121	2544.280	2307.310	16:11:01.66	14:59:47.2	19.935	0.003	9	18.938	0.007	9	19.437	0.009	6	20.785	0.009	5
122	2636.280	1366.500	16:10:52.51	14:59:59.8	20.531	0.010	5	18.267	0.007	5	19.480	0.009	6	22.050	0.011	5
123	2674.130	1149.830	16:10:50.40	15:00:05.0	21.324	0.005	6	20.691	0.007	6	21.026	0.008	6	21.784	0.009	5
124	2748.420	1011.600	16:10:49.06	15:00:15.4	20.629	0.006	3	19.088	0.006	3	19.814	0.012	6	21.917	0.014	5
125	2801.070	904.800	16:10:48.02	15:00:22.7	16.955	0.005	3	16.148	0.005	3	16.542	0.007	5	17.676	0.006	4
126	2835.020	1086.690	16:10:49.79	15:00:27.6	19.937	0.009	3	19.115	0.007	3	19.532	0.009	4	20.546	0.006	3
127	2841.220	1163.280	16:10:50.53	15:00:28.5	20.004	0.008	3	17.675	0.003	3	18.924	0.012	4	21.503	0.014	3
128	2910.900	1202.410	16:10:50.91	15:00:38.3	19.847	0.003	3	18.650	0.005	3	19.204	0.012	4	20.843	0.012	3
129	2963.860	3148.640	16:11:09.82	15:00:46.5	20.881	0.009	8	20.002	0.011	7	20.469	0.012	4	21.601	0.013	3
130	3112.300	3124.050	16:11:09.58	15:01:07.3	19.957	0.003	7	19.147	0.008	6	19.567	0.011	4	20.585	0.007	3
131	3123.770	2515.320	16:11:03.66	15:01:08.7	16.844	0.005	3	15.675	0.009	4	16.218	0.006	3	17.850	0.010	3
132	3205.420	1200.940	16:10:50.89	15:01:19.7	17.449	0.006	3	16.428	0.005	3	16.903	0.006	4	18.370	0.010	3
133	3291.180	2101.210	16:10:59.63	15:01:32.1	19.658	0.003	4	18.643	0.008	5	19.167	0.008	4	20.536	0.007	3
134	3370.540	730.300	16:10:46.31	15:01:42.7	20.165	0.006	3	19.485	0.012	3	19.836	0.013	4	20.646	0.011	3
135	3379.470	2202.680	16:11:00.62	15:01:44.5	16.928	0.006	4	15.796	0.008	4	16.315	0.006	4	17.960	0.010	3
136	3625.850	2639.170	16:11:04.85	15:02:19.3	18.431	0.004	4	17.416	0.006	4	17.907	0.006	3	19.330	0.007	3
137	3750.900	3216.830	16:11:10.46	15:02:37.1	19.864	0.003	3	19.111	0.006	4	19.513	0.010	3	20.476	0.007	3
138	3762.800	2516.120	16:11:03.65	15:02:38.5	19.732	0.006	4	18.918	0.006	4	19.341	0.010	3	20.436	0.010	3
139	3769.830	2784.180	16:11:06.26	15:02:39.6	19.158	0.003	4	17.267	0.008	4	18.218	0.009	3	20.666	0.007	3
140	3789.520	2271.990	16:11:01.28	15:02:42.2	18.925	0.004	4	17.294	0.006	4	18.088	0.005	3	20.250	0.010	3
141	3790.740	3825.410	16:11:16.38	15:02:42.9	17.195	0.009	3	16.098	0.010	3	16.614	0.011	3	18.193	0.005	3
142	4026.450	2440.300	16:11:02.91	15:03:15.6	19.617	0.003	4	18.047	0.007	4	18.818	0.009	3	20.902	0.007	3
143	4074.200	3466.410	16:11:12.88	15:03:22.6	18.870	0.008	3	18.008	0.004	3	18.460	0.011	3	19.637	0.003	3

Table 10. Stars in the Pal 14 Field with at least V and I Photometry[a]

X (pix)	Y (pix)	R.A. (J2000)	Decl. (J2000)	$< V >$	$\epsilon(V)$	n_V	$\chi^2_\nu(V)$	$< I >$	$\epsilon(I)$	n_I	$\chi^2_\nu(I)$	$< R >$	$\epsilon(R)$	n_R	$\chi^2_\nu(R)$	$< B >$	$\epsilon(B)$	n_B	$\chi^2_\nu(B)$
12.830	3762.790	16:11:15.86	14:53:51.9	21.336	0.013	3	0.98	20.342	0.015	3	1.72	20.801	0.029	2	9.51	21.980	0.018	2	0.25
30.520	3272.550	16:11:11.10	14:53:54.2	19.754	0.008	3	4.27	18.389	0.004	3	0.80	19.012	0.015	4	15.50	20.821	0.009	4	1.86
52.790	1909.790	16:10:57.86	14:53:56.9	23.437	0.062	2	1.28	20.886	0.036	3	6.20	22.407	0.030	5	3.42	—	—	1	—
52.970	3075.740	16:11:09.19	14:53:57.3	18.655	0.005	3	2.36	17.933	0.004	4	2.16	18.275	0.006	6	6.91	19.142	0.006	4	4.04
54.100	3171.720	16:11:10.12	14:53:57.5	21.087	0.010	3	2.45	18.451	0.025	4	81.22	19.867	0.010	6	10.47	22.800	0.024	4	1.90
57.040	1371.220	16:10:52.63	14:53:57.2	23.688	0.076	2	0.03	22.686	0.169	3	4.09	23.097	0.116	2	4.81	—	—	1	—
57.190	2776.150	16:11:06.28	14:53:57.8	23.279	0.053	3	1.22	22.348	0.081	3	1.66	23.025	0.065	5	4.89	23.819	0.072	4	2.53
58.800	2045.850	16:10:59.18	14:53:57.7	20.697	0.008	4	1.90	19.728	0.010	4	3.13	20.203	0.009	6	3.29	21.462	0.012	5	3.50
64.620	1469.860	16:10:53.59	14:53:58.3	20.882	0.018	4	7.77	20.438	0.014	4	1.49	20.601	0.011	6	4.42	21.193	0.014	5	6.16
65.000	653.680	16:10:45.66	14:53:58.1	18.282	0.003	3	0.26	17.332	0.005	3	2.86	17.773	0.006	4	4.84	19.144	0.006	3	3.27
72.150	3005.860	16:11:08.51	14:54:00.0	22.503	0.034	3	1.48	20.576	0.030	4	5.83	21.536	0.015	6	3.49	23.906	0.051	2	0.91
72.850	415.900	16:10:43.35	14:53:59.1	16.602	0.005	2	1.32	15.845	0.007	3	1.59	—	—	1	—	17.243	0.004	3	1.94
84.260	131.570	16:10:40.59	14:54:00.6	23.532	0.067	2	0.00	22.844	0.124	3	1.75	—	—	1	—	—	—	0	—
85.340	1673.000	16:10:55.56	14:54:01.3	24.071	0.193	2	3.18	22.798	0.227	2	3.87	23.447	0.071	2	1.00	—	—	0	—
90.960	920.600	16:10:48.25	14:54:01.8	21.997	0.037	4	5.45	21.168	0.020	4	0.21	21.565	0.008	6	0.56	22.676	0.016	5	0.94
106.410	2754.670	16:11:06.07	14:54:04.7	23.794	0.081	2	0.28	22.497	0.066	3	0.03	23.022	0.049	2	0.10	—	—	0	—
145.100	4051.890	16:11:18.67	14:54:10.6	19.474	0.004	2	0.29	17.580	0.018	2	15.48	18.519	0.031	2	46.62	20.822	0.007	2	0.08
172.600	125.720	16:10:40.53	14:54:13.0	24.205	0.120	2	0.02	21.300	0.053	2	4.18	22.974	0.046	2	0.12	—	—	0	—
172.840	2329.800	16:11:01.94	14:54:13.9	23.128	0.043	3	0.00	22.573	0.076	3	0.21	22.882	0.042	2	0.02	23.634	0.069	4	3.38
193.640	2410.030	16:11:02.72	14:54:16.8	22.960	0.039	3	0.26	22.345	0.198	2	8.08	22.663	0.022	5	0.94	23.422	0.050	4	2.57
194.310	2064.340	16:10:59.36	14:54:16.8	21.301	0.021	4	10.17	19.057	0.031	4	65.19	20.256	0.014	6	9.18	22.761	0.017	5	1.07
195.770	1203.680	16:10:51.00	14:54:16.7	22.723	0.045	3	1.79	21.318	0.025	3	0.24	21.957	0.020	5	5.38	23.969	0.050	4	0.13
199.540	3549.550	16:11:13.79	14:54:18.1	20.229	0.006	3	0.09	19.248	0.006	3	0.99	19.710	0.020	4	16.35	21.039	0.007	4	0.93
201.850	918.630	16:10:48.23	14:54:17.4	23.967	0.228	2	5.39	21.417	0.033	2	0.05	22.967	0.042	2	0.52	—	—	0	—
206.490	3770.220	16:11:15.93	14:54:19.1	21.132	0.032	2	13.14	20.177	0.033	2	3.84	20.652	0.046	2	41.47	21.828	0.023	2	1.90
231.820	3991.390	16:11:18.08	14:54:22.8	20.062	0.012	3	4.13	18.992	0.007	3	1.60	19.474	0.021	4	30.67	20.873	0.009	3	1.78
237.180	3408.930	16:11:12.42	14:54:23.3	21.544	0.013	3	0.96	19.038	0.021	4	17.35	20.415	0.013	6	7.83	23.038	0.044	4	1.67
248.180	2931.660	16:11:07.78	14:54:24.7	23.440	0.055	2	0.90	22.708	0.197	2	3.51	23.263	0.052	3	1.79	24.045	0.056	3	0.64
256.280	2983.970	16:11:08.29	14:54:25.8	23.735	0.117	2	2.66	22.410	0.072	2	0.00	23.067	0.085	3	5.65	24.572	0.092	2	0.12
257.770	2179.340	16:11:00.48	14:54:25.8	19.669	0.003	4	0.74	18.897	0.006	4	2.34	19.269	0.003	6	1.29	20.315	0.005	5	1.05
261.260	2324.360	16:11:01.88	14:54:26.3	22.876	0.033	3	0.71	22.140	0.054	3	0.65	22.490	0.029	5	2.05	23.376	0.030	4	0.06
276.840	2456.380	16:11:03.17	14:54:28.5	22.476	0.047	2	2.02	21.946	0.055	2	0.00	22.297	0.039	4	2.80	22.764	0.045	3	2.44
287.940	2340.460	16:11:02.04	14:54:30.1	23.698	0.077	2	0.00	22.858	0.116	2	0.13	23.349	0.041	3	1.01	24.166	0.063	2	0.03
292.760	3761.690	16:11:15.84	14:54:31.2	22.649	0.029	3	0.56	21.882	0.074	3	3.36	22.239	0.068	4	8.89	23.023	0.066	3	2.77
305.650	3274.540	16:11:11.11	14:54:32.9	23.396	0.103	2	2.94	21.739	0.038	2	0.53	22.456	0.067	3	6.00	—	—	1	—
317.990	1101.160	16:10:50.00	14:54:33.8	23.731	0.086	2	0.19	22.938	0.147	2	1.30	23.409	0.072	2	0.13	—	—	1	—
323.150	785.230	16:10:46.93	14:54:34.4	21.762	0.013	3	0.15	21.030	0.019	3	0.24	21.386	0.009	4	0.24	22.254	0.020	3	0.91
327.040	3781.770	16:11:16.04	14:54:36.1	20.099	0.006	3	1.12	19.292	0.007	3	1.68	19.663	0.014	4	13.40	20.666	0.006	3	0.50
349.110	530.580	16:10:44.46	14:54:38.0	23.237	0.083	2	2.46	21.333	0.066	3	9.21	22.212	0.021	2	0.54	—	—	0	—
361.340	2162.210	16:11:00.31	14:54:40.3	22.833	0.035	2	0.12	20.740	0.023	3	2.45	21.867	0.044	5	25.47	24.273	0.068	3	0.79
372.780	2580.600	16:11:04.37	14:54:42.1	18.112	0.007	4	7.22	17.260	0.005	4	3.54	17.667	0.005	6	4.77	18.793	0.003	5	1.71
373.090	3653.020	16:11:14.79	14:54:42.5	22.927	0.054	3	2.17	22.324	0.067	3	1.30	22.577	0.034	4	0.31	23.315	0.062	2	0.56
384.450	520.280	16:10:44.36	14:54:42.9	23.668	0.072	2	0.53	22.737	0.083	3	0.83	23.235	0.060	2	0.11	23.736	0.107	2	1.94
394.870	2849.250	16:11:06.98	14:54:45.3	23.468	0.064	2	0.13	22.904	0.106	2	0.85	23.129	0.044	3	1.81	23.995	0.062	3	1.26
399.170	2707.420	16:11:05.60	14:54:45.8	23.824	0.081	2	0.28	20.127	0.063	2	48.97	22.142	0.034	2	2.64	—	—	0	—
402.260	1230.280	16:10:51.25	14:54:45.7	21.919	0.031	3	4.98	20.471	0.011	4	0.56	21.133	0.005	6	0.71	23.202	0.026	4	0.99
420.260	3209.760	16:11:10.48	14:54:49.0	23.481	0.068	2	1.28	21.506	0.030	3	0.51	22.253	0.051	3	3.26	—	—	0	—
422.650	3393.110	16:11:12.26	14:54:49.4	23.640	0.097	2	1.83	21.814	0.052	3	2.26	22.755	0.071	3	4.11	—	—	0	—
433.470	880.390	16:10:47.85	14:54:50.0	23.493	0.060	2	0.39	22.604	0.096	3	1.44	22.982	0.030	3	0.04	23.746	0.041	3	0.41
436.030	748.000	16:10:46.57	14:54:50.3	23.780	0.077	2	0.03	22.246	0.143	2	5.35	23.117	0.061	2	1.50	24.313	0.136	2	0.15
440.380	1990.200	16:10:58.63	14:54:51.4	22.975	0.044	3	0.02	22.160	0.054	3	0.06	22.630	0.029	5	1.92	23.435	0.031	4	0.07
452.590	3260.730	16:11:10.97	14:54:53.5	21.979	0.015	3	0.86	20.983	0.018	4	0.49	21.484	0.017	6	4.66	22.834	0.032	5	2.05
452.820	2006.640	16:10:58.79	14:54:53.1	23.148	0.042	3	1.09	22.417	0.092	2	1.30	22.858	0.025	3	0.81	23.696	0.042	4	0.57
456.670	2600.830	16:11:04.56	14:54:53.9	23.208	0.043	3	0.68	22.556	0.083	3	1.27	22.909	0.047	3	2.44	23.683	0.040	4	0.47
458.690	3916.840	16:11:17.35	14:54:54.6	23.659	0.152	2	4.24	22.779	0.107	3	1.35	23.156	0.121	2	4.42	24.107	0.177	2	2.09
460.940	253.420	16:10:41.76	14:54:53.6	22.177	0.026	2	0.01	21.160	0.031	2	0.96	—	—	1	—	23.214	0.047	3	1.20
462.010	2011.240	16:10:58.84	14:54:54.4	23.552	0.060	2	0.30	21.709	0.047	3	2.12	22.645	0.026	3	1.48	—	—	1	—
465.120	2503.480	16:11:03.62	14:54:55.0	23.256	0.046	2	0.87	21.214	0.021	3	1.23	22.317	0.029	4	3.53	24.715	0.156	2	2.15
466.250	2052.810	16:10:59.24	14:54:55.0	19.091	0.005	4	3.47	18.337	0.007	4	5.72	18.711	0.004	6	2.49	19.676	0.004	5	1.69

[a]The full text of this table may be found at: ftp://taurus.tuc.noao.edu/pub/saha/Photseq/table10.txt

Table 11. Likely Variable Stars in the Pal 14 Field

Star ID	X (pix)	Y (pix)	R.A. (J2000)	Decl. (J2000)	$\langle V \rangle$	$\epsilon(V)$	n_V	$\chi^2_\nu(V)$	$\langle I \rangle$	$\epsilon(I)$	n_I	$\chi^2_\nu(I)$	$\langle R \rangle$	$\epsilon(R)$	n_R	$\chi^2_\nu(R)$	$\langle B \rangle$	$\epsilon(B)$	n_B	$\chi^2_\nu(B)$
V1	750.640	3667.320	16:11:14.92	14:55:35.6	23.382	0.051	6	1.71	21.336	0.078	6	23.62	22.389	0.043	4	7.03	−10.000	−1.000	1	−100.00
V2	776.070	1393.620	16:10:52.83	14:55:38.3	19.869	0.233	6	4969.24	18.881	0.034	6	95.32	19.357	0.005	4	2.88	20.700	0.013	3	4.93
V3	841.310	1739.040	16:10:56.18	14:55:47.6	19.866	0.068	6	436.13	19.241	0.010	6	5.52	19.554	0.005	6	3.03	20.341	0.015	5	10.00
V4	888.810	883.730	16:10:47.87	14:55:54.0	20.943	0.100	6	240.46	20.220	0.034	6	32.05	20.560	0.005	6	0.45	21.587	0.007	5	1.17
V5	1334.060	1962.690	16:10:58.34	14:56:57.0	21.155	0.051	9	94.90	19.843	0.005	9	1.69	20.441	0.014	6	6.72	22.200	0.031	5	6.69
V6	1487.820	1992.960	16:10:58.63	14:57:18.6	21.568	0.062	6	34.19	21.307	0.024	4	1.97	21.501	0.073	6	89.40	21.849	0.047	4	29.80
V7	1867.460	2161.920	16:11:00.26	14:58:12.0	21.315	0.022	8	13.13	20.546	0.062	8	44.30	20.881	0.020	4	8.61	22.033	0.045	4	8.70

Table 12. Mean Offsets of Various Photometry of NGC 2419 vs. this paper

Study	Mean Offsets (Study - this paper)[a] B	V	R	I
Stetson sequence	+.014 (.021)	−.014 (.004)	−.017 (.005)	−.038 (.006)
Davis sequence	+.027 (.021)	−.005 (.005)	+.001 (.007)	−.022 (.007)
Dolphin WFPC2[b]	—	+.020 (.006)	—	−.011 (.007)
Dolphin's independent calib of WIYN data	—	+.002 (.004)	—	+.003 (.007)
WIYN 0.9m data only	+.055 (.031)	−.002 (.012)	+.021 (.009)	+.032 (.018)
Sirianni et al. ACS[c]	Offsets within ±0.02 in V, R, and I			

[a]Values in parentheses indicate errors in the mean differences of the stars compared, to which the systematic error estimates from Table 2 have been added in quadrature. These may be slight underestimates, since systematic error estimates for the sequences being compared to, which should also be added in quadrature, are not generally available.

[b]The calibration is based on WFPC2 observations of ω Cen, and the photometric sequence by Walker (1994).

[c]Estimates are from privately communicated figures. Numbers not available

Table 13. Mean Residuals and Standard Errors of the Calibrating Landolt Standard stars

Object	V	$B-V$	$V-R$	$R-I$	ΔV^{a}	ϵ_V	$n(V)$	ΔI^{a}	ϵ_I	$n(I)$	ΔB^{a}	ϵ_B	$n(B)$	ΔR^{a}	ϵ_R	$n(R)$
SA101-262	14.295	0.784	0.440	0.387	0.008	—	2	0.005	—	2	0.001	—	2	0.007	—	2
SA101-268	14.380	1.531	1.040	1.200	0.005	—	2	0.021	—	2	0.017	—	2	0.009	—	2
SA101-326	14.923	0.729	0.406	0.375	−0.010	—	2	−0.022	—	2	−0.013	—	2	−0.010	—	2
SA101-330	13.723	0.577	0.346	0.338	0.004	—	2	0.001	—	2	−0.002	—	2	0.007	—	2
SA104-330	15.296	0.594	0.369	0.371	0.001	0.006	11	0.012	0.003	11	−0.024	0.003	8	0.007	0.004	8
SA104-333	15.459	0.832	0.476	0.374	−0.020	—	1	0.102	—	1	—	—	0	—	—	0
SA104-334	13.484	0.518	0.323	0.331	0.004	0.002	9	−0.008	0.002	9	0.003	0.002	9	0.001	0.002	9
SA104-336	14.404	0.830	0.461	0.403	0.002	0.003	10	0.004	0.003	10	0.009	0.002	6	−0.001	0.003	6
SA104-338	16.059	0.591	0.348	0.372	−0.022	0.004	12	−0.034	0.004	12	−0.000	0.004	9	−0.023	0.007	9
SA107-599	14.675	0.698	0.433	0.438	−0.002	0.003	5	−0.020	0.007	5	−0.048	—	1	0.000	—	1
SA107-600	14.884	0.503	0.339	0.361	0.017	0.005	4	−0.021	0.007	4	—	—	0	—	—	0
SA107-601	14.646	1.412	0.923	0.835	−0.009	0.004	4	−0.007	0.007	4	—	—	0	—	—	0
SA107-602	12.116	0.991	0.545	0.531	−0.005	0.002	5	0.002	0.009	5	−0.010	—	2	0.004	—	2
SA110-229	13.649	1.910	1.198	1.155	0.012	0.003	8	0.012	0.003	8	0.011	0.003	7	0.009	0.004	7
SA110-230	14.281	1.084	0.624	0.596	−0.001	0.003	7	−0.008	0.004	7	−0.002	0.003	4	0.000	0.005	4
SA110-232	12.516	0.729	0.439	0.450	0.008	0.002	9	0.010	0.004	9	0.013	0.004	7	0.009	0.004	7
SA110-233	12.771	1.281	0.773	0.818	−0.010	0.003	7	0.004	0.003	7	−0.017	0.004	7	−0.002	0.003	7
SA110-361	12.425	0.632	0.361	0.348	−0.015	—	2	0.004	—	2	—	—	0	—	—	0
SA110-364	13.615	1.133	0.697	0.585	−0.016	—	1	−0.047	—	1	—	—	0	—	—	0
SA92-355	14.965	1.164	0.759	0.645	−0.007	—	2	−0.005	—	2	—	—	0	—	—	0
SA92-425	13.941	1.191	0.755	0.627	0.009	—	2	0.002	—	2	—	—	0	—	—	0
SA92-430	14.440	0.567	0.338	0.338	0.002	—	2	0.010	—	2	—	—	0	—	—	0
SA95-275	13.479	1.763	1.011	0.931	0.013	—	1	0.008	—	1	—	—	0	—	—	0
SA95-276	14.118	1.225	0.748	0.646	0.002	—	1	−0.018	—	1	—	—	0	—	—	0
SA95-330	12.174	1.999	1.166	1.100	0.001	—	1	0.001	—	1	—	—	0	—	—	0
SA98-1087	14.439	1.595	0.928	0.882	0.025	—	2	0.004	—	2	—	—	0	—	—	0
SA98-650	12.271	0.157	0.080	0.086	−0.001	0.004	5	−0.006	0.005	5	−0.001	0.003	3	−0.009	0.002	3
SA98-653	9.539	−0.004	0.009	0.008	0.013	0.005	6	0.018	0.004	6	0.011	0.004	4	0.005	0.003	4
SA98-670	11.930	1.356	0.723	0.653	−0.000	0.004	4	0.005	0.007	4	0.018	—	2	0.002	—	2
SA98-671	13.385	0.968	0.575	0.494	−0.001	0.003	6	−0.002	0.004	6	−0.016	0.012	3	0.005	0.001	3
SA98-675	13.398	1.909	1.082	1.002	−0.005	—	2	0.007	—	2	—	—	0	—	—	0
SA98-676	13.068	1.146	0.683	0.673	−0.014	—	2	−0.003	—	2	—	—	0	—	—	0
SA98-682	13.749	0.632	0.366	0.352	−0.002	—	2	−0.031	—	2	—	—	0	—	—	0
SA98-685	11.954	0.463	0.290	0.280	0.001	0.003	6	−0.001	0.003	6	−0.006	0.001	4	−0.002	0.002	4
Mark-A	13.258	−0.242	−0.115	−0.125	0.010	—	2	0.012	—	2	—	—	0	—	—	0
Mark-A2	14.540	0.666	0.379	0.371	−0.004	—	2	−0.012	—	2	—	—	0	—	—	0
Mark-A3	14.818	0.938	0.587	0.510	0.002	—	2	−0.001	—	2	—	—	0	—	—	0
PG0918-A	14.490	0.536	0.325	0.336	0.001	—	1	0.010	—	1	−0.010	—	1	0.005	—	1
PG0918-B	13.963	0.765	0.417	0.370	0.001	—	1	0.008	—	1	0.015	—	1	0.001	—	1
PG0918-C	13.537	0.631	0.367	0.357	−0.003	—	1	−0.020	—	1	−0.021	—	1	−0.002	—	1
PG0918-D	12.272	1.044	0.575	0.535	−0.005	—	1	−0.009	—	1	0.014	—	1	−0.014	—	1
PG1323-086	13.481	−0.140	−0.048	−0.078	−0.001	—	1	0.013	—	1	—	—	0	—	—	0
PG1323-B	13.406	0.761	0.426	0.407	0.006	—	2	0.004	—	2	—	—	0	—	—	0
PG1323-C	14.003	0.707	0.395	0.363	0.013	—	1	−0.006	—	1	—	—	0	—	—	0
PG1323-D	12.080	0.587	0.346	0.335	0.004	—	2	0.005	—	2	—	—	0	—	—	0
PG1633+099	14.397	−0.192	−0.093	−0.116	0.004	0.002	15	0.006	0.003	15	0.007	0.003	13	0.005	0.002	13
PG1633-A	15.256	0.873	0.505	0.511	−0.005	0.004	9	−0.005	0.005	9	−0.004	0.002	6	−0.004	0.005	6
PG1633-B	12.969	1.081	0.590	0.502	0.001	0.002	18	0.001	0.002	18	0.003	0.002	14	−0.003	0.003	14
PG1633-C	13.229	1.134	0.618	0.523	0.005	0.002	15	0.003	0.003	15	0.005	0.003	12	−0.000	0.002	12
PG1633-D	13.691	0.535	0.324	0.327	−0.000	0.002	15	0.008	0.002	15	0.000	0.002	12	0.004	0.002	12
RU149	13.866	−0.129	−0.040	−0.068	0.004	0.001	4	0.006	0.006	4	0.003	0.005	4	0.000	0.003	4
RU149-B	12.642	0.662	0.374	0.354	−0.002	0.003	3	−0.011	0.005	3	0.000	0.005	3	−0.007	0.007	3
RU149-C	14.425	0.195	0.093	0.127	−0.007	0.003	3	0.015	0.006	3	−0.010	0.003	3	0.003	0.005	3
RU149-D	11.480	−0.037	0.021	0.008	0.001	0.002	3	−0.000	0.004	3	0.002	—	2	−0.002	—	2
RU149-E	13.718	0.522	0.321	0.314	0.009	0.003	4	0.002	0.002	4	0.007	0.003	4	0.008	0.008	4
RU149-F	13.471	1.115	0.594	0.538	−0.011	0.006	3	−0.023	0.004	3	−0.018	0.002	3	−0.017	0.013	3
RU152	13.014	−0.190	−0.057	−0.087	−0.008	—	2	−0.020	—	2	—	—	0	—	—	0
RU152-A	14.341	0.543	0.325	0.329	−0.010	—	1	0.018	—	1	—	—	0	—	—	0
RU152-C	12.222	0.573	0.342	0.340	−0.015	—	2	−0.018	—	2	—	—	0	—	—	0
RU152-D	11.076	0.875	0.473	0.449	−0.020	—	2	−0.021	—	2	—	—	0	—	—	0
RU152-E	12.362	0.042	0.030	0.034	−0.009	—	2	−0.002	—	2	—	—	0	—	—	0
RU152-F	14.564	0.635	0.382	0.315	0.017	—	2	0.074	—	2	—	—	0	—	—	0

[a]The sense of Δmag is “Landolt value” minus “Mean from WIYN 3.5m observations”